

Anonymous Referee #1

We thank the Referee for the thorough review of the manuscript and the constructive comments, which contributed to the improvement of this manuscript.

In response, the manuscript is substantially revised with the following:

- 1) Updated analysis of global W data to develop W(U10) parameterization.
- 2) Extended analysis of regional W data to develop W(U10,T) parameterization with SST explicitly included; this was done for both quadratic and cubic wind exponents.
- 3) Analysis for statistical significance (with Student's T-statistics and ANOVA) of new and previous W parameterizations.
- 4) Extended 'Methods' section to justify and clarify approach, data, and implementations.
- 5) Revised and extended 'Results and Discussion' section to clearly describe results and give substantive and quantitative interpretations and conclusions.

The table of contents of the revised manuscript is added after the responses for reference.

Manuscript revisions with track changes are provided in a separate pdf file.

Several comments and questions are similar in all 3 reviews (e.g., uncertainty not reduced, quadratic wind speed exponent, embedded secondary forcing, intercept interpretation). To avoid repetitions, we attempted combining responses to these common points in one file. We found, however, that one-fits-all responses do not always address the reviewers' comments and questions fully. Thus, risking some repetitions, we proceeded with a specific response to each comment.

Responses are presented below in sequence: (1) the original comment from the Referee (in bold italic), there are 10 comments; (2) our response; (3) changes in manuscript.

1.1 In general, the manuscript has poor flow. The authors jump from topic to topic with little flow between main points. There is a lot of redundancy in the text that makes it hard to follow.

1.2 We can see how a perception of "poor flow" of the manuscript can arise. The study and results presented in the manuscript are on three somewhat distinct yet interweaved topics, namely: (i) assessment of satellite-based W data; (ii) parameterization of W; and (iii) application of new W parameterization to predict SSA production. Being well aware of this, we gave a roadmap of our approach in the end of the Introduction (page 21225, lines 3-16) and occasionally listed the points considered in each subsection in short preamble (e.g., p. 21225, lines 18-20).

1.3 The manuscript is now extensively revised. The flow is different and we believe much improved.

2.1 There is no independent verification of the parameterization. Without comparison with other measured, remotely sensed or modeled data I do not see sizable contribution to scientific progress in the field.

2.2 Our intended verification of the performance of the new W(U10) parameterization was given with Fig. 12 and its discussion (old Sect. 4.2.2) as well as the extensive comparison and discussion of the SSA production estimates obtained with the new W(U10) parameterization to previous SSA production estimates (old Sect. 4.3).

2.3 We added new Fig. 13a to compare W values, obtained with new parameterizations $W(U_{10})$ and $W(U_{10}, T)$ for 10 and 37 GHz, to in situ and WindSat W data. Description and discussion of Fig. 13a are added in new Sect. 3.3.2.

Comparisons to the published in situ W data demonstrate order-of-magnitude consistency of the W values from the new parameterizations. Because there are no other remotely-sensed W data except those from WindSat, the most we can do at the moment is to evaluate how well the new parameterizations can replicate the trend and the spread of the satellite-based W . Recently, W values from a global wave model were compared to W from MOM80 and WindSat by Leckler et al. (2013), so one can evaluate where modeled W values stand in the comparison of data and parameterizations of W . All parameterized W values shown in Fig. 13a are calculated using U_{10} and T from the whitecap database, i.e., U_{10} from QuikSCAT and T from GDAS.

3.1 While the proposed parameterization for W has fair agreement with other parameterizations, the authors fail to distinguish the proposed formulation from previously proposed parameterizations after using similar retrieval algorithms (i.e. SAL13).

3.2 We do not expect to prove/show a distinctly different parameterization from that of SAL13 because, indeed, we and SAL13 use the same W data. What we show in this study (and have said in the initial text on p. 21243, lines 3-7) is that a different analysis (a ‘top down’ approach from global to regional scales) gives similar results and this proves that the outcome is robust. What is added with this work to previous analysis of the whitecap database (i.e., SAL13) is the analysis and quantification of the possible intrinsic correlation in the W data and how this could affect W predictions with the new $W(U_{10})$ expressions.

3.3 For the revised manuscript, in addition to the above, we extended the analysis to derive a $W(U_{10}, T)$ parameterization from regional W data sets in addition to the $W(U_{10})$ parameterizations at 10 and 37 GHz from the global W data set. We discuss/justify the approach for the parameterizations (new Sect. 2.1) and its implementation (new Sect. 2.3) and present the results in Sect. 3.2. The comparison to previous parameterizations, including to those of SAL13, is now extended using two metrics—percent difference between different parameterizations and tests for significant differences (new Sect. 3.3).

4.1 When applying the new parameterization to a global model which predicted SSA flux, the authors showed their parameterization reduced SSA emissions in polar regions while increasing emissions in tropical regions. Model analyzes were in the context of mass concentration and was limited to supermicron sized SSA. The argument for using supermicron sized aerosols (i.e., that sub-micron size range additionally includes organic material) does not hold water. Organic enrichment becomes important for particles with <200 nm in diameter. Such particles do not contribute considerably to overall mass. At the end, the point of this exercise is not well explained.

4.2 We agree with the Referee that the justification with the organic content is not strong and acknowledge that we should have explained our choices for estimating SSA emissions better.

4.3 We revised Sect. 2.4 in Methods to give justification for our choice of size distribution with the following arguments (new Sect. 2.4.2).

Generally, the division of the SSA particles into small, medium, and large sizes is well warranted when one considers the climatic effect to be studied. For example, submicron particles are important for scattering by SSA (direct effect) and CCN formation (indirect effect), while supermicron particles are important for heat exchange (via sensible and latent heat fluxes) and

heterogeneous chemical reactions (which need surface and volume to proceed effectively). For the purposes of this study, we do not focus on how the choice of the size distribution will affect the SSA estimates. Rather, at a fixed distribution, we want to see how W data (and W parameterizations based on them), which carry information for the influences of many factors, would affect SSA estimates. In this sense, we can use any size distribution.

The size range of 1 to 10 μm that we have chosen is in the range of medium (supermicron) SSA particles (e.g., de Leeuw et al., 2011, §8). This is the range for which Monahan et al. (1986, or M86) size distribution is valid. Table 3 in Textor et al. (2006) shows that the M86 size distribution, in its original or modified forms, is widely used. Also, Table 2 of Grythe et al. (2014) shows that this size range is a recurring part of the size ranges used in all SSSFs. As the Referee has noted, the SSA particles below $r_{80} = 0.1 \mu\text{m}$ contribute little to the overall mass ($\sim 1\%$ according to Fachini et al. (2008)). We quantify the expected discrepancy due to neglecting particles for $0.1 < r_{80} < 1 \mu\text{m}$ to be 14% using Grythe et al. (2014) estimates of SSA with M86 over two different sizes. We use this assessment in our subsequent analysis of SSA emissions (Sect. 3.4).

5.1 The total predicted sea spray aerosol mass varies by several orders of magnitude. So if the emissions inferred by the current parameterization are within this range, does that prove its validity?

5.2 Yes, it does. That emissions inferred by our new parameterization are within this range shows that our modified SSSF gives consistent estimates, which effectively proves its validity. Certainly, we do not want to be an outlier among SSA emission estimates, especially for a variability range of 2 orders of magnitude. What is more important, however, is that the spatial distribution of this total SSA emission is significantly different from those of previous SSSF predictions. Our new Fig. 14 (old Figs. 10-11) illustrates the global spatial distribution of SSA emissions and a difference map with SSA estimate using MOM80 parameterization.

5.3 We added the following text in new Sect. 3.4.

Previously modeled total dry SSA mass emissions vary by two orders of magnitude because of a variety of uncertainty sources (Sect. 1): $(2.2\text{--}22)\times 10^{12} \text{ kg yr}^{-1}$ (Textor et al., 2006, their Fig. 1a; de Leeuw et al., 2011, their Table 1); and $(2\text{--}74)\times 10^{12} \text{ kg yr}^{-1}$ for long-term averages (over 25 years) (G14, their Table 2, excluding 3 outliers). The impact of the modeling method used has to be acknowledged too. Grythe et al. (2014) suggest that the spread in published estimates of global emission based on the same M86 SSSF (Eq. (4)), from 3.3×10^{12} to $11.7\times 10^{12} \text{ kg yr}^{-1}$ (Lewis and Schwartz, 2004), can be attributed to differences in model input data and resolution differences. An example of the same SSSF yielding different results when applied in different models is also seen in the work of de Leeuw et al. (2011, their Table 1).

For a meaningful comparison of our results to SSA emissions obtained with other SSSFs, we attempt to remove (or at least minimize) the impact of the modeling method. As in this study (see Sect. 3.4), G14 used the same model (i.e., input data and configuration) to evaluate 21 SSSFs, including that of M86, against measurements. We thus can infer a “modelling” factor using our and G14 results obtained with M86 SSSF. We find that the G14 estimate of SSA emission from M86 ($4.51\times 10^{12} \text{ kg yr}^{-1}$) is 1.55 times larger than our estimate of $2.9\times 10^{12} \text{ kg yr}^{-1}$ from M86 and MOM80. We apply this factor of 1.55 to our SSA emission estimated with the new $W(U_{10}, T)$ parameterization and obtain a “model scaled” value of $6.75\times 10^{12} \text{ kg yr}^{-1}$. Our “model scaled” estimate of the SSA emission is close to the median $5.91\times 10^{12} \text{ kg yr}^{-1}$ of the SSA emission reported by G14. This shows that an SSSF with a magnitude factor derived from satellite-based W data provides reasonable and realistic predictions of the SSA emission.

6.1 The submicron range is the most likely size range influencing direct and indirect radiative forcing. The authors' analysis of SSA emissions with the new parameterization fails to highlight this reality.

6.2 We are well aware of this reality. This is seen on page 21224 where we have mentioned the importance of SSA for the direct and indirect radiative effects on climate in Lines 1-4. The importance of SSA to other climate processes is listed in the same paragraph. We have not mentioned specific sizes of the SSA suitable for each of these processes, because in Lines 1-2 on page 21225 we state that for the objective of the study we focus on the effect of W on SSA estimate.

6.3 We revised the last paragraph on page 21224 (Sect. 1) to more clearly state the focus of this study on W (the magnitude factor in the SSSF), not on the size distribution (the shape factor in the SSSF); the magnitude and shape factors are now clearly introduced in Sect. 1. Specific sizes for specific climate effects are now mentioned in our justification for the chosen size distribution (new Sect. 2.4.2) (see our response to comment 4).

7.1 There are lots of speculations in the paper that are not supported by the facts. For example, the discussion regarding 37GHz vs 10 GHz intercept is not convincing.

7.2 We agree with the Referee that our discussion on this subject could have been presented better. Yes, the interpretation of the y-intercept was speculative at the moment, and we did admit this on page 21231 (lines 21-22). Still, by providing data points globally and over all seasons, the satellite-based W data offer possibilities for new insights. The observation of different W variability for active and decaying whitecaps (approximated by W values at 10 and 37 GHz, respectively) is one example for such new insight.

7.3 We revised the manuscript to introduce the currently accepted interpretation of negative y-intercept (Sect. 2.1). Then in Sect. 3.1.1, we propose broader interpretation of the y-intercept in W(U10) expressions, be it negative or positive. Briefly, we promote the hypothesis that positive y-intercept could be interpreted as a measure of the capacity of seawater with specific characteristics, such as SST (thus viscosity), salinity, and surfactant concentration, to affect the extent of W. These secondary factors do not create whitecaps per se. Rather, they prolong the lifetime of the whitecaps thus contribute to W by altering the characteristics of submerged and surface bubbles such as stabilization and persistence by surfactants or rise velocity variations that replenishing the foam on the surface at different rates. These processes ultimately augment or decrease W and the y-intercept can be thought of as a mathematical expression of this static forcing (as opposed to dynamic forcing from the wind). In this light, our data showing negative y-intercept for W values at 10 GHz is consistent with our and SAL13 analysis that active whitecaps are less affected by secondary factors. However, secondary factors do affect strongly residual whitecaps and the positive y-intercept for our W values at 37 GHz can be interpreted and used to quantify this static influences. This is a hypothesis which is worth promoting for consideration, debate, and further verification by the community.

8.1 The discussion about the "secondary factors" being "imbedded in the exponent of the wind speed dependencies" is misleading. The influence of secondary factors can only be ascertained by the satellite based estimates of W augmented by additional data sets for directional wave spectra, currents (speed and direction), and proxies for surfactants such as ocean color, chlorophyll a, or oceanic primary production. Such studies should be conducted as case studies on regional scales.

8.2 We agree with the Referee that the most rigorous way to fully parameterize the influence of secondary factors on W is to have a large database of W values concomitant with additional variables such as those the Referee has listed. The need for such a database has justified the work of Anguelova and Webster (2006, their Sect. 2 and specifically §16 and §22) on obtaining W from satellite-borne radiometric measurements. Initial version of the database of W and additional variables built by Anguelova et al. (2010, <https://ams.confex.com/ams/pdfpapers/174036.pdf>) and described by SAL13 (their Sect. 3.1) is used in this study.

We respectfully disagree with the Referee's descriptor "misleading." Our approach to parameterize secondary forcing is now extended and clearly presented in new Sect. 2.1. We show the concept that the variability of W caused by secondary factors is expressed as a change of the wind speed exponent is not new. The Monahan and O'Muircheartaigh (1986) analysis of five data sets showed that the variability of W caused by SST (and the atmospheric stability) affect significantly the coefficients in the wind speed dependence $W(U10)$, especially the wind speed exponent. The survey of $W(U10)$ parameterizations by Anguelova and Webster (2006, their Tables 1 and 2) also clearly shows that each campaign conducted in different regions and conditions comes up with a specific wind speed exponent. This strongly suggests that the influence of secondary factors is expressed as a change of the wind speed exponent.

8.3 We extended our regional analysis to develop $W(U10,T)$ parameterizations using empirical (adjusted) and cubic wind exponents. We used significance tests (Student's T-statistics and ANOVA) to establish similarity and differences between $W(U10)$ and $W(U10,T)$ with both empirical and cubic exponents. We found that the $W(U10)$ trend predicted with a quadratic wind speed exponent does not differ significantly from the $W(U10)$ trend predicted either with quadratic or cubic $W(U10, T)$. This result clearly shows that to a large extent, the adjusted wind exponent accounts for the change in the trend caused by SST and other secondary influences. Our new Sect. 3.3.2 shows that explicitly accounting of SST (and eventually other factors) helps to model the spread, not the trend, of the W data.

We describe our approach in Sect. 2.1, the significance test used in Sect. 2.3, and give the results regarding differences between parameterizations that account for variability implicitly or explicitly in Sect. 3.3. Through the text, with each new result presented, we drive the point that the adjustment from cubic to quadratic wind exponent accounts to a large extent for secondary forcing.

9.1 The new parameterization fails to reduce uncertainty in predicting sea-spray aerosol (SSA) flux. To what degree is the uncertainty in SSA flux attributed to uncertainty in predicting W versus other aspects of traditional sea-spray source functions (SSSF)?

9.2 Indeed, we do not report reduced uncertainty in predicting SSA flux. There are many uncertainty sources yielding wide spread of predicted SSA emissions. With our study, we address only one of the uncertainty sources—that associated with the natural variability of the whitecaps.

The Referee's question prompted us to use comparisons between our and Grythe et al. (2014) results for SSA fluxes to examine and quantify variations of SSA emissions attributed to magnitude and/or shape factors.

9.3 New Sect. 3.4 is revised and extended to give our new results.

These results are summarized in the Conclusions as follows:

With or without the SST effect included in the SSSF, SSA emissions obtained with the new $W(U_{10}, T)$ parameterization vary by ~50%. Different approaches to account for SST effect yield ~67% variations. Different models for the size distribution applied to different size ranges lead to 13%-42% variations in SSA emissions.

We conclude Sect. 3.4 with the following:

On the basis of these assessments, we can state that the inclusion of the SST effect in the magnitude factor and/or the choice of the shape factor (size range and model for the size distribution) in the SSSF can explain 13%-67% of the variations in the predictions of SSA emissions. The spread in SSA emission can thus be constrained by more than 100% when improvements of both the magnitude and the shape factor are pursued. Our results on the W parameterization (Fig. 13a) suggest that accounting for more secondary forcing in the magnitude factor would explain more fully the spread among SSA emissions. Because, after wind speed, the most important secondary factor that accounts for variability in W is the wave field (SAL13), efforts to include wave parameters in W parameterizations are well justified.

10.1 Figures appear to have been generated with different software packages.

10.2 Yes, indeed. We have used Python, IDL, and Excel. Respectfully, we do not see this as a problem in presenting our results and drawing conclusions.

10.3 No changes were made regarding comment 10.

Specific Comments

Page 21221; Line 1: Awkwardly worded first sentence which fails to highlight the importance of reducing uncertainty of SSA flux.

Agreed. We removed it. The importance of reducing the uncertainty of the SSA flux is mentioned on page 21223 lines 24-25 and page 21224 lines 1-14.

Page 21223; Line 15: Acronym SSA used prior to defining SSA. SSA acronym is defined on Page 5, Line 24.

Now fixed, acronym SSA introduced on first use of “sea spray aerosols” in the Introduction.

Page 21224; Line 11: Neither evidence nor citation is made to support this statement. Suggest this as an explanation versus declaring as fact.

Yes, this was our explanation. The extensive investigation of Salisbury et al. (2013) on the W variability using year-long satellite-based W data was cited in Line 12 as a basis for this explanation. With the extensive revisions of the manuscript, this statement now is lost.

Page 21225; Line 23: Continue to use whitecap fraction instead of “ W ”. Authors flip back and forth (e.g. Page 7; Line 24) on notation. Please use W to represent whitecap fraction after defining whitecap fraction as W .

Yes, we use both “ W ” and “whitecap fraction” depending on the context. Following the Referee’s comment, the specific example and other cases have been changed from “whitecap fraction” to “ W ”

Page 2138; Line 27: Please reword.

This text is removed.

Abstract

1 Introduction

2 Methods

2.1 Approach to derive whitecap fraction parameterization

2.2 Data sets

2.2.1 Whitecap database

2.2.2 Regional data sets

2.2.3 Independent data source

2.3 Implementation

2.4 Estimation of sea spray aerosol emissions

2.4.1 Use of discrete whitecap method

2.4.2 Choice of size distribution

3 Results and Discussion

3.1 Parameterization from global data set

3.1.1 Wind speed dependence

3.1.2 Intrinsic correlation

3.2 Regional and seasonal analyses

3.2.1 Magnitude of regional and seasonal variations

3.2.2 Quantifying SST variations

3.3 New parameterization of whitecap fraction

3.3.1 Comparisons to W parameterizations

3.3.2 Comparisons to W data

3.4 Sea spray aerosol production

4 Conclusions

Data availability

Acknowledgements

References

Table 1

Figure captions

Anonymous referee #2

General impression: The paper is presenting an extensive effort of data treatment, but the results and conclusions are rather limited. The authors need to better articulate conceptual aspects of the methods used, some of which I found misinterpreted. Overall, the paper has its potential and may become publishable, but needs additional work.

We thank the Referee for the thorough review of the manuscript and the constructive comments, which contributed to the improvement of this manuscript.

In response, the manuscript is substantially revised with the following:

- 1) Updated analysis of global W data to develop $W(U_{10})$ parameterization.
- 2) Extended analysis of regional W data to develop $W(U_{10}, T)$ parameterization with SST explicitly included; this was done for both quadratic and cubic wind exponents.
- 3) Analysis for statistical significance (with Student's T -statistics and ANOVA) of new and previous W parameterizations.
- 4) Extended 'Methods' section to justify and clarify approach, data, and implementations.
- 5) Revised and extended 'Results and Discussion' section to clearly describe results and give substantive and quantitative interpretations and conclusions.

The table of contents of the revised manuscript is added after the responses for reference.

Manuscript revisions with track changes are provided in a separate pdf file.

Several comments and questions are similar in all 3 reviews (e.g., uncertainty not reduced, quadratic wind speed exponent, embedded secondary forcing, intercept interpretation). To avoid repetitions, we attempted combining responses to these common points in one file. We found, however, that one-fits-all responses do not always address the reviewers' comments and questions fully. Thus, risking some repetitions, we proceeded with a specific response to each comment.

Responses are presented below in sequence: (1) the original comment from the Referee (in bold italic), there are 8 comments; (2) our response; (3) changes in manuscript.

1.1 The main advantage over other similar W parameterisations is a quadratic form of a new parameterisation. Regardless of the well correlated linear fits of \sqrt{W} there is little justification why it should be quadratic. The resulting good correlation cannot justify it. Perhaps it can be reduced to quadratic form after careful consideration of the uncertainties, but choosing it upfront is a thing of the past when analytical approaches were limited due to computing power.

1.2 We agree with the Referee that we could have given a better justification of the approach that yielded quadratic wind speed exponent. To clarify, we didn't choose the quadratic relationship upfront. It was suggested by: (1) the data (e.g., old Fig. 3), to which we tried to fit different functional forms; and (2) our aim to apply the same approach to W data at both 10 and 37 GHz.

The finding of weaker (quadratic) wind speed dependence here is not a precedent. The first reported $W(U_{10})$ relationship of Blanchard (1963) was quadratic. With careful statistical considerations, Bondur and Sharkov (1982) derived a quadratic $W(U_{10})$ relationship for residual W (strip-like structures, in their terminology). Parameterizations of W in waters with different SST have also resulted in wind speed exponents around 2 (see Table 1 in Anguelova and Webster, 2006). Quadratic wind speed dependence is also consistent with the wind speed exponents of SAL13.

1.3 To address the Referee's concern, we have included justification for using wind speed exponent adjusted by the data in new Sects. 2.1 and 2.3. We also extended the data analysis to include parameterization using cubic wind speed dependence and compare it to the empirical quadratic expression. We report the results in new sects. 3.1.1 and 3.2.2.

2.1 Following the above the progress over the extensively referenced Salisbury et al. papers is poorly documented or highlighted.

2.2 We have stated how this work relates to the work of SAL13 in two places. In Lines 17-19 on page 21242, we state that we see the current work as complimenting the work of SAL13. In Lines 3-7 on page 21243, we point out a difference.

To recap, besides using different analyses (e.g., regional analysis), we also added analysis and quantification of the possible intrinsic correlation in the W data and how this could affect W predictions with the new W(U10) expressions. We also assessed the utility of using the satellite-based W data to estimate SSA production rate.

Yet, we agree with the Referee that we could have distinguished the two studies more clearly.

2.3 As noted at the beginning, we extended our analysis. The results on new W(U10,T) parameterization at both quadratic and cubic wind exponents (revised Sect. 3.2) and the investigation of significant differences (revised Sect. 3.3) add to the results listed above and clearly set this study apart from the analysis done in SAL13.

3.1 The main advantage of the paper might be exploration of regional differences, but the regions of extreme variability in global map (Fig.9) are poorly represented, namely, high latitude S. Atlantic, high latitude N. Pacific, high latitude North Atlantic, S. Indian Ocean. Five out of seven regions were in subtropical 60deg band. Was it due to limited clear skies? If so, that was a significant limitation of the exploratory effort.

3.2 We appreciate that the Referee acknowledges the advantage of performing regional analysis. The comment suggests that we have not presented our reasoning for the choice of the regions well. Here are some clarifications.

The cloudiness doesn't play role in the choice of the regions because radiometric measurements at microwave frequencies, used to obtain W estimates, penetrate most clouds. Radiometric observations at the ocean surface could be limited by very thick clouds (with a lot of liquid water content) and by precipitation. Such cases are flagged in the WindSat algorithm and are not used to obtain W values.

The number of samples was one of the criteria we had when choosing the regions (Line 28 on page 21227 and Line 1 on page 21228). By this criterion, there are fewer samples for latitudes above 60°S or N (see Fig. 3), mostly because WindSat and QuikSCAT have fewer matching points there (Sect. 2.1).

The latitudes between 40°S and 50°S are known as "The Roaring Forties" for the strong westerly winds there. Our region 5 is chosen in these latitudes. And because the conditions in the Southern Ocean are relatively uniform (due to lack of land masses), region 5 represents the Roaring Forties well. The regions at subtropical latitudes are placed within the Trade winds zone. These are persistent easterly winds blowing over different fetches in different oceans with different salinity and surfactants. So regions 2, 3, and 7 are representative of different cases.

Still, to address the Referee's comment, we analyzed W data in more regions.

3.3 Additional regions were chosen (updated Fig. 2); climatology for different conditions is given (new Fig. 3); extended text to justify the region choices is included (new sect. 2.2.2); and results from the extended regional analysis are given (new sect. 3.2).

4.1 The use of a chosen coarse mode SSA tool to prove usefulness of a new W parameterization is quite useless considering that available SS source functions range several orders of magnitude and would likely swamp any variability between different W parameterisations or, certainly, the impacts of secondary factors. That part is redundant in the paper as it adds very little useful knowledge. Fig. 12 is sufficient for the purpose.

4.2 We respectfully disagree with the Referee's comment because, while our modified SSSF predicts SSA production which falls within the range of variability of previously used SSSFs, we consider as an important result the fact that our SSA estimates have quite a different spatial distribution thanks to the satellite-based W data.

We updated our previous comparisons (old sect. 4.3) with additional comparisons between our and Grythe et al. (2014) results for SSA fluxes (new sect. 3.4). This gave us the possibility to examine and quantify variations of SSA emissions attributed to magnitude and/or shape factors of the SSSF.

4.3 The new results are summarized in the Conclusions as follows:

With or without the SST effect included in the SSSF, SSA emissions obtained with the new $W(U_{10}, T)$ parameterization vary by ~50%. Different approaches to account for SST effect yield ~67% variations. Different models for the size distribution applied to different size ranges lead to 13%-42% variations in SSA emissions.

We conclude Sect. 3.4 with the following:

On the basis of these assessments, we can state that the inclusion of the SST effect in the magnitude factor and/or the choice of the shape factor (size range and model for the size distribution) in the SSSF can explain 13%-67% of the variations in the predictions of SSA emissions. The spread in SSA emission can thus be constrained by more than 100% when improvements of both the magnitude and the shape factor are pursued. Our results on the W parameterization (Fig. 13a) suggest that accounting for more secondary forcing in the magnitude factor would explain more fully the spread among SSA emissions. Because, after wind speed, the most important secondary factor that accounts for variability in W is the wave field (SAL13), efforts to include wave parameters in W parameterizations are well justified.

5.1 I disagree with the author's interpretation of the intercepts arising from 10 and 37GHz datasets. Negative intercept of 10GHz dataset is physically meaningful (contrary to what authors say) as it is pointing at onset of white-capping. Contrary to what authors say, positive intercept of 37GHz dataset is meaningless, suggesting white cap at negative wind speed. Reference to residual foam is wrong as residual foam does not produce SSA as it lingers for hours, does not relate to wind speed (no bubble plume can be produced at 2m/s) and, therefore, has nothing in common with actively generated foam by bubble plumes only occurring above 3-4 m/s wind speed. A surfactant related foam while lasting a little longer is forming (and dissipating thereafter within seconds, not hours) at significant wind speeds. While data below 3m/s have little impact on W it should at least be correctly discussed.

5.2 We agree with the Referee that we didn't convey well our interpretation of the y-intercept.

5.3 We revised the manuscript to introduce the currently accepted interpretation of negative y-intercept (Sect. 2.1). Then in Sect. 3.1.1, we propose broader interpretation of the y-intercept in $W(U_{10})$

expressions, be it negative or positive. Briefly, we promote the hypothesis that positive y-intercept could be interpreted as a measure of the capacity of seawater with specific characteristics, such as SST (thus viscosity), salinity, and surfactant concentration, to affect the extent of W. These secondary factors do not create whitecaps per se. Rather, they prolong the lifetime of the whitecaps thus contribute to W by altering the characteristics of submerged and surface bubbles such as stabilization and persistence by surfactants or rise velocity variations that replenishing the foam on the surface at different rates. These processes ultimately augment or decrease W and the y-intercept can be thought of as a mathematical expression of this static forcing (as opposed to dynamic forcing from the wind). In this light, our data showing negative y-intercept for W values at 10 GHz is consistent with our and SAL13 analysis that active whitecaps are less affected by secondary factors. However, secondary factors do affect strongly residual whitecaps and the positive y-intercept for our W values at 37 GHz can be interpreted and used to quantify this static influences. This is a hypothesis which is worth promoting for consideration, debate, and further verification by the community.

6.1 I disagree with the concept of avoiding intrinsic correlation of W and U10 substituting QSCAT wind speed by ECMWF wind. In fairness, W should have been fitted directly to ECMWF data of whatever resolution because a large scatter (regardless of good overall correlation) between two wind speed datasets could have produced discernible differences in W. In conclusion the approach does not allow comparing statistical parameters of W fits.

6.2 Please note that we had done what the Referee suggests should have been done. We did make direct fit between the WindSat W values and the ECMWF wind speed values; it was presented in Fig. 8b. We assessed the differences between U10 from QSCAT and ECMWF; it was presented in Fig. 8a. Also, we did assess how much W values from parameterizations using QSCAT or ECMWF winds differ (Sect. 4.2.1, Lines 13-29 on p. 21240 and Lines 1-14 on p. 21241). The Referee's comment shows that we didn't present these results clearly.

6.3 New Sect. 2.2.3 more clearly describes the independent data set. New sect. 3.1.2 with results for intrinsic correlation is revised for completeness and clarity.

7.1 Another conceptual flaw was speculating over secondary factors influencing W quadratic relationship. The authors should have at least demonstrated that any two arbitrary chosen secondary factors were cancelling each other's influence before drawing any conclusion (or speculation in this case).

7.2 We respectfully disagree that the concept of accounting for secondary factors via change of the wind speed exponent is flawed.

Our approach to parameterize secondary forcing is now extended and clearly presented in new Sect. 2.1. In it, we show the concept that the variability of W caused by secondary factors is expressed as a change of the wind speed exponent is not new. The Monahan and O'Muircheartaigh (1986) analysis of five data sets showed that the variability of W caused by SST (and the atmospheric stability) affect significantly the coefficients in the wind speed dependence $W(U10)$, especially the wind speed exponent. The survey of $W(U10)$ parameterizations by Anguelova and Webster (2006, their Tables 1 and 2) also clearly shows that each campaign conducted in different regions and conditions comes up with a specific wind speed exponent. This strongly suggests that the influence of secondary factors is expressed as a change of the wind speed exponent.

As said in the text (Lines 5-6 on p. 21234), the secondary effects could act in opposite ways. For instance, the low viscosity of cold waters (e.g., in the Southern ocean) acts to decrease the sea surface roughness, this delays the wave growth, leading to less frequency of wave breaking, and thus decreasing W . At the same time, the high productivity of cold waters yields higher surfactant concentrations, which stabilizes the submerged and surface bubbles, so though less often created, the whitecaps in such places persist thus increasing W . The net effect of these two processes could be nominal (i.e., no change), more, or fewer whitecaps. Monahan and O'Muircheartaigh (1986) and Scott (1986, The effect of organic films on water surface motions, in *Oceanic Whitecaps*, edited by E. Monahan and G. Niocaill, pp. 159–166) have presented this physical reasoning, and Anguelova and Webster (2006) have shown that such interplay of the secondary effects may explain the spatial distribution of satellite-based W values.

While we are quite interested in investigating and quantifying the net result of such interplay, it cannot be verified with the database we have. Data for seawater properties (including surfactants, which are difficult to measure), sea surface roughness, bubble lifetime in submerged plumes, and whitecap decay times are necessary for such an investigation. Still, being well aware that such interplay is physically probable, we used it to explain the small variations between $W(U10)$ expressions derived for different regions. We, therefore, do not see this as a flaw of our approach, but more as a realization that there is much more to do to understand the natural whitecap variability and that the W database is only a start in this direction.

7.3 Because with our extended analysis we now clearly show that the effect of a secondary factor, such as SST, on W trend can be accounted for to a large extent by change of the wind speed exponent, we do not use the idea of the opposite action of the secondary factors.

Note that with our extended regional analysis, we have develop $W(U10,T)$ parameterization using both empirical (adjusted quadratic) and cubic wind exponents. We used significance tests (Student's T-statistics and ANOVA) to establish similarity and differences between $W(U10)$ and $W(U10,T)$ with both empirical and cubic exponents. We found that the $W(U10)$ trend predicted with a quadratic wind speed exponent does not differ significantly from the $W(U10)$ trend predicted either with quadratic or cubic $W(U10, T)$. This result clearly shows that to a large extent, the adjusted wind exponent accounts for the change in the trend caused by SST and other secondary influences. Our new sect. 3.3.2 shows that explicitly accounting of SST (and eventually other factors) helps to model the spread, not the trend, of the W data.

The changes in the manuscript to address this comment include: Description of the approach in Sect. 2.1, the significance test used in Sect. 2.3, and give the results regarding differences between parameterizations that account for variability implicitly or explicitly in Sect. 3.3. Through the text, with each new result presented, we drive the point that the adjustment from cubic to quadratic wind exponent accounts to a large extent for secondary influences on the trend of W with $U10$.

8.1 I have additional comment regarding leveling of W relationship at very high wind speeds. While increasing wind energy is favoring more of air entrainment and consequently larger foams the wind is also blowing directly into the foam disrupting it in the process. Such process has not been quantified yet, but is obvious in even the simplest table top experiment.

8.2 Fully agree with the Referee's comment—the leveling of W (and air-sea interaction processes associated with W) at high winds, while observed is not yet well understood and quantified. While appreciative of the comment, we decided to not speculate on the leveling off in the revised manuscript because we have a lot of new material.

The referee's suggestion, if we understand it correctly—that disruption of whitecap foam moving against the wind could explain the leveling of (at least partially)—is an interesting one and,

frankly, new to us. Perhaps this is akin to spume droplets, just relates to the spume (synonymous of froth and foam) itself, not to the droplets formed from the spume. In any case, this is an idea which should be promoted by the Referee.

Abstract

1 Introduction

2 Methods

2.1 Approach to derive whitecap fraction parameterization

2.2 Data sets

2.2.1 Whitecap database

2.2.2 Regional data sets

2.2.3 Independent data source

2.3 Implementation

2.4 Estimation of sea spray aerosol emissions

2.4.1 Use of discrete whitecap method

2.4.2 Choice of size distribution

3 Results and Discussion

3.1 Parameterization from global data set

3.1.1 Wind speed dependence

3.1.2 Intrinsic correlation

3.2 Regional and seasonal analyses

3.2.1 Magnitude of regional and seasonal variations

3.2.2 Quantifying SST variations

3.3 New parameterization of whitecap fraction

3.3.1 Comparisons to W parameterizations

3.3.2 Comparisons to W data

3.4 Sea spray aerosol production

4 Conclusions

Data availability

Acknowledgements

References

Table 1

Figure captions

Interactive comment by Ian Brooks and Dominic Salisbury:

We thank our colleagues Ian Brooks and Dominic Salisbury for the thorough review of the manuscript and the constructive comments, which contributed to the improvement of this manuscript.

In response, the manuscript is substantially revised with the following:

- 1) Updated analysis of global W data to develop $W(U_{10})$ parameterization.
- 2) Extended analysis of regional W data to develop $W(U_{10}, T)$ parameterization with SST explicitly included; this was done for both quadratic and cubic wind exponents.
- 3) Analysis for statistical significance (with Student's T -statistics and ANOVA) of new and previous W parameterizations.
- 4) Extended 'Methods' section to justify and clarify approach, data, and implementations.
- 5) Revised and extended 'Results and Discussion' section to clearly describe results and give substantive and quantitative interpretations and conclusions.

The table of contents of the revised manuscript is added after the responses for reference.

Manuscript revisions with track changes are provided in a separate pdf file.

Several comments and questions are similar in all 3 reviews (e.g., uncertainty not reduced, quadratic wind speed exponent, embedded secondary forcing, intercept interpretation). To avoid repetitions, we attempted combining responses to these common points in one file. We found, however, that one-fits-all responses do not always address the reviewers' comments and questions fully. Thus, risking some repetitions, we proceeded with a specific response to each comment.

Responses are presented below. The original comments are in bold italic; we enumerated those (23 comments) for easy reference.

General comments:

1. This paper aims to improve the accuracy of sea spray source function defined via the whitecap method – where the source flux is defined as the product of whitecap fraction, W , and the aerosol produced per unit area whitecap over the lifetime of the whitecap. It aims to improve the accuracy of this approach by reducing the uncertainty in the parameterization of W “by better accounting for its natural variability”. We feel it fails to demonstrate such a reduction in uncertainty.

We acknowledge that as formulated, our objective was not met. We revised Sect. 1 to introduce magnitude and shape factors comprising the SSSF and how uncertainties from each factor contribute to the uncertainty of the SSSF. This allows us to clearly define our objective as “a study investigating the second of these two routes, namely—how using W values carrying information for secondary factors would influence the SSA production flux.”

We use comparisons between our and Grythe et al. (2014) results for SSA fluxes to examine and quantify variations of SSA emissions attributed to magnitude and/or shape factors. The results are in new Sect. 3.4. These results are summarized in the Conclusions as follows: With or without the SST effect included in the SSSF, SSA emissions obtained with the new $W(U_{10}, T)$ parameterization vary by ~50%. Different approaches to account for SST effect yield ~67% variations. Different models for the size distribution applied to different size ranges lead to 13%-42% variations in SSA emissions.

We conclude Sect. 3.4 with the following:

On the basis of these assessments, we can state that the inclusion of the SST effect in the magnitude factor and/or the choice of the shape factor (size range and model for the size distribution) in the SSSF can explain 13%-67% of the variations in the predictions of SSA emissions. The spread in SSA emission can thus be constrained by more than 100% when improvements of both the magnitude and the shape factor are pursued. Our results on the W parameterization (Fig. 13a) suggest that accounting for more secondary forcing in the magnitude factor would explain more fully the spread among SSA emissions. Because, after wind speed, the most important secondary factor that accounts for variability in W is the wave field (SAL13), efforts to include wave parameters in W parameterizations are well justified.

2. While the paper focuses on the issue of parameterizing W , it is worth noting that this is not the only source of uncertainty in the parameterization of the sea spray source function by this method; there is also uncertainty in the aerosol produced per unit area whitecap – this is inherently assumed here to be a constant, but is almost certainly not. A study on which one of the co-authors here is also a coauthor (Norris et al. (2013)) has demonstrated that the aerosol flux per unit area whitecap varies with the wind/wave conditions.

We fully agree with Brooks and Salisbury comment and are well aware of the limitation of the whitecap method, specifically its basic assumptions. We included new Sect. 2.4.1 to more fully discuss the uncertainties coming from the whitecap method. However, the whitecap method (in the form of Monahan et al., 1986, or M86) has been widely used in many models for SSA flux (e.g., Table 3 in Textor et al., 2006). Therefore, to those who have worked with M86 until now, a meaningful way to demonstrate how the new satellite-based W data and new parameterizations $W(U10)$ or $W(U10,T)$ based on them would affect estimates of SSA flux is to hold constant the shape factor and clearly show differences caused solely by the use of the new expressions.

3. Much of the material in the paper is very similar to that presented in Salisbury et al. (2013, 2014 –both widely cite throughout). The authors could use this to their advantage by removing repeated background material, most notably in section 2.

We mentioned this fact in Line 25 on p. 21225 and consciously proceeded to “briefly” describe the W database (as said in Line 1 on p. 21226). The comment here suggests that we should shorten Sects. 2.1 and 2.2 even more. We agree: Sects. 2.1 and 2.2 (72 lines) have been combined and revised to a shorter new Sect. 2.2.1 (41 lines).

4. The recent paper by Paget et al, (2015) needs to be considered too given that it uses the same data set and one of its main focuses is parameterisation of satellite W . In particular, Paget et al. address the use of equivalent neutral winds in the satellite W database. Here, the inherent difference between QuikSCAT winds and ECMWF winds is an important point, and warrants more than a passing comment (section 4.2.1).

Paget et al. (2015) didn't derive $W(U10)$ parameterization from the satellite-based W data. Paget et al. investigated and quantified variations of W values when different wind speed sources are employed to derive $W(U10)$ parameterizations. Paget et al. did that by coupling in situ W data with in situ (thus stability-dependent) and satellite (thus stability-corrected) wind speed values, then analyzing how the coefficients in $W(U10)$ expressions change. The satellite-based W database was

used to assess differences between $W(U10)$ expressions obtained from in situ W and different wind sources.

In contrast, we used both satellite-based W data and $U10$ from the W database to derive $W(U10)$ expression. For the revised manuscript, we extended our regional analysis to derive also $W(U10,T)$ parameterization. In the revised manuscript, we cite Paget et al. (2015) in Sect. 2.2.3 regarding stability effects on $U10$ data sources.

Use of independent wind speed:

5. A novel aspect of the paper, and a key difference from the Salisbury et al. studies, is the aim to assess the impact of intrinsic correlation between W and the QuikSCAT-derived U_{10} values used in the Salisbury et al papers, because the same U_{10} data is used in part of the W retrieval. However, the approach adopted fails to properly address the issue.

To avoid the potential self-correlation of W and $U_{QuikSCAT}$ the simple approach would be to fit W to the independent measure of U_{10} . Here the ECMWF model values, U_{ECMWF} , are adopted; however, instead of this, the authors fit W to $U_{QuikSCAT}$ (eqn 7), then fit U_{ECMWF} to $U_{QuikSCAT}$ (eqn 8), rearrange (8) and substitute U_{ECMWF} for $U_{QuikSCAT}$ in (7) to give (9). There are multiple problems here, both conceptual, and in implementation.

We plot U_{ECMWF} vs. $U_{QuikSCAT}$ to assess how the $U10$ values from the two sources differ. We find this necessary as we comment that it is not easy to find truly independent $U10$ data (Lines 27-28 on p. 21229). The small difference of 5% between U_{ECMWF} and $U_{QuikSCAT}$ prove this point to some extent. The fit between the U_{ECMWF} and $U_{QuikSCAT}$ (made over approximately 700 000 data points) is useful because a reader might have either QSCAT or ECMWF data and this fit offers an easy and reliable conversion between the two wind speed sources.

Implementation issues:

6. 1) A potentially minor issue, but in fitting U_{ECMWF} to $U_{QuikSCAT}$ the authors adopt a fit forced through zero, rather than an unconstrained fit. No justification is given for doing so.

We did not need to give a justification because we did both unconstrained and zero-forced fits of $U_{QuikSCAT}$ to U_{ECMWF} . Both were shown in (old) Fig. 8a with dashed and solid lines, respectively. It is seen in the figure that the two fits are very close (almost overlap) with corr. coef. almost identical. The comment suggests that the closeness of the two fits should be clearly pointed out in order to be noticed. We do that in the new Sect. 2.2.3 and in the figure caption (new Fig. 4).

7. 2) When substituting U_{ECMWF} for $U_{QuikSCAT}$ in (7), the authors completely neglect the scaling coefficient with the result that (9) is identically equal to (7) – the authors even note this themselves, and that it is a result of rounding the coefficients, and that the error introduced is up to 10%! There is no justification for doing this. In effect the authors are using the parameterization of W in terms of $U_{QuikSCAT}$, and claiming it is in terms of an independent U_{ECMWF} .

We acknowledge that this was not the best way to pursue the $W(U10)$ parameterization. Updated and extended analysis of the data now provides $W(U10)$ on a global scale and $W(U10,T)$ derived from the regional analysis. New Sect. 2.3 describes the implementation of the parameterizations. New Sect. 3.1.1 present the updated $W(U10)$ expression. New Sect. 3.2 shows the derivation of $W(U10,T)$. Revised Sect. 3.3 compares both $W(U10)$ and $W(U10,T)$ to parameterized W values and to W data.

8. As an aside, equation (8) essentially states “ $ax=y$ implies $x = y/a$ ” – this is so trivial that it really shouldn’t need stating.

We agree. We revised Eq. (8) (new Eq. (7)).

Conceptual issues:

9. A serious problem here is that even if the substitution of U_{ECMWF} for $U_{QuickSCAT}$ was correctly done (no rounding of coefficients), this approach would not give an estimate of W unbiased by any inherent correlation with $U_{QuickSCAT}$, it would simply scale the value of $W^{0.5}$ by the coefficient relating U_{ECMWF} and $U_{QuickSCAT}$. In order to achieve what the authors claim to do, W must be fitted to U_{ECMWF} directly. Note that there is considerable scatter between U_{ECMWF} and $U_{QuickSCAT}$, thus any given estimate of W is likely to be paired with a different value of U_{ECMWF} than $U_{QuickSCAT}$ and the functional form of the fit may be different.

This point essentially invalidates one of the stated aims/conclusions of the paper.

The comment suggests that we did not convey clearly what we have done. So, to clarify:

We made time-space matchups between the WindSat W data and wind speed from ECMWF. For each $W-U_{QuickSCAT}$ pair from the original W database, we have a corresponding $W-U_{ECMWF}$ pair of data. These data are used to make the scatter plots in (old) Fig. 8.

We did make direct fit between the \sqrt{W} values and the ECMWF wind speed values (it was shown in Fig. 8b) and used it to obtain $W(U_{10ECMWF})$. We thus have direct $W(U_{10})$ parameterizations for the two wind speed sources.

To address the comment, we revised the text to more clearly present the formation of “independent” data set (new Sect.2.2.3) and the results (new Sect. 3.1.2).

Functional form of $W(U_{10})$ parameterization

10. When fitting W as a function of U_{10} , the authors adopt an assumed quadratic relationship. No justification is given for this assumption, and it is largely unsupported by previous studies. As the authors themselves noted, Salisbury et al. (2013) found different power laws for W_{10} and W_{37} ($U^{2.26}$ and $U^{1.59}$) respectively for the same data set used here.

We agree that we could have given a better justification of the approach that yielded quadratic wind speed exponent. See below.

11. Cubic or quadratic forms have been forced in previous studies based on theoretical arguments. But these arguments are based on idealised conditions such as a wind input – wave dissipation energy balance. If anything, secondary factors could be expected to lead to a deviation from a strict quadratic or cubic dependence on U_{10} alone.

We have the same understanding on this and fully agree with this statement.

The presentation of our approach to parameterize secondary forcing is now extended and clarified in new Sect. 2.1. In it, we show that previous experience strongly suggests that the influence of secondary factors is expressed as a change of the wind speed exponent. This has guided our analysis. We didn’t choose the quadratic relationship upfront. It was suggested by: (1) the data (e.g., old Fig. 3), to which we tried to fit different functional forms (including cubic); and (2) our aim to apply the same approach to W data at both 10 and 37 GHz. So the quadratic wind speed exponent is, in fact, the adjustment which we expect from whatever idealized wind speed dependence there is (we usually assume cubic) to that dictated by the satellite-based W data. And, in accord with the previous experience mentioned above, this adjustment does represent some implicit account of secondary influences.

The finding of weaker (quadratic) wind speed dependence here is not a precedent. The first reported $W(U_{10})$ relationship of Blanchard (1963) was quadratic. With careful statistical considerations, Bondur and Sharkov (1982) derived a quadratic $W(U_{10})$ relationship for residual W (strip-like structures, in their terminology). Parameterizations of W in waters with different SST have also resulted in wind speed exponents around 2 (see Table 1 in Anguelova and Webster, 2006). Quadratic wind speed dependence is also consistent with the wind speed exponents of Salisbury et al. (2013).

To address this comment, we included justification for using wind speed exponent adjusted by the data in new Sects. 2.1 and 2.3. We also extended the data analysis to include parameterization using cubic wind speed dependence and compare it to the empirical quadratic expression. We report the results in new sects. 3.1.1 and 3.2.2.

12. In general making an a priori assumption about the exponent in such relationships is likely to lead to biases over at least part of the wind speed range. Here it is evident from figure 4 and figure 5(a,b) that the adopted function does not fit the data at either very low or very high wind speeds. There is no reason why the exponent should be an integer value, and it seems likely that many of the results and conclusions in this paper (e.g. Section 3.1.2) are a direct result of this unjustified choice.

Quadratic $W(U_{10})$ fits well W data for wind speeds from 3 m/s (whitecap inception) to 20 m/s (chosen to minimize uncertainty of satellite-based W data at higher winds). In the updated analysis all fits are done for this range (new Fig. 8).

The quadratic wind exponent represents well the weaker wind speed dependence of the satellite-based W data. We show this in new Fig. 13a described in new Sect. 3.3.2. This confirms that the quadratic wind exponent is the deviation we expect due to secondary factors. We have checked with Student's T-statistics and ANOVA tests that indeed quadric $W(U_{10})$ parameterization is not statistically different from the SAL13 $W(U_{10})$ parameterizations with more specific wind exponents.

13. The authors state (p21232, line 5) that “The $\sqrt{W(U_{10})}$ values at 10GHz for wind speeds below 3 m s⁻¹ were discarded in the analysis because, as shown in Fig. 4, the linear relationship breaks up at about this wind speed” – the fact that a portion of the data doesn’t fit a functional form that has been chosen without justification is not a good reason for discarding it. This is tantamount to cherry picking data that fits a pre-conceived idea. The fact that the data doesn’t follow the chosen function is evidence that the function is not appropriate.

Yes, we state this in Line 5 p. 21232. And we continue in the next sentence to state that either discarding or taking into account these data points, does not significantly influence the position of the linear fit.

Discarding W data for wind speeds below 3 m s⁻¹ is something we all usually do because we all recognize that this is the wind speed threshold for whitecap formation in most conditions (of course, the threshold wind speed vary). Moreover, in Line 10 on p. 21243, we give justice to SAL13 that they more carefully evaluated the W data to be used in their study by discarding those with large std. deviations. Coincidentally, most of these discarded W data were for wind speed below 3 m s⁻¹.

More generally, it is well known that W data, whether in situ or satellite-based, have the largest uncertainty at both low and high winds. Following faithfully their trends at these wind speed regimes is not always productive. We thus introduce the range of wind speed from 3 to 20 m/s used for all fits (new Sect. 2.3). So there is no cherry picking of the data here to fit pre-conceived idea, rather we follow a reasonable and well established practice of quality control of W data.

Regional W distributions

14. The analysis of $W(U_{10})$ functions by geographical region is a potentially interesting and useful approach. Both this study and Salisbury et al. (2013, 2014) note the significant difference between global maps of W parameterized from this data set and by Monahan and O’Muircheartaigh (1980). The prime reason for that difference is that the Monahan and O’Muircheartaigh (1980) study used tropical data only, and thus represented a specific wind/wave/water-temperature regime, and further with a maximum wind speed of order 17 m s^{-1} , much lower than common high wind speeds at high latitudes. Monahan has emphasised that this is a regionally specific function, but its widespread adoption in models means it commonly gets applied globally, and at wind speeds well above its range of validity.

We fully agree with this statement. We state similar understanding in Lines 9-12 on p. 21242. The revised manuscript has this information too—in Sect. 1 and the end of Sect. 3.3.2.

15. The different functions obtained here for different regions should similarly represent different wind/wave regimes, and the influence of other environmental factors such as sea surface temperature (SST), surfactant concentrations, etc. This point is touched on, but then the various functions are simply averaged to give a single ‘globally applicable’ function. In fact, as is demonstrated by the differing regional functions, this single function is not truly globally applicable at all – although the bias in any given region may be modest, it will be a mean bias, not random variability, and hence potentially significant in terms of global budgets.

We agree. With the extended significance analysis, we found that the slopes and intercepts of the regional νW to U_{10} fits are statistically significant; the seasonal variations are not. New Sect. 3.2.1 presents these results; we illustrate the results with Fig. 8 (old Fig. 5) and two additional new figures.

16. The analysis and discussion of the regional/seasonal relationships seems superficial, and perhaps misleading. The authors suggest that the smaller variability in fits with month of year in region 5 vs that between all the different regions for the month of march implies “extreme yet sporadic seasonal values of the major forcing factor such as U_{10} at a given location contribute less to the W variations than varying environmental conditions from different locations” – but the comparison is of dissimilar effects. The regional differences result from differences in mean conditions (wind/wave regime, SST, surfactant concentrations,...), whereas ‘extreme yet sporadic’ events will by their nature affect only a small fraction of the data points. Further, region 5 is not necessarily representative of other areas; figure 6 indicates that region 4 (North Atlantic) has a much larger seasonal cycle than other regions, while region 6 (tropical) has very little seasonal cycle. The statements cited above thus draw rather general conclusions from a small, and not necessarily representative, subset of the data.

The “extreme yet sporadic” text is now removed. Analysis is now extended for 12 regions in order to cover the full range of global oceanic conditions and represent diverse regional conditions. New Sect. 2.2.2, updated Fig. 2, and additional Fig. 3 describe the regional W data sets.

17. The analysis of regional/seasonal variations presented in figures 6 and 7 seems a curious approach.

Only the intercepts of the linear fits of νW_{37} to U_{10} are examined – these are effectively the mean offsets in νW_{37} between regions & month of year, the value of νW_{37} at $U_{10} = 0$. As noted above, the fits do not represent the data well at low wind speeds, the intercepts thus greatly overestimate W at $U_{10} = 0$ – theoretically W should be zero here.

The justification given for examining the intercept only is that the intercepts show more variability than the gradients (according to the values given the standard deviation of the gradients is ~3%

and that of the intercepts about 20%). We would question the validity of this. Note that when the linear fits of \sqrt{W} are expanded to give W , the gradient scales U^2 while the intercept affects the mean offset and U . As an example we reproduce figure 5f below, with the two fits with extreme gradients highlighted in black and green. For reference the black line is copied as a dotted line with its intercept adjusted to match that of the green line, allowing the relative influence of intercept and gradient to be assessed – clearly they have a similar overall impact.

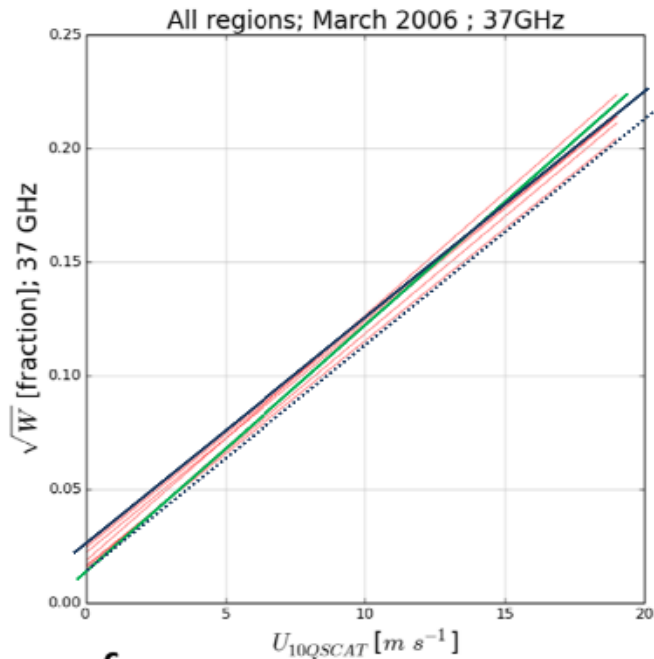
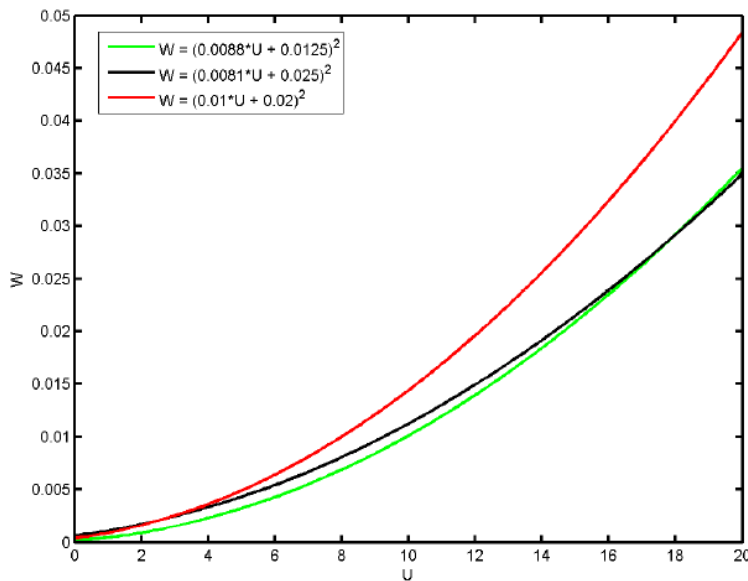


Figure 5f, Green line gradient = 0.0088, black line gradient = 0.0081, a difference of approximately 8%.

We agree that the initial regional analysis was incomplete. The new analysis is on both slopes and intercepts, for both 10 and 37 GHz, applied to all 12 regions for all months with both the adjusted quadratic and the physical cubic relationships. New Sect. 2.3 describes the implementation of the analysis. New Sect. 3.2.2 gives results for quantifying the SST effect. Parameterization $W(U_{10}, T)$ is developed as a quadratic (or cubic) wind speed dependence $W(U_{10})$ whose coefficients vary with SST; this is justified in new Sect. 2.1.

18. It is easier to see the true impact if we plot W instead of \sqrt{W} .



The black and green curves are as in figure 5f above, the difference in gradient more than compensates for the difference in intercepts. More dramatic is the comparison with the red line- the 'global' function given as eqn 7: $vW = 0.01U_{10} + 0.02$. It is clear here that this 'global' function is far from representative of some of the individual regions for specific seasons.

These equations are now updated (new Eqs. (11-12)). The two new parameterizations, $W(U10)$ from the global data set and the $W(U10,T)$ from the regional analysis, are much closer, almost overlapping. Student's T-statistics and ANOVA tests show them to be statistically not different. Note that this is so for the trend of W with $U10$ shown in figures like the one above. The new $W(U10)$ and $W(U10,T)$ parameterizations give statistically different results when used with real $U10$ and T data because $W(U10,T)$ is capable to model the spread of the W data while $W(U10)$ only the trend.

19. In their discussion of the variations in gradients the authors give a rather vague description of why they believe the gradients vary little between regions, suggesting first that the use of a quadratic fit somehow accounts for the influence of secondary environmental forcing factors, which is clearly not possible, then suggesting that maybe multiple environmental factors cancel each other out, which is plausible but pure speculation without any evidence provided. In the discussion of the intercepts of the fits the authors then contradict the earlier claims by suggesting that the gradient accounts for the wind-speed dependence and the other environmental factors are accounted for by the intercept. Again, it is plausible that environmental factors such as SST or surfactant concentration would affect the mean offset in W_{37} but no evidence is presented to support the claim here.

Though the action of secondary factors in opposite directions, and thus cancelling out effects, is viable (Monahan and O'Muircheartaigh, 1986; Scott, 1986, The effect of organic films on water surface motions, in Oceanic Whitecaps, edited by E. Monahan and G. Niocaill, pp. 159–166), we do not use this idea anymore because we cannot show this with our data.

As said above (comments 11 and 12), the quadratic wind exponent is the adjusted (empirical) wind exponent dictated by the satellite-based W data, so it represents a deviation from physical cubic due to secondary factors. We now prove that quadratic $W(U10,T)$ replicates the satellite-based data well, while cubic $W(U10,T)$ cannot. We present extensive discussion on this with two new figs. 12 and 13 in new sects. 3.3.1 and 3.3.2.

As for the intercept, we revised the manuscript to introduce the currently accepted interpretation of negative y-intercept (Sect. 2.1). Then in Sect. 3.1.1, we propose broader interpretation of the y-intercept in $W(U10)$ expressions, be it negative or positive. Briefly, we promote the hypothesis that positive y-intercept could be interpreted as a measure of the capacity of seawater with specific characteristics, such as SST (thus viscosity), salinity, and surfactant concentration, to affect the extent of W . These secondary factors do not create whitecaps per se. Rather, they prolong the lifetime of the whitecaps thus contribute to W by altering the characteristics of submerged and surface bubbles such as stabilization and persistence by surfactants or rise velocity variations that replenishing the foam on the surface at different rates. These processes ultimately augment or decrease W and the y-intercept can be thought of as a mathematical expression of this static forcing (as opposed to dynamic forcing from the wind). In this light, our data showing negative y-intercept for W values at 10 GHz is consistent with our and SAL13 analysis that active whitecaps are less affected by secondary factors. However, secondary factors do affect strongly residual whitecaps and the positive y-intercept for our W values at 37 GHz can be interpreted and used to quantify this static influences. This is a hypothesis which is worth promoting for consideration, debate, and further verification by the community.

20. A relationship with SST is claimed from figure 7, where time series of the intercepts of monthly mean fits of \sqrt{W}_{37} to U_{10} are plotted by region, along with similar time series of monthly mean SSTs. The authors claim an inverse relationship between the intercept and SST. This is (we presume) inferred by the progression of increasing SST from regions 5 \rightarrow 4 \rightarrow 6 and the corresponding decrease in intercept between the same regions (in a mean sense, there are individual points that do not follow the trend). However, this assumes all the differences between regions are a result of SST, and does not allow for the co-variation of, for example, SST and biology, and hence surfactant concentration, or of SST with latitude and hence wind/wave regime. Also, it is hard to determine anything but the most general relationship from a plot of overlaid time series. If you want to determine the relationship between the intercepts and SST, plot a scatterplot of intercept (y axis) against SST (x axis) and look for a functional relationship.

We now plot the slopes and intercepts of the $W(U10)$ relationships in all regions and for all months as a function of SST (new Fig. 11). From these plots we derive expressions for the SST variations of the coefficients in the $W(U10)$ dependence. The figure shows the inverse relationship between the intercept and SST.

Agree, we cannot account for the interplay between the secondary factors in different regions with the data we use in this study. However, with new Fig. 13a (in new Sect. 3.3.2) we show that including SST in the W parameterization explains only part of the spread/variability of the satellite-based W data. This suggests that besides SST, other secondary factors have to be included explicitly to fully replicate the variability of the satellite-based W data.

Aerosol Flux

21. The whitecap method for parameterization of the sea spray source flux is built upon the premise that W can be used as a scaling factor. That is, for a given shape function (the size-resolved interfacial flux from a unit area whitecap), any change in the production flux is linearly related to the change in W . Though it has been noted that this premise is likely to be incorrect (Norris et al. 2013), given the need for relatively simple parameterisations of SSA production rates in global climate and aerosol models, the community is not yet at the stage where the whitecap method can be developed to reflect this fact.

Therefore in presenting new globally-averaged estimates (or global maps) of SSA emission rates calculated via the whitecap method (in its current form), little new information is gained.

We respectfully disagree with this comment because we consider as an important result the fact that our SSA estimates have quite a different spatial distribution thanks to the satellite-based W data. To demonstrate these differences, the widely used whitecap-based SSSF in this form is a useful baseline for comparison; we justify this in new Sect. 2.4.1 (see also comment 2). Also, with our and previous results, we were able to examine and quantify the variations of SSA emissions attributed to magnitude and/or shape factors in the whitecap-based SSSF (see comment 1).

22. *One could argue that it is worthwhile comparing the resulting new estimates of globally-averaged SSA production rates with those of previous studies, but often these estimates simply lie somewhere within the large spread of previous estimates, and no further illuminating conclusions can be deduced.*

That SSA emission inferred by our new parameterization is within the range of previous estimates of SSA emissions shows that our modified SSSF gives consistent estimates. Certainly, we do not want to be an outlier among SSA emission estimates, especially knowing their large spread. Again, what is more important is that the spatial distribution of this total SSA emission is significantly different from those of previous SSSF predictions. And, again, our estimates of the total SSA emission proved useful to evaluate variations due to magnitude and/or shape factors in the SSSF (see earlier comments 1, 2, and 21).

23. *All the new and novel information is contained within the new W estimates and their spatial variation (Figure 9). Figure 10, therefore, adds little to the paper, especially when followed by the difference map [Figure 11]. We suggest that maps of the difference (bias) between W from the new parameterisation and those obtained from a previous parameterisation are more easily interpretable.*

Salisbury et al. (2014) show global maps of the new satellite-based W data. Old Figs. 9 and 10 showed global maps from W parameterizations, not W data. In our view, it is informative for the readers to see global maps of W and SSA with the absolute values obtained with the new $W(U10)$ parameterization.

Still, we agree that difference maps for W and SSA with reference values from MOM80 and M86, respectively, is a more informative and focused way to demonstrate differences. So Fig. 9 (new Fig. 13b) is revised to show difference between W from MOM80 and W from our quadratic $W(U10,T)$. Old Figs. 10 and 11 are combined in a new Figure 14 with top panel showing SSA from the M86 SSSF using our quadratic $W(U10,T)$, and lower panel showing difference map with M86 SSSF using MOM80 $W(U10)$.

References

- Norris, S. J., I. M. Brooks, B. I. Moat, M. J. Yelland, G. de Leeuw, R. W. Pascal, B. J. Brooks, 2013: Near-surface measurements of sea spray aerosol production over whitecaps in the open ocean. *Ocean Science*, 9, 133–145, doi: 10.5194/os-9-133-2013
- Paget, A. C., M. A. Bourassa, and M. D. Anguelova (2015), Comparing in situ and satellite-based parameterizations of oceanic whitecaps, *J. Geophys. Res. Oceans*, 120, 2826–2843, doi:10.1002/2014JC010328

Abstract

1 Introduction

2 Methods

2.1 Approach to derive whitecap fraction parameterization

2.2 Data sets

2.2.1 Whitecap database

2.2.2 Regional data sets

2.2.3 Independent data source

2.3 Implementation

2.4 Estimation of sea spray aerosol emissions

2.4.1 Use of discrete whitecap method

2.4.2 Choice of size distribution

3 Results and Discussion

3.1 Parameterization from global data set

3.1.1 Wind speed dependence

3.1.2 Intrinsic correlation

3.2 Regional and seasonal analyses

3.2.1 Magnitude of regional and seasonal variations

3.2.2 Quantifying SST variations

3.3 New parameterization of whitecap fraction

3.3.1 Comparisons to W parameterizations

3.3.2 Comparisons to W data

3.4 Sea spray aerosol production

4 Conclusions

Data availability

Acknowledgements

References

Table 1

Figure captions

Parameterization of oceanic whitecap fraction based on satellite observations

M. F. M. A. Albert¹, M. D. Anguelova², A. M. M. Manders¹, M. Schaap¹, and G. de Leeuw^{1,3,4}

[1]{TNO, P.O. Box 80015, 3508 TA Utrecht, The Netherlands}

[2]{Remote Sensing Division, Naval Research Laboratory, Washington, DC 20375}

[3]{Climate Research Unit, Finnish Meteorological Institute, Helsinki, Finland}

[4]{Department of Physics, University of Helsinki, Helsinki, Finland}

Correspondence to: M. F. M. A. Albert (monique.albert@tno.nl)

Abstract

In this study the utility of satellite-based whitecap fraction (W) values for the prediction of sea spray aerosol (SSA) emission rates is explored. More specifically, the study is aimed at evaluating how an account for natural variability of whitecaps in the W parameterization would affect SSA mass flux predictions when using a sea spray source function (SSSF) based on the discrete whitecap method. The starting point is a data set containing W data for 2006, together with matching wind speed U_{10} , sea surface temperature (SST) T_s and statistical data. Whitecap fraction W was estimated from observations of the ocean surface brightness temperature T_B by satellite-borne radiometers at two frequencies (10 and 37 GHz). A global scale assessment of the data set revealed a quadratic correlation between W and U_{10} . A new global $W(U_{10})$ parameterization was developed and used to evaluate an intrinsic correlation between W and U_{10} that could have been introduced while estimating W from T_B . A regional scale analysis over different seasons indicated significant differences of the coefficients of regional $W(U_{10})$ relationships. The effect of SST on W is explicitly accounted for in a new $W(U_{10}, T)$ parameterization. The analysis of W values obtained with the new $W(U_{10})$ and $W(U_{10}, T)$ parameterizations indicates that the influence of secondary factors on W is for the largest part embedded in the exponent of the wind speed dependence. In addition, the $W(U_{10},$

- Deleted: improving the accuracy of the
- Deleted: derived by using
- Deleted: through the reduction of the uncertainties in the parameterization of W by better accounting for its natural variability
- Deleted: ,
- Deleted: environmental
- Deleted: , for 2006
- Deleted: to evaluate the wind speed dependence of W
- Deleted: , as well as a relatively larger spread in the 37 GHz data set
- Moved (insertion) [17]
- Deleted: A
- Deleted: was determined, evaluated and presumed to lie within the error margins of the newly derived $W(U_{10})$ -parameterization
- Deleted: The latter could be attributed to secondary factors affecting W in addition to U_{10} . To better visualize these secondary factors, a
- Deleted: assessment
- Deleted: was performed. This assessment
- Deleted: s
- Deleted: i

T) parameterization is capable to partially model the spread (or variability) of the satellite-based W data. The satellite-based parameterization $W(U_{10}, T)$ was applied in an SSSF to estimate the global SSA emission rate. The thus obtained SSA production rate for 2006 of $4.4 \times 10^{12} \text{ kg yr}^{-1}$ is within previously reported estimates, however with distinctly different spatial distribution.

1 Introduction

Whitecaps are the surface phenomenon of bubbles near the ocean surface. They form at wind speeds of around 3 m s^{-1} and higher, when waves break and entrain air in the water which subsequently breaks up into bubbles which rise to the surface (Thorpe, 1982; Monahan and Ó'Muircheartaigh, 1986). The estimated global average of whitecap cover, i.e., the fraction of the ocean surface covered with whitecaps W , is 2 to 5% (Blanchard, 1963). Being visibly distinguishable from the rough sea surface, whitecaps are the most direct way to parameterize the enhancement of many air-sea exchange processes including gas- and heat transfer (Andreas, 1992; Fairall et al., 1994; Woolf, 1997; Wanninkhof et al., 2009), wave energy dissipation (Melville, 1996; Hanson and Phillips, 1999), and the production rate of sea spray aerosols (SSA) (e.g., Blanchard, 1963; 1983; Monahan et al., 1983; O'Dowd and de Leeuw, 2007; de Leeuw et al., 2011), because all these processes involve wave breaking and bubbles.

Measurements of the whitecap fraction W are usually extracted from photographs and video images collected from ships, towers, and air planes (Monahan, 1971; Asher and Wanninkhof, 1998; Callaghan and White, 2009; Kleiss and Melville, 2011). Whitecap fraction is commonly parameterized in terms of wind speed at a reference height of 10 m, U_{10} . Wind speed is the primary driving force for the formation and variability of W (Monahan and Ó'Muircheartaigh, 1986; Salisbury et al., 2013, hereafter SAL13). Whitecap fractions predicted with conventional $W(U_{10})$ parameterizations show a large spread between reported W values (Lewis and Schwartz, 2004; Anguelova and Webster, 2006). Part of these variations is due to differences in methods of extracting W from still and video images. Indeed, the spread of W values has decreased in recently published in situ data sets as image processing improved and data volume increased (de Leeuw et al., 2011). However, an order-of-magnitude scatter of W values remains, suggesting that U_{10} alone cannot fully predict the W variability. Other factors such as atmospheric stability (often expressed in terms of air-sea

Moved up [17]: An intrinsic correlation between W and U_{10} that could have been introduced while estimating W from T_B was determined, evaluated and presumed to lie within the error margins of the newly derived $W(U_{10})$ -parameterization.

Deleted: Hence no further improvement can be expected by looking at effects of other factors on the variation in W explicitly. From the regional analysis, a new globally applicable quadratic $W(U_{10})$ parameterization was derived.

Deleted: compared to parameterizations from other studies and was

Deleted: 1

Deleted: While recent studies that account for parameters other than U_{10} explicitly could be suitable to improve predictions of SSA emissions, we promote our new $W(U_{10})$ parameterization as an alternative approach that implicitly accounts for these different parameters and helps to improve SSA emission estimates equally well.

Deleted: There are many reasons why it is important to study whitecaps, not the least because they are still surrounded by significant uncertainties (de Leeuw et al., 2011).

Deleted: ; Thorpe, 1982

Deleted: SSA

Deleted: particles

Deleted: in situ

1 | temperature difference), sea surface temperature (SST) T or friction velocity (combining wind
2 | speed and thermal stability (e.g., Wu, 1988; Stramska and Petelski, 2003)) have been
3 | indicated to affect W with implications for the SSA production. Thus, parameterizations of W
4 | that use different, or include additional (secondary), forcing parameters to better account for
5 | W variability have been sought (Monahan and Ó'Muircheartaigh, 1986; Zhao and Toba, 2001;
6 | Goddijn-Murphy et al., 2011; Norris et al., 2013b; Ovadnevaite et al., 2014; Savelyev et al.,
7 | 2014).

Deleted: whitecap fraction

Moved (insertion) [18]

Deleted: (

Deleted:)

Deleted: and

Deleted: (

Deleted:)

8 | An alternative approach to address the variability of W is to use whitecap fraction
9 | estimates from satellite-based observations of the sea state, because such observations provide
10 | long-term global data sets which encompass a wide range of meteorological and
11 | environmental conditions, as opposed to local measurement campaigns during which a limited
12 | variation of conditions is usually encountered. Brightness temperature T_B of the ocean surface
13 | measured from satellite-based radiometers at microwave frequencies has been successfully
14 | used to retrieve geophysical variables, including wind speed (Wentz, 1997; Bettenhausen et
15 | al., 2006; Meissner and Wentz, 2012). The feasibility of estimating W from T_B has also been
16 | demonstrated (Wentz, 1983; Pandey and Kakar, 1982; Anguelova and Webster, 2006).
17 | Anguelova et al. (2006; 2009) used WindSat data (Gaiser et al., 2004) to further develop the
18 | method of estimating W from T_B , and compiled a database of satellite-based W accompanied
19 | with additional variables. Figure 1a shows an example of the global W distribution from
20 | WindSat for a randomly chosen day.

Deleted: whitecap fraction

Moved (insertion) [9]

21 | Salisbury et al. (2013) showed that satellite-based W values carry a wealth of
22 | information on the variability of W . In particular, these authors showed that the global
23 | distribution of satellite-based W values differs from that obtained using a conventional $W(U_{10})$
24 | parameterization with important implications for modeling SSA production rate in global
25 | climate models (GCMs) and chemical transport models (CTMs) (Salisbury et al., 2014).
26 | Salisbury et al. (2013) proposed a new $W(U_{10})$ parameterization in power law form using
27 | satellite-based W data over the entire globe for a full year. They derived wind speed
28 | exponents which are approximately quadratic for different data sets:

Deleted: emissions

Deleted: estimates

Deleted: and linear

$$\begin{aligned}
 29 \quad W_{10} &= 4.6 \times 10^{-3} \times U_{10}^{2.26}; & 2 < U_{10} \leq 20 \text{ m s}^{-1}, \\
 30 \quad W_{37} &= 3.97 \times 10^{-2} \times U_{10}^{1.59}; & 2 < U_{10} \leq 20 \text{ m s}^{-1},
 \end{aligned}
 \tag{1}$$

1 where W is expressed in % and the subscripts denote the T_B frequencies used to obtain W .

2 These exponents are significantly different from the cubic and higher wind speed

3 dependences proposed by **Callaghan et al. (2008, hereafter CAL08)**:

4 $W = 3.18 \times 10^{-3} (U_{10} - 3.70)^3; \quad 3.70 < U_{10} \leq 11.25 \text{ m s}^{-1}$

5 $W = 4.82 \times 10^{-4} (U_{10} + 1.98)^3; \quad 9.25 < U_{10} \leq 23.09 \text{ m s}^{-1}$

6 and Monahan and O'Muircheartaigh (1980, hereafter MOM80):

7 $W(U_{10}) = 3.84 \times 10^{-4} U_{10}^{3.41}$

8 The MOM80 parameterization was derived on the basis of the data sets of Monahan (1971)
9 and Toba and Chaen (1973). Most of the wind speed values from these two data sets are up to
10 12 m s^{-1} with only 10% of the data points for winds up to 19 m s^{-1} . The range of SST is from
11 17 to 31°C . Monahan and O'Muircheartaigh (1986) emphasized that this is a regionally
12 specific function, but its widespread adoption in global models led to its application at wind
13 speeds and SSTs well above its range of validity.

14 In this study we explore the utility of the satellite-based W data from a standpoint of
15 predicting SSA production rate. Whitecaps are used as a proxy for the amount of bubbles at
16 the ocean surface. When these bubbles burst, they generate sea spray droplets which in turn
17 transform to SSA when they equilibrate with the surroundings (Blanchard, 1983). Bursting
18 bubbles produce film and jet droplets, whereas at high wind speeds, exceeding about 9 m s^{-1} ,
19 additional sea spray is directly produced as droplets which are blown off the wave crests
20 (Monahan et al., 1983). These spume droplets are larger than the bubble-mediated SSA
21 droplets (Andreas, 1992). In this study we will focus on bubble-mediated production of sea
22 spray.

23 Sea spray aerosols are important for the climate system because, due to the vast extent
24 of the ocean, SSA are amongst the largest aerosol sources globally (de Leeuw et al., 2011).
25 SSA particles contribute to the scattering of short-wave electromagnetic radiation and thus the
26 direct radiative effect on climate. Also, having high hygroscopicity, SSA particles are a
27 source for the formation of cloud condensation nuclei (Ghan et al., 1998; O'Dowd et al.,
28 1999) and as such influence cloud microphysical properties and thus exert indirect radiative
29 effects on the climate system. While residing in the atmosphere, SSA provide surface and
30 volume for a range of multiphase and heterogeneous chemical processes (Andreae and

Deleted: Monahan and O'Muircheartaigh (1980, hereafter MOM80):
 $W(U_{10}) = 3.84 \times 10^{-4} U_{10}^{3.41}$
(2)
and Callaghan et al. (2008):

Deleted: 3

Field Code Changed

Deleted: The reason for such differences is that Eqs. (2) and (3) were developed from data taken on a regional scale with U_{10} measured locally, while the data used by Salisbury et al. (2013) for Eq. (1) implicitly account for the influence of secondary factors on a global scale.

Deleted: values

Deleted: emission rates of

Deleted: aerosol

Deleted: (SSA)

Deleted: and

Deleted: provide a major

Deleted: ion

Deleted: (de Leeuw et al., 2011)

Deleted: H

Deleted: O'Dowd et al., 1999;

Moved down [19]: Sea spray aerosol particles mainly consist of sea salt and, in biologically active regions, of organic matter in the submicron size range (O'Dowd et al., 2004; Facchini et al., 2008; Partanen et al., 2014).

Crutzen, 1997). Through such chemical processes, the SSA contribute to the production of inorganic reactive halogens (Cicerone, 1981; Graedel and Keene, 1996; Keene et al., 1999; Saiz-Lopez and von Glasow, 2012), participate in the production or destruction of surface ozone (Keene et al., 1990; Barrie et al., 1988; Koop et al., 2000), and provide a sink in the sulfur atmospheric cycle (Chameides and Stelson, 1992; Luria and Sievering, 1991; Sievering et al., 1992; 1995).

The modeling of all these processes in GCMs and CTMs starts with calculation of the production rate of SSA particles (termed also SSA production flux, SSA generation, or SSA emission). Sea spray source function (SSSF) is used to calculate SSA production flux—the number of SSA particles produced per unit of sea surface area per unit time. The most commonly used SSSF, proposed by Monahan et al. (1986, hereafter M86), estimates SSA emission by the indirect, bubble-mediated mechanism. Based on the discrete whitecap method, the SSSF of M86 is formulated in terms of $W(U_{10})$, as defined by MOM80 (Eq. (3)), whitecap decay timescale τ , and the aerosol productivity per unit whitecap dE/dr :

$$\frac{dF}{dr_{80}} = \frac{W(U_{10})}{\tau} \frac{dE}{dr_{80}} = 1.373 \cdot U_{10}^{3.41} \cdot r_{80}^{-3} (1 + 0.057 r_{80}^{1.05}) \times 10^{1.19e^{-B^2}}, \quad (4)$$

In Eq. (4), the timescale is a constant $\tau = 3.53$ s, r_{80} is the droplet radius at a relative humidity of 80%, and the exponent B is defined as $B = (0.38 - \lg r_{80})/0.65$. The term dE/dr , associated with the sea spray size distribution, determines the shape of the SSSF (i.e., shape factor); the term W/τ is a scaling (or magnitude) factor as it links predetermined SSA production per unit whitecap area with the amount of whitecapping in different regions at different seasons. Refer to Lewis and Schwartz (2004), de Leeuw et al. (2011), and Callaghan (2013) for clear distinction of the discrete whitecap method from the continuous whitecap method.

Estimates of SSA production fluxes using the discrete whitecap method still vary widely (Lewis and Schwartz, 2004; de Leeuw et al., 2011) precluding reliable estimates of the direct and indirect effects by SSA in GCMs, as well as the outcome of heterogeneous chemical reactions taking place in and on SSA particles in CTMs. The wide spread of predicted SSA emissions is caused by a combination of uncertainties coming from both the magnitude and the shape factors of the used SSSFs. The uncertainties associated with the magnitude factor include difficulties of measuring W and τ and their natural variability, which affects the $W(U_{10})$ parameterizations. The assumptions of the discrete whitecap method

Deleted: thus

Deleted: ing

Deleted: ;

Deleted:

Deleted: ing

Deleted: ;

Deleted: ing

Deleted: emission rate of SSA particles, i. e.,

Deleted: the number of SSA particles produced per unit of sea surface area per unit time, needed in climate models and chemical transport models, is described by a

Deleted: s

Deleted: (

Deleted: ,

Deleted: (referred

Deleted: as

Deleted:)

Deleted: that

Deleted: generation

Deleted: s

Deleted: the whitecap fraction

Deleted: in

Deleted: and the production of

Deleted: SSA

Formatted: English (United States)

Deleted: .

Deleted: with

(detailed in Sect. 2.4) also contribute to the uncertainty. Added to these are the uncertainties associated with the shape factor, such as its natural variability and the model chosen to parameterize the SSA size distribution. A source of uncertainty is the difficulty of directly measuring SSA fluxes which are used to develop and/or constrain SSSFs. When measurements of SSA concentrations are used to develop an SSSF, uncertainty comes from the deposition velocity model used to convert the concentrations to fluxes (e.g., Smith et al., 1993; Savelyev et al., 2014).

Aside from addressing uncertainties due to measuring techniques, there are two possible ways to improve the performance of a whitecap-based SSSF as regards the physical processes involved. One way is to address variations and uncertainties in the size-resolved productivity dE/dr_{80} (i.e., the shape factor in the SSSF), for instance by including the organic matter contribution to SSA at sub-micron sizes (O'Dowd et al., 2004; Albert et al., 2012) and/or by accounting for its variations with environmental factors instead of keeping it constant for all conditions (de Leeuw et al., 2011; Norris et al., 2013a; Savelyev et al., 2014). Another way is to address the variations and uncertainties in the whitecap fraction W (i.e., the magnitude factor in the SSSF) by steady improvements of the W measurements and by accounting for its natural variability. Both approaches are expected to reduce, or at least to better account for, the variations and uncertainties in parameterizing SSA flux.

Here we report on a study investigating the second of these two routes, namely—how using W data, which carry information for secondary factors, would influence the SSA production flux. The objective is to assess how much of the uncertainty in the SSA flux can be explained with the natural variability of W . Our approach (Sect. 2) involves three steps. We first assess the satellite-based whitecap database to evaluate the wind speed dependence of W over as wide a range of U_{10} values as possible (sect. 3.1.1). In assessing the W database, we also evaluate the impact of an intrinsic correlation between W and U_{10} , which could have been introduced in the process of estimating W from T_B (SAL13) (Sect. 3.1.2). We next apply the established wind speed dependence to W on regional scales in order to gain insights into the influence of secondary factors in different locations during different seasons (Sect. 3.2). In this second step, we use the results of our regional analysis to derive a new W parameterization that incorporates the effect of sea surface temperature (SST) T on W . The new $W(U_{10}, T)$ parameterization is compared to those of MOM80, CAL08, and SAL13 (Sect.

- Deleted:** P
- Deleted:** method
- Deleted:** are
- Deleted:** : (i)
- Deleted:** to reduce the uncertainties in
- Deleted:** production flux dF
- Deleted:** , and (ii)
- Deleted:** to reduce the uncertainties in the parameterization of
- Deleted:** to better
- Deleted:** aiming at improving
- Deleted:** The study presented here is on three somewhat distinct yet interweaved topics, namely: (i) assessment of satellite-based W data; (ii) parameterization of W ; and (iii) application of the new W parameterization to predict SSA production. ¶
- Deleted:** thus
- Deleted:** , and our results (Sect. 3) and discussion (Sect. 4) each address these three interlaced topics. Specifically,
- Deleted:** w
- Deleted:** start with an
- Deleted:** ment
- Deleted:** of
- Deleted:** W
- Deleted:** on a global scale
- Deleted:** the whitecap fraction
- Deleted:** alisbury et al., 20
- Deleted:** Stepping on this assessment,
- Deleted:** w
- Deleted:** consider variations of
- Deleted:** whitecap fraction
- Deleted:** e
- Deleted:** , globally applicable
- Deleted:** (U_{10})
- Deleted:** a correction for the possible intrinsic correlation between
- Deleted:** and U_{10} .
- Moved (insertion) [6]**
- Deleted:** n
- Deleted:** of
- Deleted:** allaghan et al. (20
- Deleted:**)
- Deleted:** Salisbury et al. (2013)

3.3). The utility of the new $W(U_{10}, T)$ parameterization is evaluated by using it to estimate SSA emissions and comparing to previous predictions of SSA emissions (Sect. 3.4).

2 Methods

2.1 Approach to derive whitecap fraction parameterization

Reasoning on a series of questions shaped our approach to parameterizing W and justified the choices we made for its implementation (Sect. 2.3). We first considered, Why do we need to parameterize W instead of using satellite-based W data directly? A major benefit of using satellite-based W data directly in an SSSF is that these data reflect the amount and persistence of whitecaps as they are formed by both primary and secondary forcing factors acting at a given location. This approach limits the uncertainty to that of estimating W from satellite measurements and does not add uncertainty from deriving an expression for $W(U_{10})$ or $W(U_{10}, T, \text{etc.})$. However, such an approach would limit global predictions of SSA emissions to monthly values because a satellite-based W data set does not provide daily global coverage; i.e., one would need data like that in Fig. 1a for at least two weeks (and more for good estimates of the uncertainties) in order to have full coverage of the globe.

Alternatively, a parameterization of whitecap fraction derived from satellite-based W data can provide daily estimates of SSA emissions using readily available daily data of wind speed and other variables. Importantly, such a parameterization will be globally applicable because the whitecap fraction data cover the full range of meteorological conditions encountered over most of the world oceans. Because the availability of a large number of W data would ensure low error in the derivations of the $W(U_{10})$ or $W(U_{10}, T, \text{etc.})$ expressions, we proceed with deriving a parameterization for W using the data in the whitecap database (Sect. 2.2.1).

The next question to consider was, How to account for the influence of secondary factors? Generally, to fully account for the variability of whitecap fraction, a parameterization of W would involve wind speed and many additional forcings explicitly to derive an expression $W(U_{10}, T, \text{etc.})$ (MOM80; Monahan and Ó'Muircheartaigh, 1986; Anguelova and Webster, 2006). The SAL13 analysis showed substantial variations of W as a function of different variables, including SST. Because SST and wind speed are readily available variables, it would be useful to start with parameterization $W(U_{10}, T)$.

Deleted: 4.2

Deleted: Finally, t

Deleted: t. The results of this study are

Deleted: ed

Deleted:

Deleted: the $W(U_{10})$ parameterization of MOM80, Callaghan et al. (2008), Salisbury et al. (2013) as well as to available in situ W data (Sect. 4.2), and

Moved up [6]: $W(U_{10})$ parameterization of MOM80, Callaghan et al. (2008), Salisbury et al. (2013) as well as to available in situ W data (Sect. 4.2)

Deleted: ¶ reasoning and inga A new parameterization for the whitecap fraction is derived using satellite data which are described in Sect. 2.1. The data sets used, the approach to derive the new parameterization, and the method estimating SSA emission are described in Sect.(s) 2.2-2.4.

Formatted: Indent: First line: 0"

Moved (insertion) [4]

Deleted: The assessment of the satellite-based estimates of whitecap fraction (Sect. 3.1) informs our decision how to most effectively use these data to improve a whitecap-method based SSSF. The

Deleted: w

Deleted: were,

Deleted: (1)

Deleted: develop a $W(U_{10})$

Deleted: ation

Deleted: ; and (2) How to account for the influence of secondary factors in W parametrization

Deleted: .:

Deleted: explicitly, including them in the parameterization, e.g., $W(U_{10}, \text{SST}, \text{atmospheric stability, etc.})$ or implicitly. These questions are addressed below. ¶

Deleted: statistics

Deleted: wind speed

Deleted: a

Deleted: T

Deleted: the most important

Deleted: , Salisbury et al., 2013

Deleted: , especially those readily available from either observations or meteorological forecasts, such as U_{10} , SST, etc. However, a parameterization requiring the use of many variables is not conduct(...

Deleted: .

Deleted: , along with

Deleted: ,

Deleted: is

Deleted: b

The question that arises next is, How to combine the different dependences of W ? One possibility is to use a single-variable regression to extract the W dependence on each variable separately, e.g., $W(U_{10})$ and $W(T)$. Then, these can be combined to derive an expression for their effects in concert, e.g., $W(U_{10}, T) = W(U_{10})W(T)$. While variables like T , atmospheric stability, surfactants, etc. influence W , they do not cause whitecapping. So a parameterization formulated with dedicated $W(T)$ and other expressions may put undue weight on such influences. This approach can be pursued when we have enough information to judge the relative importance of each influence (e.g., Anguelova et al., 2010, their Fig. 6) and include it in a combined expression with a respective weighting factor.

Previous experience points to another possibility to combine causal variables like U_{10} and influential variables like T and the likes. The Monahan and O’Muircheartaigh (1986) analysis of five data sets showed that the variability of W caused by SST (and the atmospheric stability) affect significantly the coefficients in the wind speed dependence $W(U_{10})$, especially the wind speed exponent. The survey of $W(U_{10})$ parameterizations by Anguelova and Webster (2006, their Tables 1 and 2) also clearly shows that each campaign conducted in different regions and conditions comes up with a specific wind speed exponent. This strongly suggests that the influence of secondary factors is expressed as a change of the wind speed exponent. On the basis of their principal component analysis, ~~SAL13~~ also suggested that in describing the W variability, it is more effective to combine individual variables with wind speed. On this ground, we proceed to obtain $W(U_{10}, T)$ as a wind speed dependence $W(U_{10})$ whose regression (or parametric) coefficients vary with SST. This goal can be realized by first identifying a general wind speed dependence to use as a reference, then quantifying the variations of its regression coefficients in different regions and seasons.

The important question now is, What functional form should we use for the general (reference) $W(U_{10})$ dependence? Equations (1)-(3) exemplify the functional forms usually employed to express $W(U_{10})$:

$$W = aU_{10}^n \quad (5a)$$

$$W = a(U_{10} + b)^3 \quad (5b).$$

Deleted: Salisbury et al. (2013)

Field Code Changed

Field Code Changed

A general $W(U_{10})$ dependence derived using Eq. (5a) would provide an empirical wind speed exponent n determined from available data sets, as MOM80 did using the available data sets at the time (Sect. 1). The wider the range of conditions represented by the data sets is, the closer the resulting $W(U_{10})$ dependence would be to average conditions globally and seasonally.

A general $W(U_{10})$ dependence derived using Eq. (5b) would provide a physically-based wind speed exponent $n = 3$ consistent with dimensional (scaling) arguments. Namely, because W is related to the rate at which the wind supplies energy to the sea, W should be proportional to the cube of the friction velocity u_* (Monahan and O’Muircheartaigh, 1986; Wu, 1988). On this basis, Monahan and Lu (1990) related $W^{1/3}$ to U_{10} and derived the cubic power law in Eq. (5b). Subsequently, this relationship was used successfully in whitecap data analyses (e.g., Asher and Wanninkhof, 1998; CAL08). Coefficient b in Eq. (5b) is included because it is preferable for a $W(U_{10})$ relationship to involve a finite y -intercept (Monahan and O’Muircheartaigh, 1986). A negative y -intercept determines b from an x -intercept and is usually interpreted as the threshold wind speed for whitecap inception.

A modified version of Eq. (5) combines the merits of both formulations into the form:

$$W = a(U_{10} + b)^n \quad (6)$$

where the wind speed exponent is adjustable and a finite y -intercept is included. A general $W(U_{10})$ dependence derived using Eq. (6) would provide a wind speed exponent as dictated by the whitecap database that is applicable to all satellite-based W data. Being representative of globally averaged conditions, this general $W(U_{10})$ dependence can be applied with the same n to different regional scales and seasonal timeframes affording quantification of its variations with SST via coefficients a and b . Any of the three formulations (Eqs. (5 and 6)) can produce a viable general $W(U_{10})$ dependence, the empirical one representative of the average conditions of the world oceans and the physical one supported by sound reasoning.

Deleted: It has been argued that

Moved (insertion) [10]

Deleted: should be proportional to the

Deleted: flux supplied by wind which

Deleted: is

Deleted: resulting in a cubic $W(u_*)$ and above cubic $W(U_{10})$ parameterizations (Wu, 1988)

Deleted: .

Field Code Changed

2.2 Data sets

To implement the approach thus formulated, we use the whitecap database on a global scale for the general $W(U_{10})$ dependence, and regional W subsets extracted from the whitecap database for the SST analysis. In describing the data sets used, we start with the whitecap database (Sect. 2.2.1). The considerations given to extract regional data sets from it are described in Sect. 2.2.2. We also introduce the data from the European Centre for Medium range Weather Forecasting (ECMWF) used in this study as an independent source to investigate possible intrinsic correlation among the entries of the whitecap database (Sect. 2.2.3).

2.2.1 Whitecap database

Anguelova and Webster (2006) describe in detail the general concept of retrieving the whitecap fraction W from measurements of the brightness temperature T_B of the ocean surface with satellite-borne microwave radiometers. Salisbury et al. (2013) describe the basic points of the retrieval algorithm estimating W (hereafter referred to as the $W(T_B)$ algorithm). Briefly, the algorithm obtains W by using measured T_B data for the composite emissivity of the ocean surface and modelled T_B data for the emissivity of the rough sea surface and areas that are covered with foam (Bettenhausen et al., 2006; Anguelova and Gaiser, 2013). Minimization of the differences between the measured and modelled T_B data in the $W(T_B)$ algorithm ensures minimal dependence of the W estimates on model assumptions and input parameters. An atmospheric model is necessary to evaluate the contribution from the atmosphere to T_B .

Wind speed U_{10} is one of the required inputs to the atmospheric, roughness and foam models (Anguelova and Webster, 2006; Salisbury et al., 2013). Wind speed data come from the SeaWinds scatterometer on the QuikSCAT platform or from the Global Data Assimilation System (GDAS), whichever matches up better with the WindSat data in time and space within 25 km and 60 min; hereafter we refer to both QuikSCAT or GDAS wind speed values as U_{10} from QuikSCAT or $U_{10\text{QSCAT}}$. The use of $U_{10\text{QSCAT}}$ in the estimates of satellite-based W is anticipated to lead to some intrinsic correlation when/if a relationship between W and $U_{10\text{QSCAT}}$ is sought.

The W data used in this study are obtained from T_B at 10 and 37 GHz, W_{10} and W_{37} ; data for 37 GHz are shown in Fig. 1a. The W_{10} and W_{37} data approximately represent different stages of the whitecaps because of different sensitivity of microwave frequencies to foam

Deleted: Satellite-based estimates of whitecap fraction

Deleted: by

Deleted: The whitecap fraction estimates used in this study are obtained from the WindSat T_B data.

Deleted: The T_B algorithm has been updated with physics based models for the roughness and foam emissivities (Bettenhausen et al., 2006; Anguelova and Gaiser, 2013) replacing the simple, empirical models used in the initial implementation of Anguelova and Webster (2006).

Deleted: additionally, a

Deleted: is used to provide the atmospheric correction

Deleted: for the retrieval of ocean surface T_B

Deleted: WindSat measurements at the top of the

Deleted: WindSat measures T_B at five microwave frequencies, ranging from 6 to 37 GHz. Because different microwave frequencies probe the ocean surface at different skin depths, they have different sensitivity to the thickness of the foam layer (Anguelova and Gaiser, 2011): with frequency increasing, the sensitivity to thinner foam layers increases. As a result, information on different stages of whitecap evolution can be obtained.

Deleted: I

Deleted: only two frequencies

Deleted: used

Deleted: ,

Deleted: .

thickness (Anguelova and Gaiser, 2011). Data W_{10} are an upper limit for predominantly active wave breaking (stage A whitecaps (Monahan and Woolf, 1989)) partially mixed with decaying (stage B) whitecaps, while W_{37} data quantify both active and decaying whitecaps. Because decaying foam covers a much larger area of the ocean surface than active whitecaps (Monahan and Woolf, 1989), W_{37} data are larger than W_{10} data. Comparisons to historic and contemporary in situ W data in Fig. 1b confirm the approximate representations of stage A whitecaps (cyan squares) and A + B whitecaps (blue diamonds) by W_{10} (green) and W_{37} (magenta), respectively. Anguelova et al. (2009) have quantified the differences between satellite-based and in situ W data using both previously published measurements and time-space match-ups of W and discussed possible reasons for the discrepancies.

The satellite-based W data are gridded into a $0.5^\circ \times 0.5^\circ$ grid cell together with the variables accompanying each W data point, namely $U_{10QSCAT}$, T from GDAS, time (average of the times of all samples falling in each grid cell), and statistical data generated during the gridding including the root-mean-square (rms) error, standard deviation (SD), and count (the number of individual samples in a satellite footprint averaged to obtain the daily mean W for a grid cell). In this study, we used daily match-ups of W , U_{10} , and T data for each grid cell for the year 2006. Due to large data gaps in both space and time, the daily W data cannot be interpolated to provide better coverage (Fig. 1a). Therefore, only the available data are used without filling the gaps for areas where data are lacking. This global data set was used to assess the globally averaged wind speed dependence of W .

2.2.2 Regional data sets

The annual global W distributions show regions with valid data points ranging from 100 to 300 samples per grid cell per year when both ascending and descending satellite passes are considered. There are fewer samples for latitudes beyond $60^\circ S$ or N (see Fig. 1a) because WindSat and QuikSCAT have fewer matching points there (Sect. 2.2.1). Thus, different regions were selected using two criteria, namely (i) consider regions with a high number of valid data points, and (ii) obtain a selection representative of different conditions in the northern and southern hemispheres (NH and SH).

With these criteria, 12 regions of interest were selected (Fig. 2) and W , U_{10} , and T data for each region were extracted from the whitecap database. The coordinates of the selected regions are listed in Table 1, together with the corresponding number of samples and

Deleted: At 10 GHz

Deleted: ,

Deleted: thick foam that is associated with initial,

Deleted: could be observed, while thinner foam layers associated with

Deleted: are detected only partially

Deleted: . Because 37 GHz frequency is more sensitive to thin foam patches,

Deleted: can be observed, resulting in a larger signal at 37 GHz b

Deleted: values

Deleted: is

Deleted: values

Deleted: The $W(T_B)$ algorithm provides W values at satellite resolution of $50 \times 71 \text{ km}^2$. Both ascending and descending passes of the satellite platform are available, thus providing satellite data at a given spot on the Earth surface twice a day, in the morning and in the evening. The W values are gridded into a $0.5^\circ \times 0.5^\circ$ box together with the variables accompanying each W value, namely $U_{10QSCAT}$, SST from GDAS, time (average of the times of all samples falling in each grid cell), and statistical data generated during the gridding including the root-mean-square (rms) error, standard deviation, and count (the number of individual samples in a satellite footprint averaged to obtain the daily mean W for a grid cell). ¶
<#>Data sets ¶

Deleted: satellite-based estimates of whitecap fraction at 10 and 37 GHz are

Deleted: in

Deleted: pairs

Deleted: and

Deleted:

Deleted: values

Deleted: Only W values for horizontal H polarization were considered because W is a surface feature and in radiometric experiments the sensitivity of H polarization to changes in wind, and thus to whitecap formation, was found to be larger than t(...

Moved up [9]: Figure 1 shows an example of ¶ ...

Deleted: The figure shows that the daily data d(...

Deleted: the high variability

Deleted: the

Deleted: and devise a method to analyse region(...

Deleted: either relatively low or relatively high(...

Deleted: ,

Deleted: data points

Deleted: both

Deleted: In this way

Deleted: 7

Deleted: ,

minimum, maximum, mean, and median values for wind speed and SST for January and July. For 90% of the regional and monthly data used in the study, the percent difference (PD, defined as the difference between two values divided by the average of the two values) between mean and median values of U_{10} and T is less than 4% and 9.5%, respectively. With medians and means approximately the same, the U_{10} and T data have normal distributions; i.e., outliers, though existing, do not affect the mean values significantly. All analyses presented here use the mean U_{10} and T values. Figure 3 shows the seasonal cycles of the mean U_{10} and T values for four of the selected 12 regions visualizing the full range of U_{10} and T data (Table 1).

Regions 2-11 are all in the open ocean, region 1 was selected for its landlocked position. Region 6 in the Pacific Doldrums is used as a reference for the lower limit of U_{10} (Fig. 3a), while region 12 is included to represent the lowest T values (Fig. 3b). Four regions (2, 3, 7, and 8) are at latitudes between 0 and 30°S and N (Tropics and Subtropics) representing the Trade winds zone with persistent (Easterly) winds blowing over approximately the same fetches (except region 8) in oceans with different salinity (Tang et al., 2014) and primary production (Falkowski et al., 1998) (a proxy for surfactant concentrations). Region 4 is in the NH temperate zone representing long-fetched Westerly winds. Region 5 covers the latitudes between 40°S and 50°S known as “The Roaring Forties” for the strong Westerly winds there, but is characterized with shorter fetch. Differences in the seasonal cycles of U_{10} and T in regions 4 and 5 (Fig. 3) suggest more uniform conditions and longer fetches in the SH temperate zone. We have chosen regions 8 and 9 to represent different zonal conditions and to gauge the effect of narrower range of SST variations (as compared to the SST range in region 5). Chosen at the same latitude, regions 9-11 have approximately the same SST, salinity, and surfactants but represent different wind fetches, shortest for region 9 and longest for region 11. Overall, the chosen regions cover the full range of global oceanic conditions and are representative of diverse regional conditions.

2.2.3 Independent data source

Ideally, when deriving a $W(U_{10})$ parameterization, the data for W and U_{10} should come from independent sources. The intrinsic correlation between W and U_{10} that might have arisen from the use of U_{10} from QuikSCAT in the estimates of W from T_B (Sect. 2.2.1), might affect the relationship between W and U_{10} developed here. To evaluate the magnitude of such intrinsic

Deleted: range

Deleted: mean

Deleted: Whereas r

Deleted: 7

Deleted: to identify the effect of short fetches

Deleted: Although region 7 has, regarding its size, a relatively low number of W samples compared to regions 1-6, it is included in the list to compensate for the otherwise limited representation of the Northern Atlantic Ocean. The results for this region could also show the degree to which the number of samples affects the information W can give.

Deleted: Following the results of the global data set assessment (Sect. 3.1.1), for each selected region, scatterplots of the square root of W against U_{10} were generated, and the best linear fits were determined. For the seasonal dependencies, scatterplots were generated using all available daily data per month, ranging from 22 to 31 days of data.

Deleted: <#>¶

Following the formulated approach (Sect. 2.1), the assessment of the satellite-based estimates of whitecap fraction (Sect. 3.1) informs our decision how to most effectively use these data to improve a whitecap-method based SSSF. The questions we considered were, (1) Why develop a $W(U_{10})$ parameterization instead of using satellite-based W data directly; and (2) How to account for the influence of secondary factors: explicitly, including them in the parameterization, e.g., $W(U_{10}, SST, \text{atmospheric stability, etc.})$ or implicitly. These questions are addressed below. ¶ A major benefit of using satellite-based W data directly in an SSSF is that these data reflect the amount and persistence of whitecaps as they are formed by both primary and secondary forcing factors acting at a given location. This approach limits the uncertainty to that of estimating W from satellite measurements and does not add uncertainty from deriving an expression for $W(U_{10})$. However, such an approach would limit global predictions of SSA emissions to monthly values because a satellite-based W data set does not provide daily global coverage; i.e., one would need data like that in Fig 1 for at least two weeks (and more for good statistics) in order to have full coverage of the globe. ¶ Alternatively, a parameterization of whitecap fraction derived from satellite-based W data can provide daily estimates of SSA emissions using readily available wind speed daily data. Importantly, such a parameterization will be globally applicable because the whitecap fraction data cover the full range of meteorological conditions encountered over most of the world oceans. The availability of a large number of W data would ensure low error in the derivations of the $W(U_{10})$ expression. ¶ Generally, to fully account for the variability of whitecap fraction, a parameterization of W would (...)

Moved up [4]: The assessment of the satellite-based estimates of whitecap fraction (Sect. 3.1) informs our decision how to most effectively use these data to improve a whitecap-method based SSSF. The questions we considered were, (1) Why develop a $W(U_{10})$ parameterization instead of usin(...)

Deleted: effect

Deleted: this

correlation, we used U_{10} from the ECMWF ($U_{10ECMWF}$), which is considered to be a more independent source; note though that even the ECMWF data are generated by assimilating observational data sets (e.g., from buoys) in a coupled atmosphere-wave model (Goddijn-Murphy et al., 2011).

To compile this “independent” data set, we made time-space matchups between the W_{10} and W_{37} data and $U_{10ECMWF}$. In this way, for each $W-U_{10QSCAT}$ pair from the original W database, we have a corresponding $W-U_{10ECMWF}$ pair of data. To speed up calculations, and because this already provides a statistically significant amount of data, we used only ascending satellite overpasses. Wind speeds above 35 m s^{-1} were discarded. Besides ECMWF wind data, for consistency we also extracted ECMWF SST values.

Figure 4a shows all ECMWF wind speed data that have been matched in time and space with the available $U_{10QSCAT}$ data for March 2006. The majority of the data is clustered in the range of $5\text{-}10 \text{ m s}^{-1}$. To characterize the difference between the two wind speed sources, the correlation between U_{10} from ECMWF and U_{10} from QuikSCAT was determined as the best linear fit forced through zero:

$$U_{10ECMWF} = 0.952U_{10QSCAT} \quad (7)$$

with $R^2 = 0.844$. For comparison, the unconstrained fit between $U_{10QSCAT}$ and $U_{10ECMWF}$ is also shown in Fig. 4a (dashed line); both fits are very close (they almost overlap) with almost identical correlation coefficients ($R^2 = 0.845$ for the unconstrained fit). Similarly, Fig. 4b compares T from ECMWF and GDAS showing almost 1:1 correlation. That is, the two data sources provide almost the same values for T .

On average, U_{10} from ECMWF is about 5% lower than U_{10} from QuikSCAT. This U_{10} difference can be explained to some extent with the effect of atmospheric stability because QuikSCAT provides equivalent neutral wind which accounts for the stability effects on the wind profile (Kara et al., 2008; Paget et al., 2015), while the ECMWF model gives stability dependent wind speeds (Chelton and Freilich, 2005).

Having the correlations between U_{10} and T from the whitecap database and ECMWF quantified, one can evaluate differences caused by the use of different data sources. Equation (7) could also be useful when one decides to use ECMWF data because of their availability at 6 or 3 h intervals as compared to the availability of W , U_{10} , and T match-ups twice a day (Sect. 2.2.1).

- Deleted: $U_{10QSCAT}$ is replaced with
- Formatted: Font: Not Italic
- Deleted: European Centre for Medium range Weather Forecasting (
- Deleted:)
- Formatted: Font: Not Italic
- Moved (insertion) [14]
- Deleted: It is, therefore, preferred to derive a $W(U_{10})$ parameterization that is based on ECMWF wind speed dQuantifying the intrinsic correlation between W and U_{10} from QuikSCAT comes down to quantifying how closely U_{10} from QuikSCAT and U_{10} from ECMWF correlate, for which these two quantities needed to be matched in time and space.
- Deleted: processes
- Deleted: were used in the analysis
- Deleted: to use later in our analysis

- Deleted: An
- Moved (insertion) [11]
- Deleted: e
- Deleted: s
- Deleted: between QuikSCAT and ECMWF

- Deleted: additional advantage of quantifying
- Formatted: Not Highlight
- Deleted: QuikSCAT
- Deleted: U_{10} from
- Deleted: is
- Deleted: of the latter
- Deleted: -
- Deleted: pairs

2.3 Implementation

We aim to develop an expression capable of modeling both the trend of W with U_{10} and the spread of the satellite-based W data (see green and magenta symbols in Fig. 1b). We analyze the global data set of satellite-based W_{10} and W_{37} data and derive a general $W(U_{10})$ expression that represents average wind conditions in different geographical environments (i.e., the trend of W with U_{10}). Following Monahan and Lu (1990), we derive an expression in the form of Eq. (6) by plotting $W^{1/n}$ as a function of $U_{10\text{QSCAT}}$. Applying linear regression, we find an expression:

$$W^{1/n} = mU_{10} + c \quad (8)$$

which is then rearranged and raised to the power n providing coefficients $a = m^n$ and $b = c/m$ in Eq. (6) (results in Sect. 3.1.1). All linear fits are done on the W data points associated with U_{10} from 3 to 20 m s⁻¹. The lower limit of 3 m s⁻¹ is chosen as a threshold for observing whitecaps. This restriction is reasonable in light of the SAL13 analysis in which W data with a relative standard deviation (σ_w/W) > 2 were removed. The discarded W data were about 10% of all W data, mostly in regions with low wind speeds of around 3 m s⁻¹. We exclude the high wind speed regime in order to avoid uncertainty due to (i) fewer data points in this regime; and (ii) anticipated larger uncertainty in the W data from the $W(T_B)$ algorithm. With the wind speed threshold imposed in this way, we propose a broader interpretation of regression coefficient b (sect. 3.1.1).

For the intrinsic correlation analysis, the $W-U_{10\text{ECMWF}}$ data pairs are used in a similar fashion to make $W^{1/n}(U_{10\text{ECMWF}})$ linear fits and derive from them a relationship between the satellite-based W data and the ECMWF wind speeds. The two global $W(U_{10})$ parameterizations for the two wind speed sources are then compared to evaluate the magnitude of the intrinsic correlation (results in Sect. 3.1.2).

Because Eq. (7) gives the possibility to evaluate discrepancies due to the use of different sources for U_{10} and T , we use U_{10} and T from the whitecap database in all subsequent analyses and results. In this way, with the intrinsic correlation characterized, we restrict the uncertainty in our analyses by using the close matching-up of W , U_{10} , and T data in the whitecap database. This decision is reasonable considering that both data sets can be used in practice for different applications. The collocated data in the whitecap database (involving QuikSCAT) are most handy for analysis (as done in this study). Meanwhile, W data from the

Moved up [14]: It is, therefore, preferred to derive a $W(U_{10})$ parameterization that is based on ECMWF wind speed. Quantifying the intrinsic correlation between W and U_{10} from QuikSCAT comes down to quantifying how closely U_{10} from QuikSCAT and U_{10} from ECMWF correlate, for which these two quantities needed to be matched in time and space. To speed up calculation processes, and because this already provides a statistically significant amount of data, only ascending satellite overpasses were used in the analysis. Wind speeds above 35 m s⁻¹ were discarded.

whitecap database combined with forcing data from a global model (such as ECMWF or other) are useful for forecasts and climate simulations.

With n for the general wind speed dependence determined, we then apply Eq. (6) with the same n to the regional monthly sub-sets of W_{10} and W_{37} data. All available data per month were used, ranging from 22 to 31 days of data. Once again, scatter plots of $W^{1/n}(U_{10})$ were generated and the best linear fits were determined providing coefficients m and c for each region for each month for W_{10} and W_{37} . The regional and seasonal variations of coefficients m and c , as well as a and b , are analyzed to judge to what extent these variations warrant parameterization in term of SST $a(T)$ and $b(T)$ (results in Sect. 3.2).

To quantify how $a(T)$ and $b(T)$ are influenced by the functional form of the general wind speed dependence—our empirically determined wind speed exponent n (Eq. (6)) and the physically reasoned cubic wind speed dependence (Eq. (5b))—we also analyzed scatter plots of $W^{1/3}(U_{10})$ and derived a respective set of coefficients $a(T)$ and $b(T)$.

We analyzed the variations of coefficients m and c with the Student's T-statistics and Analysis of variance (ANOVA) tests. The Student test verifies whether two data sets (or sample populations) have significantly different means by confirming or rejecting the null hypothesis (the default statement that there is no difference among data sets). A small significance value (e. g., $p < 0.05$) for any pair of regional m and c data sets would indicate that the regional means of coefficients m and c are significantly different. The ANOVA test essentially does the same but for a group of three or more data sets simultaneously. ANOVA rejects the null hypothesis if two or more populations differ with statistical significance. In this sense, an ANOVA test is less specific than a Student test. Because the ANOVA assumptions (that the data sets are normally distributed and they have approximately equal variances) may not always be true for our data, the ANOVA results were verified with the more general Kruskal-Wallis H test (referred to as H test) which does not have any of these assumptions.

We quantify differences between new and previously published parameterizations with two metrics (results in Sect. 3.3): (i) the PD between W values obtained with different parameterizations; and (ii) significance tests (Student, ANOVA, and H) of the differences between W values obtained with new and previous W parameterizations.

2.4 Estimation of sea spray aerosol emissions

The newly formulated $W(U_{10}, T)$ parameterization is applied to estimate the global annual SSA emission using SSSF of M86 (Eq. (4)). Dividing Eq. (4) by Eq. (3), we modify the M86 SSSF to clearly separate the magnitude and shape factors (re-written here as Eq. (4')):

$$\frac{dF}{dr_{80}} = W(U_{10}, T) \cdot \left[3.5755 \times 10^5 \cdot r_{80}^{-3} (1 + 0.057 r_{80}^{1.05}) \times 10^{1.19e^{-B^2}} \right] \quad (4')$$

with B as defined in Sect. 1 and the timescale τ absorbed in the shape factor (the expression in the brackets). The size range for M86 validity is $r_{80} = 0.8\text{--}8\text{ }\mu\text{m}$. We calculate the SSA flux for radii r_{80} ranging from 1 to 10 μm .

2.4.1 Use of discrete whitecap method

The basic assumptions of M86 for the SSSF based on the discrete whitecap method—constant values for τ and dE/dr (Sect. 1)—are usually questioned (Lewis and Schwartz, 2004; de Leeuw et al., 2011; Savelyev et al., 2014). It is not expected for both of these assumptions to hold for wave breaking at various scales and under different conditions in different locations. The SSSF proposed by Smith et al. (1993) on the basis of measured size-dependent aerosol concentrations is one of the first formulations to demonstrate that the shape factor cannot be constant. Norris et al. (2013a) also demonstrated that the aerosol flux per unit area whitecap varies with the wind and wave conditions.

Recently, Callaghan (2013) showed that the whitecap timescale is another source of often overlooked variability in SSSF parameterizations based on M86. Because W typically includes foam from all stages of whitecap evolution, Callaghan (2013) suggested that the adequate timescale for the aerosol productivity from a discrete whitecap is not just its decay time (as in Eqs. (4) and (4')), but the sum of the whitecap formation and decay timescales τ' . The value of τ' varies from breaking wave to breaking wave, but an area-weighted mean whitecap lifetime can be calculated for any given observational period to account for this natural variability. Analyzing the lifetimes of 552 oceanic whitecaps from a field experiment, Callaghan (2013) found that the area-weighted mean τ' varies by a factor of 2.7 (from 2.2 to 5.9 s). We refer the reader to Callaghan (2013) for an SSSF that accounts for SSA flux variability by explicitly incorporating whitecap timescale τ' .

Deleted: coarse mode

Field Code Changed

Despite these questionable assumptions, the SSSF based on the discrete whitecap method in the form of M86 has been widely used in many models (Textor et al., 2006). Therefore, to those who have worked with M86 until now, a meaningful way to demonstrate how the new satellite-based W data, and W parameterizations based on them, would affect estimates of SSA flux is to hold everything else constant (e.g., the whitecap timescale and productivity in the shape factor) and clearly show differences caused solely by the use of new W expression(s) as a magnitude factor. On these grounds, the choice of the SSSF based on the M86 whitecap method is a suitable baseline for comparisons.

2.4.2 Choice of size distribution

Though the chosen size range of 1–10 μm for SSA particles is limited, it is well justified for the purposes of this study with the following arguments.

Deleted: with sizes r_{90} ranging from 1 to 10 μm .

Generally, the division of the SSA particles into sizes of small, medium, and large modes (de Leeuw et al., 2011, their §8) is well warranted when one considers the climatic effect to be studied (Sect. 1). For example, sub-micron particles are important for scattering by SSA (direct effect) and the formation of cloud condensation nuclei (indirect effect), while super-micron particles are important for heat exchange (via sensible and latent heat fluxes) and heterogeneous chemical reactions (which need surface and volume to proceed effectively). However, in this study we do not focus on how the choice of the size distribution will affect the SSA estimates. Nor do we aim to present estimates of specific forcing of the climate system. Rather, with a fixed size distribution, we explore how parameterizing W data, which carry information for the influences of many factors, would affect estimates of SSA emission (Sect. 1). In this sense, we can choose to use any published size distribution as a shape factor.

The chosen size range is the range of medium (super-micron) mode of SSA particles. This is the range for which the size distribution of M86 is valid (Sect. 2.4). The M86 size distribution, in its original or modified form, is widely used in GCMs and CTMs (Textor et al., 2006, their Table 3). This size range is a recurrent part of the various size ranges used in all (or at least most) SSSFs (see Table 2 in Grythe et al. (2014, hereafter G14)).

The chemical composition of the SSA particles is another argument favoring the chosen size range. The super-micron particles consist, to a good approximation, solely of sea salt, whereas, in biologically active regions, the sub-micron size range additionally includes

Deleted: in the coarse mode

organic material, with an increasing contribution as particle size decreases (O'Dowd et al., 2004, Facchini et al., 2008; Partanen et al., 2014). Since the organic mass fraction in sub-micron SSA particles is still highly uncertain (Albert et al., 2012), we focus on the medium mode SSA emissions.

We evaluate the discrepancy expected due to neglecting particles below 1 μm using the G14 report of SSA production rate for dry particle diameters $D_p = r_{80}$ obtained with M86 over two different size ranges: $4.51 \times 10^{12} \text{ kg yr}^{-1}$ for the size range of $0.8 \mu\text{m} < r_{80} < 8 \mu\text{m}$ and $5.20 \times 10^{12} \text{ kg yr}^{-1}$ for size range of $0.1 \mu\text{m} < r_{80} < 10 \mu\text{m}$. The different size ranges bring a difference between the two G14 estimates of about 14%. Neglecting particles with $r_{80} < 0.1 \mu\text{m}$ would not change significantly the results presented here because they contribute on the order of 1% to the overall mass (Facchini et al., 2008).

Because total whitecap fraction, rather than only the active breaking crests, provides bubble-mediated production of SSA, we use W_{37} data to estimate the emission of medium mode SSA. The calculations use a modeling tool (Albert et al., 2010) in which the $W(U_{10})$ parameterization of MOM80, as integrated in Eq. (4), was replaced with the newly derived $W(U_{10}, T)$ parameterization (Eq. (4')). The resulting size-segregated droplet number emission rate was converted to mass emission rate using the approximation $r_{80} = 2r_d = D_p$, where r_d and D_p are the particle dry radius and diameter, respectively (e.g., Lewis and Schwartz, 2004; de Leeuw et al., 2011), and a density of dry sea salt of 2.165 kg m^{-3} .

3 Results and Discussion

The graphs showing our results visualize the W data points available for wind speeds from 0 to 35 m s^{-1} , but all fits are valid for $3 \leq U_{10} \leq 20 \text{ m s}^{-1}$ (Sect. 2.3).

3.1 Parameterization from global data set

Figure 5 shows global W data estimated from WindSat measurements for March 2006 as function of $U_{10\text{QSCAT}}$, at 10 GHz (Fig. 5a) and 37 GHz (Fig. 5b). For comparison, the MOM80 relationship (Eq. (3)) is also plotted in each panel. There are three noteworthy observations in Fig. 5. First, we note the different variability of W_{10} and W_{37} data. The 10 GHz data show far less variability than those at 37 GHz. The W_{37} data at a certain wind speed vary over a much wider range, with the strongest variability for wind speeds of $10\text{--}20 \text{ m s}^{-1}$. This supports the

Moved (insertion) [19]

Deleted: (Facchini et al., 2008). Sea spray aerosol particles mainly consist of sea salt and, in biologically active regions, of organic matter in the submicron size range

Deleted: sea spray aerosol...SA particles is still...

Moved (insertion) [22]

Deleted: With regard to the size range, note that the contribution of the mass of submicron ...artic...

Moved (insertion) [23]

Deleted:Grythe et al. (2014) report two SSA...

Deleted: As suggested by Salisbury et al. (2014)...

Deleted: Assessment of satellite-based whitecap fraction data

Moved down [1]: Wind speed dependence

Deleted: from global data set

Deleted: 3... shows global W data estimated fr...

1 suggestion that other variables, in addition to U_{10} , influence the whitecap fraction, such as
 2 SST or wave field; SAL13 quantify this variability.

Deleted: sea state
 Deleted: . Salisbury et al. (2013)

3 Another observation in Fig. 5 is noted at low wind speeds. The 10 GHz scatter plot
 4 does not show W data for wind speeds lower than about 2 m s^{-1} because at these low wind
 5 speeds no active breaking occurs (Sect. 1). In contrast, non-zero W_{37} data are retrieved at wind
 6 speeds $U_{10} < 2 \text{ m s}^{-1}$. Salisbury et al. (2013) suggested that the presence of foam on the ocean
 7 surface at these low wind speeds could be due to residual long-lived foam. This residual foam
 8 might be stabilized by surfactants, which increases its lifetime (Garrett, 1967; Callaghan et
 9 al., 2013). Another explanation could be production of bubbles and foam from biological
 10 activity (Medwin, 1977). However, there is not enough information currently to prove any of
 11 these conjectures.

Deleted: values
 Deleted: , as mentioned in the introduction
 Deleted: at 37 GHz
 Deleted: whitecap fraction values

12 The comparison of the MOM80 relationship (Eq. (3)) to W_{10} and W_{37} data clearly
 13 reveals the most important feature in Fig. 5—the wind speed dependence of satellite-based W
 14 data deviates from cubic and cubic-like relationship.

15 3.1.1 Wind speed dependence

Moved (insertion) [1]

16 Following the arguments of our approach (Sect. 2.1) and trying different expressions, we
 17 found that a quadratic wind speed exponent ($n = 2$) fits both W_{10} and W_{37} data sets best. For
 18 the same data shown in Fig. 5, Fig. 6 shows the linear regression of the square root of W
 19 versus U_{10} :

$$20 \quad \sqrt{W} = 0.01U_{10} - 0.011 \quad 10 \text{ GHz} \quad (9a)$$

$$21 \quad \sqrt{W} = 0.01U_{10} + 0.019 \quad 37 \text{ GHz} \quad (9b)$$

Deleted: In
 Deleted: 4
 Deleted: the same data are plotted as in Fig. 3 but instead of the value of W we plot
 Deleted: , to weigh both axes evenly, and fit a linear relationship to the resulting scatterplots
 Deleted: 5
 Deleted: 6

22 with coefficients of correlation R^2 of 0.996 and 0.956, respectively. From Eq. (9), we obtain
 23 the following global average wind speed dependence of W using U_{10} from QuikSCAT:

$$24 \quad W_{10} = 1 \times 10^{-4} (U_{10} - 1.1)^2 \quad (10)$$

$$25 \quad W_{37} = 1 \times 10^{-4} (U_{10} + 1.9)^2 \quad (11)$$

Deleted: The $\sqrt{W(U_{10})}$ values at 10 GHz for wind speeds below $\sim 3 \text{ m s}^{-1}$ were discarded in the analysis because, as shown in Fig. 4, the linear relationship breaks up at about this wind speed. However, either discarding or taking into account these data points, does not significantly influence the position of the linear fit.
 Field Code Changed
 Field Code Changed

26 where W is a fraction (not %).

27 The finding of weaker (quadratic) wind speed dependence here is not a precedent. The
 28 first reported $W(U_{10})$ relationship of Blanchard (1963) was quadratic. With careful statistical

1 considerations, Bondur and Sharkov (1982) derived a quadratic $W(U_{10})$ relationship for
2 residual W (strip-like structures, in their terminology). Parameterizations of W in waters with
3 different SST have also resulted in wind speed exponents around 2 (see Table 1 in Anguelova
4 and Webster, 2006). Quadratic wind speed dependence is also consistent with the wind speed
5 exponents of SAL13 in Eq. (1).

6 The y-intercept for W_{10} (Eq. (10)) is negative and, following the usual interpretation,
7 yields a threshold wind speed of 1.1 m s^{-1} for whitecap inception. This is in the range of
8 previously published values from 0.6 (Reising et al., 2002) to 6.33 (Stramska and Petelski,
9 2003). Meanwhile, the positive y-intercept b for W_{37} (Eq. (11)) is meaningless at first glance
10 and intriguing upon some pondering. While foam from biological sources is possible (Sect.
11 3.1), it is not known whether such mechanism is capable of providing a measurable amount of
12 foam patches which produce bubble-mediate sea spray efficiently.

13 We propose broader interpretation of b in Eqs. (10-11), be it negative or positive.
14 Generally, it is expected that the atmospheric stability (Kara et al., 2008) and fetch (through
15 the wave growth and development) cause inception of the whitecaps at lower or higher wind
16 speed. One can consider the range of values for b mentioned above (0.6 to 6.33) as an
17 expression of such influences. We suggest that b can also incorporate the effect of the
18 seawater properties on the extent of W . The net result of all secondary factors may be either
19 negative or positive b .

20 Specifically, we promote the hypothesis that a positive y-intercept b can be interpreted
21 as a measure of the capacity of seawater with specific characteristics, such as viscosity and
22 surface tension—which are governed by SST, salinity, and surfactant concentration—to affect
23 W . Undoubtedly, none of these secondary factors creates whitecaps per se. Rather, they
24 prolong or shorten the lifetime of the whitecaps via processes governed by the seawater
25 properties. For instance, surfactants and salinity influence the persistence of submerged and
26 surface bubbles. This yields variations of bubble rise velocity that replenishes the foam on the
27 surface at different rates. Long-lived decaying foam added to foamy areas created by
28 subsequent breaking events would augment W ; conversely, conditions that shorten bubble
29 lifetimes would reduce W (or at least not add to W).

30 A positive y-intercept can be thought of as a mathematical expression of this static
31 forcing (as opposed to dynamic forcing from the wind) that given seawater properties can

Moved down [15]: quadratic trends of W with U_{10} in Fig. 4 are in contrast to the known cubic and higher wind speed dependences such as in the MOM80 relationship. Using satellite W data therefore results in a higher estimate of W at wind speeds lower than about 10 m s^{-1} (based on Fig. 3a, obtained with 10 GHz data) and about 15 m s^{-1} (based on Fig. 3b, with 37 GHz data), and a lower estimate for higher wind speeds. Wind speeds are generally lower than 10 or 15 m s^{-1} (cf. Fig. 3) and thus a $W(U_{10})$ parameterization based on these data will most of the time lead to higher W estimates than those obtained from using the MOM80 relationship.

sustain. That is, at any given location, this static forcing acts as though higher wind speed of magnitude $(U_{10} + b)$ is producing more whitecaps than U_{10} alone. By parameterizing coefficients a and b in terms of different variables, one can evaluate how much the static forcing affects W in different geographic regions. By developing parameterizations $a(T)$ and $b(T)$ (Sect. 2.1), here we quantify only one static influence.

For completeness, we have also investigated the effect of either rising or waning winds on the $W(U_{10})$ relationship; increasing-decreasing winds are considered as a proxy for undeveloped-developed seas (Stramska and Petelski, 2003; CAL08). The rise-wane wind effect, as detected in this study, is not pronounced compared to findings in previous studies that use in situ wind speed data. Goddijn-Murphy et al. (2011) studied wind history and wave development dependencies on in situ W data using wave model (ECMWF), satellite (QuikSCAT), and in situ data for U_{10} . These authors detected significant effects only with in situ U_{10} . The absence of a significant wind history effect in our study might therefore be traced back to the method through which U_{10} was determined: wind speeds from satellites are spatial averages of scatterometric or radiometric observations that take a snapshot of the surface as it is affected by both history and local conditions, whereas in situ data for wind speed are single point values averaged over a short time and hence representative for a relatively small area. The effect of the spatial averaging of the satellite data over a much larger area (i.e., the satellite footprint) might be that information on wind history is lost in the process. The effect of the wind history, therefore, is not further sought in this study.

3.1.2 Intrinsic correlation

To quantify the possible intrinsic correlation in the derived $W(U_{10})$ parameterization (Eqs. (10-11)), we derived $W(U_{10})$ using ECMWF wind speeds instead of the QuikSCAT wind speeds (Sect. 2.3). Figure 7 shows a scatter plot of $W^{1/2}$ versus $U_{10\text{ECMWF}}$ (only data for 37 GHz are shown); dashed and solid lines show unconstrained and zero-forced fits, respectively. The linear regression (given in the figure legend) is used to obtain the global average wind speed dependence using U_{10} from ECMWF as follows:

$$W_{37} = 8.1 \times 10^{-5} (U_{10} + 3.33)^2 \quad (12).$$

The positive intercept here is interpreted as in Sect. 3.1.1.

Moved (insertion) [7]

Deleted: Although the value of W has been observed to be somewhat higher for waning than for rising winds, these differences are not statistically relevant. An effect of the wind history, therefore, is not included in the resulting $W(U_{10})$ parameterization (Eq. 9). ¶

Deleted: (undeveloped-developed sea)

Deleted: effect

Deleted: very

Deleted: (Stramska and Petelski, 2003; Callaghan et al., 2008; Goddijn-Murphy et al., 2011)

Deleted: -

Deleted: either ECMWF

Deleted: data

Deleted: QuikSCAT

Deleted: data

Deleted: or

Deleted: only

Deleted: data for

Deleted: this

Deleted:

Moved (insertion) [2]

Deleted: 9

Deleted: have

Deleted: ed

Deleted: 3

Field Code Changed

Field Code Changed

To evaluate the significance of the intrinsic correlation, we look at the change of the correlation coefficient of the $W(U_{10})$ relationship when QuikSCAT winds are substituted with the ECMWF winds. Physically, we expect a strong correlation between $W^{1/2}$ and U_{10} , and we see this clearly in Fig. 6b which shows a correlation coefficient $R^2 = 0.956$ for $W^{1/2}$ and $U_{10\text{QSCAT}}$. However, the correlation coefficient might not be as high as in Fig. 6 if U_{10} were from a more independent source. We see this when comparing Figs. 6b and 7. The $W^{1/2}$ - U_{10} correlation is still strong in Fig. 7, but the plot shows more scatter and slightly lower correlation with $R^2 = 0.826$. This is a sign that probably some intrinsic correlation contributes to the $W(U_{10\text{QSCAT}})$ relationship which, therefore, is stronger than $W(U_{10\text{ECMWF}})$.

The slopes in Figs. 6b and 7 differ by about 11%. We evaluate how this translates into differences in W_{37} values using Eqs. (11) and (12). We found the PD between $W_{37}(U_{10\text{QSCAT}})$ and $W_{37}(U_{10\text{ECMWF}})$ to be less than $\pm 9\%$ for wind speeds of 7–23 m s⁻¹. Specifically, the W_{37} values obtained with $U_{10\text{QSCAT}}$ and $U_{10\text{ECMWF}}$ are equal for wind speed of 11 m s⁻¹. Below 11 m s⁻¹, $W_{37}(U_{10\text{ECMWF}})$ is higher than $W_{37}(U_{10\text{QSCAT}})$ by up to 8.8%. Above 11 m s⁻¹, $W_{37}(U_{10\text{ECMWF}})$ is smaller than $W_{37}(U_{10\text{QSCAT}})$ by up to 8.4%. The difference goes up to 30% for wind speeds of 3 m s⁻¹.

While R^2 values for the regressions in Figs. 6b and 7 suggest that the intrinsic correlation may contribute to these differences, this is not the only possible reason for the discrepancies. The difference of about 5% between the U_{10} values from the two different sources (Fig. 4a) also contributes to the W discrepancies from Eqs. (11) and (12). Of course, we have to consider these differences in the light of other uncertainties in Eqs. (11) and (12) such as the uncertainties in determining $U_{10\text{QSCAT}}$ and $U_{10\text{ECMWF}}$ and the satellite-based W data itself. We, therefore, conclude that the effect of the intrinsic correlation alone on W is most likely less than about 4%.

3.2 Regional and seasonal analyses

3.2.1 Magnitude of regional and seasonal variations

Figure 8 shows examples of the $W^{1/2}$ versus $U_{10\text{QSCAT}}$ for different regions and seasons. Figures 8a and 8b show scatter plots for the Gulf of Mexico (region 1) at both frequencies for January 2006. Statistics are presented at the top of the figures and the fit lines are shown in red. Figures 8c and 8d show the fit lines $W^{1/2}(U_{10})$ for 10 and 37 GHz in region 5 for all

- Deleted: We
- Moved (insertion) [3]
- Deleted: two aspects of the W , $U_{10\text{QSCAT}}$, and $U_{10\text{ECMWF}}$ data used to obtain the $W(U_{10})$ (...)
- Deleted: ing
- Field Code Changed
- Deleted: 4
- Deleted: squared
- Deleted: of
- Field Code Changed
- Deleted: 4
- Deleted: is
- Deleted: show
- Deleted: in
- Deleted: 8b which is similar to Fig. 4 but uses (...)
- Deleted: -
- Field Code Changed
- Deleted: clearly seen
- Deleted: in Fig. 8b
- Deleted: the squared
- Deleted: coefficient is
- Moved (insertion) [12]
- Deleted: 4
- Deleted: 8b
- Deleted: up to
- Deleted: 0
- Deleted: , a difference comparable to that of usi (...)
- Moved (insertion) [13]
- Deleted: the parameterization
- Deleted: goodness of the relationship between
- Deleted: We do not have a good estimate of (...)
- Deleted: ,
- Deleted: presumed to lie within the error margi (...)
- Deleted: variations
- Deleted: 5
- Field Code Changed
- Deleted: square root of W
- Deleted: against
- Deleted: 5a
- Deleted: 5b
- Deleted: retrieved ove
- Deleted: 5
- Deleted: 5
- Field Code Changed
- Deleted: \sqrt{W}

months, while Figs. 8e and 8f demonstrate variations of the fit lines $W^{1/2}(U_{10})$ for both frequencies over all regions for March 2006. Figure 8 shows that the variations of the $W^{1/2}(U_{10})$ relationships at 10 GHz are smaller than those for 37 GHz, confirming the same observation reported by SAL13 but obtained with a different analysis. Focusing on the results for 37 GHz, we note that geographic differences from region to region for a fixed time period (Fig. 8f) yield more variability in the $W^{1/2}(U_{10})$ relationship than seasonal variations at a fixed location (Fig. 8d).

Figure 9 shows the seasonal cycles of m and c of the $W^{1/2}(U_{10})$ relationships at 37 GHz in regions 4, 5, 6, and 12. The annual variations of each curve and the variations between the curves confirm the observation from Fig. 8—the variations of m and c over the year are smaller than their variations from region to region. Figure 9 also shows that the seasonal cycles of m and c do not mimic the seasonal cycles of either U_{10} or T (Fig. 3). This implies that m and c are not merely scaling and offsetting the $W^{1/2}(U_{10})$ relationships, as Eq. (8) suggests, but rather carry more information for the regional and seasonal influences.

As anticipated from Figs. 8a, 8c, and 8e, seasonal cycles for the 10 GHz data reveal much less regional and seasonal influences (not shown). Because the 37 GHz data provide more information for secondary forcing than the 10 GHz data, the remainder of the data analysis in this study is illustrated with results for W_{37} data. Note, however, that all the procedures and analyses described for W_{37} data have been also carried out for the W_{10} data and some final results are reported (e.g., sect. 3.3.1).

Figures 8 and 9 show that variations of $W^{1/2}$ caused by U_{10} from 3 to 20 m s⁻¹ are much larger than the regional and seasonal variations of $W^{1/2}$. While this is expected (because U_{10} is a primary forcing factor), this also points that we need to evaluate whether these regional and seasonal variations are statistically significant. For this, we grouped the data for m and c , as well as for a and b , in two ways: (1) by month with the full range of geographical variability (over all 12 regions) for each month; and (2) by region with the full range of seasonal variability (over all 12 months) for each region. ANOVA and H tests applied to both groups showed that the seasonal variations are not statistically significant, while the regional variations are.

We illustrate this in Fig. 10 with values for b ; similar graphs for m , c , and a show the same results. Figure 10a shows the seasonal cycle for the regionally averaged b values with

Deleted: 5

Deleted: 5

Deleted: \sqrt{W}

Field Code Changed

Deleted: ¶

Deleted: 5

Field Code Changed

Deleted: \sqrt{W}

Deleted: Salisbury et al. (2013)

Deleted: tical approach

Deleted: Figs. 5d and 5f show

Field Code Changed

Deleted: \sqrt{W}

Deleted: even for a location like region 5 where extreme seasonal changes could be observed

Moved down [8]: The standard deviation of the slopes in Fig. 5d is 3×10^{-4} , while that in Fig. 5f is 4×10^{-4} . We surmise that obtaining whitecap fraction data at different locations can ensure a wider range of meteorological and oceanographic conditions that influence W than data at a fixed location for different seasons. This suggests that extreme yet sporadic seasonal values of the major forcing factor such as U_{10} at a given location contribute less to the W variations than varying environmental conditions from different locations. Such observation has implications for collecting W data with the purpose of capturing and parameterizing the natural variability of whitecap formation and extent. For example, even if twice a day, satellite-based observations of W on a global scale are still an effective way to record influences of secondary factors. For in situ data collection, as could be expected, long-leg cruises would provide more information on the effect of secondary factors, while long-term monitoring at a specific location will be more suitable to capture the wind speed effect alone. ¶

Field Code Changed

Field Code Changed

Field Code Changed

Field Code Changed

error bars (\pm one SD) representing the regional variability. It is clear that the seasonal variations of the regionally averaged b values lay within the regional variability. This suggests that variations of b from month to month are statistically undistinguishable. Figure 10b illustrates why variations of b from region to region are significantly different. The graph shows the annually averaged b values for each region with error bars representing the seasonal variability. It is clear that overall the geographical variations are not lost in the seasonal variability.

Note in Fig. 10b that some regional variations might not be distinguished within their seasonal variability. For example, the annual means for regions 1, 4, 7, 8, and 9 all lay within their seasonal variability; likewise, for the annual means for regions 5, 9, and 10. To pinpoint regions with significant differences of b (as well as a , m , and c), we applied the Student test to all possible pairs of regions; e.g., region 1 paired with each region from 2 to 12, region 2 paired with each region from 3 to 12, and so on to a total of 66 pairings of different regions. The Student tests showed statistically different values of b from region to region in 78% of all cases and 58% for a .

3.2.2 Quantifying SST variations

The results of the significance tests give a rationale for developing the SST dependences $a(T)$ and $b(T)$. Following the data representation in Fig. 10b, we derived $a(T)$ and $b(T)$ for data at 37 GHz by relating annually averaged a and b values to the annually averaged T for each region (Fig. 11). Figure 11c shows the monthly means of the coefficients b for each region and thus demonstrates how the data points in Fig. 11b have been formed; a similar procedure is used for the data points in Fig. 11a. As in Fig. 10b, the error bars (\pm one SD) represent the seasonal variability for SST (horizontal bars) and the coefficients a and b (vertical bars). A second order polynomial is fitted to the data points in Fig. 11a; a linear fit is applied to the data in Fig. 11b. The correlation coefficients for the derived SST dependences are $R^2 = 0.57$ for $a(T)$ and $R^2 = 0.87$ for $b(T)$. Such R^2 values are consistent with the expectation that SST, being a static secondary factor, affects W more via the offset b than via the slope a .

To evaluate the effect of using quadratic versus cubic wind speed dependence in Eq. (8), we also derived the SST dependences $a(T)$ and $b(T)$ for $n = 3$ following the same procedure as for the case of $n = 2$. We applied Eq. (8) with $n = 3$ (Eq. (5b)) to W_{37} data for all months in regions 4, 5, 6, and 12; we verified that differences due to the use of four instead of

twelve regions are not significant. The absolute values of m and c increase compared to their values obtained with $n = 2$. Specifically, the slopes m in each of the four regions change by 30% to 50%, while their regional variability (i.e., SD) increased by a factor of 3. The y -intercepts c in the four regions become larger than the c values obtained with $n = 2$ by a factor of 4.6, with regional variability increasing by a factor of 2. However, put together, the fit lines $W^{1/3}(U_{10})$ in region 5 for all months and in all four regions for March 2006 (not shown) behave like those in Figs. 8d and 8f; namely, seasonal variations are smaller than variations from region to region. Coefficients a and b are calculated from the m and c values and graphs similar to those in Fig. 11 are produced. Linear fits for both a and b were applied to these graphs. The correlation coefficients for these fits are $R^2 = 0.87$ for $a(T)$ and $R^2 = 0.91$ for $b(T)$.

The reason for the different values of m and c (thus a and b) for different n is that each set of coefficients (n, m, c) accounts for primary (i.e., U_{10}) and secondary factors differently. When the expected cubic law is applied to regional data sets which exhibit quadratic wind speed dependences (following from Figs. 5-6), the large differences are reconciled solely by m and c ; their values are therefore high. Conversely, smaller values for m and c are required to quantify regional variations when the wind speed exponent is already adjusted to follow the quadratic trend of the data. This confirms the reasoning in Sect. 2.1 that the change from cubic to quadratic wind speed exponent is a major change that the additional parameters impart on the $W(U_{10})$ relationship. The question then is which set of parameters—($n = 2, m, c$) or ($n = 3, m, c$)—better reproduce measured W data. In other words, if the wind speed exponent n is not adjusted but follows the physically determined cubic dependence, can the parametric coefficients m and c alone account for all observed variations of W ? We quantify and discuss this point in Sect. 3.3.

3.3 New parameterization of whitecap fraction

A new parameterization for the whitecap fraction $W(U_{10}, T)$ was obtained by replacing the fixed coefficients $A = 1 \times 10^{-4}$ and $B = 1.9$ in Eq. (11) with SST-dependent coefficients:

$$W = a(T)[U_{10} + b(T)]^2 \quad (13)$$

where

$$a(T) = a_0 + a_1 T + a_2 T^2 \quad (14a)$$

$$b(T) = b_0 + b_1 T \quad (14b)$$

Field Code Changed

Deleted: Though noticeable, overall Fig. 5 shows small variations: the slopes of the resulting $\sqrt{W}(U_{10})$ parameterizations for 12 months for all regions are found to be similar for all determined fits, about 0.01 with a standard deviation of 3×10^{-4} . In contrast to the slope result, the intercept (i.e., the value for W at zero wind speed, hereafter referred to as residual W) obtained with the 37 GHz W data shows strong variability (Fig. 6), with a mean value of 0.019, and a standard deviation of 0.004. These intercept variations at 37 GHz quantify the variations in absolute values of W by region and season seen in Fig.(s) 5d and 5f. The intercepts that were obtained with the 10 GHz data show much less variability with a mean value of -0.011 and a standard deviation of 9×10^{-4} . Sampling differences between the regions (e.g., fewer samples in region 7 than in any other region) do not seem to cause significant differences between the resulting $\sqrt{W}(U_{10})$ fits. Also, the results from region 1 do not noticeably differ from the results from the other regions, or at least are within the spread of the different results. These outcomes do not provide sufficient information to draw conclusions on effects of short fetches. These small variations in the derived wind speed dependencies across retrieval frequency, season, or location is in contrast to our expectation to reveal influences of environmental factors other than wind speed on W , in particular SST which influences viscosity. However, the high correlation coefficients suggest that U_{10} explains the variation in W to a very large extent. One possible explanation is that the additional influences have already been accounted for, at least partially, by using a quadratic power law.

Deleted: T

Deleted: is,

Deleted: law

Deleted: the

Deleted: Another suggestion might be that space and time variations of the secondary factors exist, but because they affect W in opposite ways (e.g., Monahan and O'Muircheartaigh, 1986), these influences cancel each other. Hence no further improvement can be expected by looking at effects of other factors on the variation in W explicitly, especially when the $W(U_{10})$ dependence is derived from a database covering a wide range of conditions. ¶

Deleted: Therefore, whereas 10 GHz data mainly provide the wind speed dependence of W , the 37 GHz data set provides information useful to quantify the influence of secondary factors on W , such as SST, the presence and amount of surfactants, or the local relaxation time of foam, depending on conditions like viscosity (Salisbury et al., 2013). ¶ These conditions are not only determined by the actual circumstances but also by the processes through which they developed, i.e. the history of ...

Deleted: P

Deleted: A parameterization of W in terms of U_{10} was obtained by averaging the $\sqrt{W} - U_{10}$ relationships for each region and for all months of 2006. The thus obtained relationship is similar to ...

Deleted: 7

and the coefficients are:

$$\begin{aligned} a_0 &= 8.462 \times 10^{-5} \\ a_1 &= 1.625 \times 10^{-6} \\ a_2 &= -3.348 \times 10^{-8} \\ b_0 &= 3.354 \\ b_1 &= -6.206 \times 10^{-2} \end{aligned} \tag{14c}$$

The whitecap fraction is calculated with Eqs. (10-12 and 13-14) and compared to both parameterized W values and to W data. The W values from SAL13 (37 GHz) and MOM80 are used as references for PD calculations and significance tests (Sect. 2.3).

3.3.1 Comparisons to W parameterizations

All parameterizations shown here are run for wind speeds from 3 to 20 m s⁻¹. The global quadratic $W(U_{10})$ (Eq. (11)) is compared to the published parameterizations of SAL13 (at 10 and 37 GHz), CAL08, and MOM80 (Eqs. (1-3)) in Fig. 12a. The PD between the global quadratic $W(U_{10})$ and SAL13 at 37 GHz ranges from 0.5% to 10% over the wind speed range. ANOVA and Student tests show that such differences are not statistically significant. That is, the global quadratic $W(U_{10})$ parameterization replicates the trend of the satellite-based W data as well as the SAL13 parameterization, which has a more specific wind speed exponent. Note that we do not expect our $W(U_{10})$ parameterization to be distinctly different from that of SAL13 because both studies use the same W database.

The PD between the trends of the global quadratic $W(U_{10})$ and MOM80 $W(U_{10})$ is from 5% up to 175% with the largest PDs for wind speeds below 7 m s⁻¹. Though Fig. 12a shows visibly different trends from both parameterizations, they seem to fall within each other uncertainties because both ANOVA and Student tests show no significant difference between them. However, if applied for winds up to 25 m s⁻¹ (Table 1), significant differences occur. That is, the use of the new global quadratic $W(U_{10})$ expression brings important changes to the trend of W compared to that from MOM80 $W(U_{10})$ at high winds.

Figure 12b shows W values from the new $W(U_{10}, T)$ parameterization at three fixed SST values ($T = 28, 12$, and 1 °C); the parameterizations of SAL13 for 37 GHz and MOM80 are shown for reference. Physically (from the SST dependence of the seawater viscosity), at

the same wind speed, W is expected to be higher in warm waters and lower in cold waters (Monahan and Ó'Muircheartaigh, 1986). Figure 12b shows a more complicated behavior of W . The highest W values (green line) are for moderate SST of 12 to 20 °C. At extreme SSTs (2 and 28 °C, blue and red lines, respectively), the SST influence on W changes depending on the wind speed: W is the lowest in cold waters and high winds, but is higher than W in warm waters at low winds. The trends of coefficients a and b in Fig. 11 suggests that we can expect such reversal.

According to Fig. 12b, changes of SST from 1 to 28 °C bring relatively small variations in the wind speed trend of W , PD no more than 15%. Applying Student tests, we find that the W values at any T remain statistically the same. In addition, W values at any T are not significantly different from the W predictions of the global quadratic $W(U_{10})$ parameterization. These results support the anticipated notion (Sect. 3.2.2) that by using quadratic wind speed exponent either in $W(U_{10})$ or $W(U_{10}, T)$, we can indeed account implicitly (i.e., only via adjustment of the U_{10} exponent) for most of the SST (and other) influences.

Figure 12c compares W values obtained with the quadratic and cubic $W(U_{10}, T)$ parameterizations at $T = 20$ °C; MOM80 and SAL13 at 37 GHz are shown for reference. With $p > 0.05$ for any fixed T , the W values from the cubic $W(U_{10}, T)$ parameterization are not statistically different from those obtained with either the quadratic $W(U_{10}, T)$ or MOM80. Still, the different trends of the W values seen in Fig. 12c suggest that accounting explicitly for SST via $a(T)$ and $b(T)$ in the physically expected cubic wind speed dependence is not sufficient to replicate the satellite-based W values. That is, when using $n = 3$, one needs to include more secondary forcing in order to reproduce the weaker wind speed dependence from the W database.

3.3.2 Comparisons to W data

Comparisons to the published in situ W data demonstrate order-of-magnitude consistency of the W values from the new parameterizations. Because there are no other remotely-sensed W data except those from WindSat, the most we can do at the moment is to evaluate how well the new parameterizations can replicate the trend and the spread of the satellite-based W . Recently, W values from a global wave model were compared to W from MOM80 and WindSat by Leckler et al. (2013), so one can evaluate where modeled W values stand in the

comparison of data and parameterizations of W . All parameterized W values shown here are calculated using U_{10} and T from the whitecap database, i.e., U_{10} from QuikSCAT and T from GDAS (Sect. 2.2.1).

Figure 13a compares W values predicted with both new parameterizations, $W(U_{10})$ and $W(U_{10}, T)$, to the same in situ and satellite-based W data for 10 and 37 GHz plotted in Fig. 1b; comparisons to satellite-based W data on any other day of 2006 are the same. Once again, it is confirmed that the new global quadratic $W(U_{10})$ parameterizations (black symbols in the figure) follow closely the wind speed trends of the satellite-based W data. This lends confidence in the use of the proposed quadratic $W(U_{10})$ parameterization to model a W trend with secondary influences implicitly included.

The W values predicted with the new $W(U_{10}, T)$ parameterization (red and cyan symbols in Fig. 13a) represent the spread of the satellite-based W data fairly well; tests show that they do not differ significantly. The cluster of W values are, however, statistically different from both the new quadratic and the MOM80 $W(U_{10})$ parameterizations. This is the most important result of this study: when we model only the trend of W with U_{10} , new and old parameterizations differ significantly only for extreme conditions (e.g., winds above 20 m s^{-1} in cold waters, Sect. 3.3.1). In contrast, when we model both the trend *and* the spread of the W values, the result is a significant difference with any, new or old, $W(U_{10})$ parameterization at any conditions.

In Fig. 13a, one can notice that the new $W(U_{10}, T)$ parameterization does not predict the spread of the satellite-based W data entirely. This suggests that accounting explicitly for SST in a W parameterization is not enough to replicate all the natural variability of W . This is consistent with our general understanding of the need to explicitly include many secondary factors in W parameterizations, not just SST (Sect. 2.1).

Though SST entails small variations in the trend of W with U_{10} (Fig. 12b), the most important consequence of the newly derived quadratic $W(U_{10}, T)$ parameterization is that it shapes significantly different spatial distribution compared to cubic and higher wind speed dependences like that of the MOM80. The complex behavior seen in Fig. 12b attests to this because different combinations of SST and U_{10} could be encountered over the globe. Meanwhile, the recreation of the spread of the satellite-based W data in Fig. 13a confirms that a $W(U_{10}, T)$ expression can model such situations.

Deleted: ¶

The method used to quantify the intrinsic correlation between W and U_{10} from QuikSCAT is described in Sect. 2.3. Figure 8 shows all ECMWF wind speed data that has been matched in time and space with the available $U_{10\text{QSCAT}}$ data for March 2006. The majority of the data is clustered in the range of $5\text{--}10 \text{ m s}^{-1}$. The correlation between U_{10} from ECMWF ($U_{10\text{ECMWF}}$) and U_{10} from QuikSCAT was determined as the best linear fit, forced through zero:¶

$$0.952 \cdot U_{10\text{QSCAT}} = U_{10\text{ECMWF}} \rightarrow U_{10\text{QS}} \quad (8)¶$$

with $R^2 = 0.844$. On average, U_{10} from ECMWF is about 5% lower than U_{10} from QuikSCAT.¶

We cast Eq. (7) in terms of $U_{10\text{ECMWF}}$ by combining it with Eq. (8). This allows for correction of the possible intrinsic correlation between W and U_{10} , which is applied in the resulting $W(U_{10})$ parameterization:¶

$$W = (U_{10\text{ECMWF}}^2 + 4U_{10\text{ECMWF}} + 4) \times 10^{-3} \quad (9)¶$$

Deleted: T

Deleted: is

Deleted: parameterization

Figure 13b shows a difference map between the global annual average W distributions for 2006. The MOM80 relationship yields a wider W range with higher values in regions with the highest wind speeds. In particular, this occurs between about 40° and 70° in the Southern ocean and in the North Atlantic. The latitudinal variations from the Equator to the poles are more pronounced when using the MOM80 relationship as compared to Eqs. (13-14). The new $W(U_{10}, T)$ parameterization provides a global spatial distribution with similar patterns, but the absolute values are lower at high latitudes and higher at low latitudes.

Note that in most studies, as in this study, $W(U_{10})$ of MOM80 is extrapolated beyond the range of the data from which it was derived (Sect. 1). Therefore, at higher wind speeds (and especially in cold waters), the W values that are obtained using the MOM80 parameterization are somewhat questionable. At the same time, the QuikSCAT instrument, which provided the U_{10} satellite data used in this study, has a decreased sensitivity for wind speeds over 20 m s^{-1} (Quilfen et al., 2007). All results regarding higher wind speeds should, therefore, be handled with caution. Only continuous comparison of directly measured W data to parameterized W values can help to better constrain predictions of whitecap fraction.

3.4 Sea spray aerosol production

The newly derived quadratic $W(U_{10}, T)$ parameterization (Eqs. (13-14)) was used to estimate the global annual average emission of super-micron SSA using M86 SSSF (Eq. (4')). The total (i.e., size integrated) annual SSA mass emission for 2006 is $4359.69 \text{ Tg yr}^{-1}$ ($4.4 \times 10^{12} \text{ kg yr}^{-1}$). This is about 50% larger than that calculated with the M86 SSSF using MOM80 (Eq. (4)), 2915 Tg yr^{-1} ($2.9 \times 10^{12} \text{ kg yr}^{-1}$). Because we have shown that the new quadratic $W(U_{10}, T)$ and MOM80 $W(U_{10})$ are significantly different (Sect. 3.3.2), we infer that the SSA emissions based on SSSFs using these two parameterizations also differ significantly. The two estimates of SSA emissions are calculated using the same modelling tool (Sect. 2.4) and the same input data (Sect. 2.2.1). Without any change in the shape factor, this guarantees that the 50% difference is due solely to the explicit accounting for the SST effect on W .

The spatial distribution of the mass emission rates obtained with SSSFs using the new $W(U_{10}, T)$ is shown in Fig. 14a. The SSA emissions obtained with the new and the MOM80 $W(U_{10})$ parameterizations mimic the patterns of the W distributions. The differences are mapped in Fig. 14b.

Deleted: (Eq. 2) in Fig. 9, which shows

Deleted: obtained with Eqs. (2) and (9) and wind speeds from ECMWF

Deleted: , as expected (see Sect. 3.1.1)

Deleted: over the southern oceans

Deleted: between about 40 and 70 N

Deleted: 9

Moved (insertion) [15]

Deleted: quadratic trends of W with U_{10} in Fig. 4 are in contrast to the known cubic and higher wind speed dependences such as in the MOM80 relationship. Using satellite W data therefore results in a higher estimate of W at wind speeds lower than about 10 m s^{-1} (based on Fig. 3a, obtained with 10 GHz data) and about 15 m s^{-1} (based on Fig. 3b, with 37 GHz data), and a lower estimate for higher wind speeds. Wind speeds are generally lower than 10 or 15 m s^{-1} (cf. Fig. 3) and thus a $W(U_{10})$ parameterization based on these data will most of the time lead to higher W estimates than those obtained from using the MOM80 relationship. In Fig. 12 the parameterization derived in this study (Eq. 9) is compared to $W(U_{10})$ parameterizations obtained by MOM80, Callaghan et al. (2008), and Salisbury et al. (2013). The differences between the MOM80 parameterization and Eq. 9 are discussed in Sect. 3.2.

Moved (insertion) [5]

Deleted: this parameterization was derived

Deleted: that

Deleted: that are

Deleted: ¶

Deleted: Specifically,

Moved (insertion) [20]

Deleted: how it affects

Deleted: coarse mode sea spray aerosol (Fig. 10

Deleted: t

Deleted: supermicron

Deleted: 2915

Deleted: 2.9

Deleted: when using the MOM80 W

Moved (insertion) [21]

Deleted: 4

Deleted: 2

Deleted: giving higher emission rates over a lar

Moved (insertion) [24]

Deleted: made in this study, obtained with the

Deleted: s

Deleted: shown in Fig. 9

Deleted: This is expected because the M86 SSS

Deleted: between the distributions of SSA mass

Moved up [21]: The annual emission rate

Moved up [20]: Specifically, the total

Previously modeled total dry SSA mass emissions vary by two orders of magnitude because of a variety of uncertainty sources (Sect. 1): $(2.2\text{--}22)\times 10^{12}$ kg yr⁻¹ (Textor et al., 2006, their Fig. 1a; de Leeuw et al., 2011, their Table 1); and $(2\text{--}74)\times 10^{12}$ kg yr⁻¹ for long-term averages (over 25 years) (G14, their Table 2, excluding 3 outliers). The impact of the modeling method used has to be acknowledged too. Grythe et al. (2014) suggest that the spread in published estimates of global emission based on the same M86 SSSF (Eq. (4)), from 3.3×10^{12} to 11.7×10^{12} kg yr⁻¹ (Lewis and Schwartz, 2004), can be attributed to differences in model input data and resolution differences. An example of the same SSSF yielding different results when applied in different models is also seen in the work of de Leeuw et al. (2011, their Table 1).

For a meaningful comparison of our results to SSA emissions obtained with other SSSFs, we attempt to remove (or at least minimize) the impact of the modeling method. As in this study, G14 used the same model (i.e., input data and configuration) to evaluate 21 SSSFs, including that of M86, against measurements. We thus can infer a “modelling” factor using our and G14 results obtained with M86 SSSF. We find that the G14 estimate of SSA emission from M86 (4.51×10^{12} kg yr⁻¹) is 1.55 times larger than our estimate of 2.9×10^{12} kg yr⁻¹ from M86 and MOM80. We apply this factor of 1.55 to our SSA emission estimated with the new $W(U_{10}, T)$ parameterization and obtain a “model scaled” value of 6.75×10^{12} kg yr⁻¹. Our “model scaled” estimate of the SSA emission is close to the median 5.91×10^{12} kg yr⁻¹ of the SSA emission reported by G14. This shows that an SSSF with a magnitude factor derived from satellite-based W data provides reasonable and realistic predictions of the SSA emission.

To narrow down this broad assessment, we now look at the SSSFs evaluated by G14 which account for the SST effect on SSA emissions. There are four such SSSFs in the G14 study (see their Table 2): S11T of Sofiev et al. (2011), G03T of Gong (2003), J11T of Jaeglé et al. (2011), and G13T of G14. To minimize differences caused by using different size ranges, we focus on S11T and G13T, both applied to dry SSA diameters $D_p = r_{80}$ (Sect. 2.4) from 0.01 to 10 µm. The upper limit is the same as in our study, while the lower limit is extended to sub-micron sizes, which, as we have seen (Sect. 2.4.2), introduces a discrepancy of about 14%.

The original Sofiev et al. (2011) SSSF is based on the M86 SSSF (Eq. (4)) combined with data from laboratory experiments by Mårtensson et al. (2003) to account for SST and

Moved (insertion) [8]

Moved up [10]: It has been argued that W should be proportional to the energy flux supplied by wind which is proportional to the cube of the friction velocity u_* resulting in a cubic $W(u_*)$ and above cubic $W(U_{10})$ parameterizations (Wu, 1988).

Deleted: Discussion ¶
<#>Assessment of satellite-based whitecap fraction data¶

The choice to use W data that was obtained at two different frequencies has led to more insight about the different stages of W . Based on the findings obtained with 10 GHz data, it can be concluded that for stage A whitecaps, for open ocean, the only real forcing factor is U_{10} , which mostly drives the absolute value of W with little variations caused by other factors. Following from the analysis of the 37 GHz data, more information was obtained on stage B whitecaps, namely that the amount of stage B whitecaps also clearly depends on the wind speed, but effects of other factors contribute to larger variations of the absolute values. ¶

When taking a closer look at the data cloud distributions of the scatterplots in Figs. 3 and 4, one can notice that the 10 GHz data show a relatively sharp cut-off on the bottom side of the data cloud whereas for the 37 GHz data one can see a sharp cut-off on the upper side. This might imply that at a certain wind speed there is a clear minimum of W produced by active wave breaking, and a well set maximum of the total sum of W . Apparently at a certain wind speed only up to a certain amount of foam can exist. One could speculate on foam stability maxima constrained by wind speed but it should be considered that this might as well be an artifact of the $W(T_B)$ algorithm. ¶

Considering our analyses of the W data sets, a lot seems to be explained by U_{10} . Although not very significant compared to those that are U_{10} -related, we do find some additional features as described below. ¶ First, Fig. 3 (the same applies for Fig. 5, showing data on regional scale) shows that at both 10 and

Deleted: t...he impact of the modell...ng meth...

Moved up [24]: The two estimates made in this study, obtained with the M86 SSSF, including either the original MOM80 or the newly derived Eq.9

Deleted: The two estimates made in this study, obtained with the M86 SSSF, including either the original MOM80 or the newly derived Eq.9

Moved up [23]: Specifically, using M86, Grythe et al. (2014) report two SSA emissions: an SSA estimate of $4.51\times 10^{12} \pm 0.44$ kg yr⁻¹ for the size range of $0.8 \mu\text{m} < r_{80} < 8 \mu\text{m}$, where the estimated value

Deleted: .

Moved up [22]: With regard to the size range, note that the contribution of the mass of submicron particles with $D_p < 1 \mu\text{m}$ to the total mass of partic

Deleted:These Grythe et al. estimates are

Formatted: Highlight

Deleted: Comparison of this value to the Grythe et al estimates shows that our estimate is in the lower range of the ...eported global annual mass

Deleted: This model corrected value is also of the same order as the estimates ...f the ...ofiev et al.

Deleted: experimental

salinity effects and a field experiment by Clarke et al. (2006) to increase the size range. In the G14 study, the salinity weight proposed by Sofiev et al. (2011) is not applied. At a reference salinity of 33 ‰, S11T estimates an SSA emission of 2.59×10^{12} kg yr⁻¹. Without the SST effect (the SST factor set to unity), the SSA emission estimated with S11 is 5.87×10^{12} kg yr⁻¹. With everything else the same except for the SST factor in source functions S11 and S11T, we evaluate that accounting for the SST effect results in changes by 56%. Correcting for 14% discrepancy due to extended lower size limit, we infer a 42% change when the SST effect is included in the SSSF. This is comparable to the 50% change due to SST in our case. We surmise that parameterizing additional influences on W is a viable way to account and explain for some of the uncertainty of SSA emissions.

Grythe et al. (2014) used a large data set of ship observations to develop G13T by changing both the magnitude and the shape factors. The authors modified the SSSF of Smith and Harrison (1998) (a sum of two log-normal distributions) to add an extra log-normal mode to cover the accumulation mode. They also added the empirically based SST factor (a third order polynomial) proposed by Jaeglé et al. (2011). With G13T, G14 estimate an SSA emission of 8.91×10^{12} kg yr⁻¹. The functional forms of the magnitude (involving the SST effect) and shape (modelling the size distribution) factors of G13T and S11T are very different. This makes it difficult to evaluate the relative contribution of the magnitude and shape factors for variations in SSA emissions. Our results can help.

The shape factors of S11T and our SSSF using $W(U_{10}, T)$ have a similar (not identical) functional form (that of M86, original and modified), but the functional forms accounting for SST are different. Our SSA emission estimate is about 62% higher than that of S11T. Allowing for 14% discrepancy due to the lower size limit, we find that different approaches to account for SST lead to about 67% variation in SSA emissions. Compared to G13T, our SSSF using $W(U_{10}, T)$ has a different shape factor (that of M86 versus log-normal), and a similar (but not identical) functional form for the SST effect (polynomial). Our SSA emission estimate is about 32% lower than that of G13T. Allowing for 14% size discrepancy, we find that different shape factors lead to about 13% variation in SSA emissions.

On the basis of these assessments, we can state that the inclusion of the SST effect in the magnitude factor and/or the choice of the shape factor (size range and model for the size distribution) in the SSSF can explain 13%-67% of the variations in the predictions of SSA emissions. The spread in SSA emission can thus be constrained by more than 100% when

- Deleted:** validity
- Deleted:** but also to account for SST and salinity effects
- Deleted:** However,
- Deleted:** i
- Deleted:** work by
- Deleted:** rythe et al. (20
- Deleted:**)
- Deleted:** resulting in
- Deleted:** estimate
- Deleted:** ± 0.33
- Deleted:** , at a reference salinity of 33 ‰ (referred to as S11T in Grythe et al. (2014))
- Deleted:** Grythe et al. (2014) also calculated an
- Deleted:** from the
- Deleted:** ofiev et al. (20
- Deleted:**) SSSF, leaving out temperature dependence, resulting in an estimate
- Deleted:** of
- Deleted:** ± 0.57
- Deleted:** ,
- Deleted:** at a reference salinity of 33 ‰ and a reference temperature of 25°C (referred to as S11 in
- Deleted:**)
- Moved (insertion) [25]**
- Deleted:** Grythe et al. (2014) SSSF was obtained by
- Deleted:** ying
- Deleted:** SSSF, based on observational data, by
- Deleted:** ing
- Deleted:** and including temperature dependence
- Deleted:** The
- Deleted:** estimate that was obtained using this SSSF (
- Deleted:** ± 0.61
- Deleted:**)
- Deleted:** was, compared to the other reviewed source functions by Grythe et al. (2014), found to be closest to the observations considered in the same work, and only about 1.5 times higher compared to our new satellite-based estimate

improvements of both the magnitude and the shape factor are pursued. Our results on the parameterization (Fig. 13a) suggest that accounting for more secondary forcing in the magnitude factor would explain more fully the spread among SSA emissions. Because, after wind speed, the most important secondary factor that accounts for variability in W is the wave field (SAL13), efforts to include wave parameters in W parameterizations are well justified.

4 Conclusions

The objective of the study presented here is to evaluate how accounting for natural variability of whitecaps in the parameterization of the whitecap fraction W would affect mass flux predictions when using a sea spray source function based on the discrete whitecap method. The study uses satellite-based W data estimated from measurements of the ocean surface brightness temperature T_B by satellite-borne microwave radiometers at frequencies of 10 and 37 GHz, W_{10} and W_{37} . Global and regional data sets comprising W_{10} and W_{37} data, wind speed U_{10} , and sea surface temperature T for 2006 were used to derive parameterizations $W(U_{10})$ and $W(U_{10}, T)$. The SSSF of Monahan et al. (1986) combined with the new $W(U_{10}, T)$ was used to estimate sea spray aerosol emission. The conclusions of the study are the following.

Assessment of the global W data set revealed a quadratic correlation between W and U_{10} (Eqs. (10-11)). The unconventional positive y -intercept for $W_{37}(U_{10})$ could be interpreted as a mathematical expression of the static forcing that given seawater properties (e.g., effects of SST, salinity, and surfactant concentrations) impart on whitecaps. Parameterization $W(U_{10})$ derived with an independent data set (U_{10} from ECMWF instead of QuikSCAT) helps to determine that the intrinsic correlation between W and U_{10} is most likely less than about 4%. The derived $W(U_{10})$ for both W_{10} and W_{37} replicate the trend of the satellite-based data well (Fig. 13a). That is, the adjusted quadratic wind speed exponent in $W(U_{10})$ accounts implicitly for most of the SST variations. The new quadratic $W(U_{10})$ predicts whitecap fraction significantly different from that obtained with the widely used $W(U_{10})$ of MOM80 only at extreme conditions (high winds and cold waters).

Applying the global quadratic $W(U_{10})$ parameterization on regional scale shows that the seasonal variations of its regression coefficients a and b are not statistically significant, while the regional variations are. On this basis, by relating annually averaged a and b values to the annually averaged T for each region (Fig. 11), the SST dependences $a(T)$ and $b(T)$ for data at 37 GHz were derived. The new quadratic $W(U_{10}, T)$ parameterization (Eqs. (13-14))

Deleted: The Grythe et al. (2014) S11 estimate is, as expected, close to the M86E estimate. Including temperature dependence, a lower estimate was found (S11T). In contrast, our estimate is assumed to implicitly account for temperature and salinity dependence through the $W(U_{10})$ parameterization, and results in a higher estimate compared to M86E. This cannot be caused by inclusion of salinity dependence because the fixed reference salinity is that of the oceans, and including varying salinities almost exclusively includes lower salinity values, resulting in lower emission estimates. This thus

Moved up [18]: Norris et al. (2013) and

Deleted: ¶

Moved up [25]: The Grythe et al. (2014) SSSF

Deleted: .

Deleted: ¶

Moved down [16]: Savelyev et al. (2014)

Moved (insertion) [16]

Deleted: ¶

Deleted: here aimed at improving the accuracy

Deleted: a

Deleted: -method based sea spray source functi

Deleted: the uncertainties

Deleted: approach was based on a

Deleted: data set containing

Deleted: two

Deleted: (

Deleted:)

Deleted: together with matching environmental

Deleted: .

Formatted: Indent: First line: 0.49"

Deleted: global a

Deleted: to evaluate the wind speed dependence

Deleted: The relatively large spread in the 37 G

Deleted: was

Deleted: as a function of

Deleted:

Deleted: only, as it is simple enough for global

Deleted: T_B was evaluated by using a more

Deleted: . The $U_{10ECMWF}$ values were found to b

Deleted: on

Deleted: is presumed to lie within the error

Deleted:)

Deleted: parameterization. Also, the effect of w

Deleted: relationship was examined and was fo

Deleted: parameterization for global application

Deleted: the

Deleted: parameterization derived in this study

predicts small variations in the trend of W for different SST values (Fig. 12b). However, it replicates the variability (spread) of the satellite-based W data well (Fig. 13a). The capability of the new $W(U_{10}, T)$ parameterization to model both the trend and the spread of the W data sets it apart from all other $W(U_{10})$ parameterizations. Results show that besides SST, one needs to include explicitly other secondary factors in order to model the full spread of the satellite-based W . Including the SST effect via $a(T)$ and $b(T)$ in the physically expected cubic wind speed dependence is not sufficient to replicate the trend of the satellite-based W values.

Application of the new quadratic $W(U_{10}, T)$ parameterization in the Monahan et al. (1986) SSSF resulted in a total (integrated only over super-micron sizes) SSA mass emission estimate of $4359.69 \text{ Tg yr}^{-1}$ ($4.4 \times 10^{12} \text{ kg yr}^{-1}$) for 2006. Scaled for modeling differences (Sect. 3.4), this estimate is $6.75 \times 10^{12} \text{ kg yr}^{-1}$, which is comparable to previously reported estimates. Comparing our and previous total SSA emissions, we have been able to assess to what degree accounting for the SST influence on whitecaps can explain the spread of SSA emissions. With or without the SST effect included in the SSSF, SSA emissions obtained with the new $W(U_{10}, T)$ parameterization vary by $\sim 50\%$. Different approaches to account for SST effect yield $\sim 67\%$ variations. Different models for the size distribution applied to different size ranges lead to 13%–42% variations in SSA emissions. Understanding and constraining the various sources of uncertainty in the SSSF would eventually improve the accuracy of SSSF predictions. Including the natural variability of whitecaps in the SSSF magnitude factor is a viable way toward such accuracy improvement.

Data availability

The data analysis and the results reported in this study are available from the corresponding author M.F.M.A. (Monique) Albert (monique.albert@tno.nl).

Acknowledgements

This study is partly funded by SRON, Netherlands Institute for Space Research, through the Dutch Users Support Programme GO-2. MDA was sponsored by the Office of Naval Research, NRL Program element 61153N, WU 4500. GdL by was supported by the European Space Agency (Support to Science Element: Oceanflux Sea Spray Aerosol, contract No. 4000104514/11/I-AM), the Centre on Excellence in Atmospheric Science funded by the Finnish Academy of Sciences Excellence (project no. 272041), the CRAICC project (part of the Top-level Research Initiative).

Deleted: supermicron

Deleted: 082

Deleted: 1

Deleted: , which is comparable to previously reported estimates

Deleted: Several recent studies were found to move towards SSSFs that use different parameters, other than U_{10} , which would better suit to describe SSA emissions. Considering our new $W(U_{10})$ parameterization that implicitly accounts for these different parameters, it is plausible that our approach using satellite-based W data to reduce the uncertainties in the parameterization of W , will help to improve future SSA emission estimates. ¶

Formatted: Line spacing: 1.5 lines

References

- Albert, M. F. M. A., Schaap, M., de Leeuw, G., and Builtjes, P. J. H.: Progress in the determination of the sea spray source function using satellite data, *Journal of Integrative Environmental Sciences*, **7**, 159-166, 2010.
- Albert, M. F. M. A., Schaap, M., Manders, A. M. M., Scannell, C., O'Dowd, C. D., and de Leeuw, G.: Uncertainties in the determination of global sub-micron marine organic matter emissions, *Atmos. Environ.*, **57**, 289-300, 2012.
- Andreae, M. O. and Crutzen, P. J.: Atmospheric aerosols: biogeochemical sources and role in atmospheric chemistry, *Science*, **276**, 1052-1058, 1997.
- Andreas, E. L.: Sea Spray and the turbulent air-sea heat fluxes, *J. Geophys. Res.*, **97**, 11429-11441, 1992.
- Anguelova, M. D. and Gaiser, P. W.: Skin depth at microwave frequencies of sea foam layers with vertical profile of void fraction, *J. Geophys. Res.*, **116**, C11002, 2011.
- Anguelova, M. D. and Gaiser, P. W.: Microwave emissivity of sea foam layers with vertically inhomogeneous dielectric properties, *Remote Sens. Environ.*, **139**, 81-96, 2013.
- Anguelova, M. D. and Webster, F.: Whitecap coverage from satellite measurements: A first step toward modeling the variability of oceanic whitecaps. *J. Geophys. Res.*, **111**, C03017, 2006.
- Anguelova, M. D., Bettenhausen, M. H., and Gaiser, P. W.: Passive remote sensing of sea foam using physically-based models, in: *Proceedings of the IGARSS 2006: IEEE International Geoscience and Remote Sensing Symposium*, Denver, Colorado, USA, 31 July-4 August, 3659-3662, 2006.
- Anguelova, M. D., Bettenhausen, M. H., Johnston, W. F., Gaiser, P. W.: First extensive whitecap database and its use to study whitecap fraction variability, in: *Proceedings of the 17th Air-Sea Interaction Conference*, AMS, Annapolis, Maryland, USA, 26 - 30 September, 2010 (<http://ams.confex.com/ams/pdfpapers/174036.pdf>).
- Anguelova, M. D., Bobak, J. P., Asher, W. E., Dowgiallo, D. J., Moat, B. I., Pascal, R. W., and Yelland, M. J.: Validation of satellite-based estimates of whitecap coverage: approaches and initial results, in: *Proceedings of the 16th Air-Sea Interaction conference*, AMS, Phoenix, Arizona, USA, 10-15 January, 2009, (<http://ams.confex.com/ams/pdfpapers/143665.pdf>).

Deleted: (2)

Deleted: (NO. C7)

Deleted: 14 pp.,

1 Asher, W. E. and Wanninkhof, R.: The effect of bubble-mediated gas transfer on purposeful
2 dual-gaseous tracer experiments, *J. Geophys. Res.*, 103, 10,555-10,560, 1998.

3 Barrie, L. A., Bottenheim, J. W., Schnell, R. C., Crutzen, P. J., and Rasmussen, R. A.: Ozone
4 destruction and photochemical reactions at polar sunrise in the lower Arctic atmosphere,
5 *Nature*, 334, 138–141, 1988.

6 Bettenhausen, M. H., Smith, C. K., Bevilacqua, R. M., Wang, N. -Y., Gaiser, P. W., and
7 Cox, S.: A nonlinear optimization algorithm for WindSat wind vector retrievals, *IEEE T.*
8 *Geosci. Remote*, 44, 597-610, 2006.

9 Blanchard, D. C.: The electrification of the atmosphere by particles from bubbles in the sea,
10 *Prog. Oceanogr.*, 1, 73-112, 1963.

11 Blanchard, D. C.: The production, distribution, and bacterial enrichment of the sea-salt
12 aerosol, in: *Air-sea exchange of gases and particles*, Liss, P. S. and Slinn, W. G. N., D. Reidel
13 Publishing Company, Dordrecht, The Netherlands, 407-454, 1983.

14 Bondur, V., and Sharkov, E.: Statistical properties of whitecaps on a rough sea, *Oceanology*,
15 22, 274– 279, 1982.

16 Callaghan, A. H.: An improved whitecap timescale for sea spray aerosol production flux
17 modeling using the discrete whitecap method, *J. Geophys. Res.-Atmos.*, 118, 9997-10010,
18 2013.

19 Callaghan, A. H. and White, M.: Automated processing of sea surface images for the
20 determination of whitecap coverage, *J. Atmos. Ocean. Tech.*, 26, 383-394, 2009.

21 Callaghan, A. H., de Leeuw, G., Cohen, L., and O'Dowd, C. D.: Relationship of oceanic
22 whitecap coverage to wind speed and wind history, *Geophys. Res. Lett.*, 35, L23609, 2008.

23 Callaghan, A. H., Deane, G. B., and Stokes, M. D.: Two Regimes of Laboratory Whitecap
24 Foam Decay: Bubble-Plume Controlled and Surfactant Stabilized, *J. Phys. Oceanogr.*, 43,
25 1114-1126, 2013.

26 Chameides, W. L. and Stelson, A. W.: Aqueous-phase chemical processes in deliquescent
27 sea-salt aerosols: a mechanism that couples the atmospheric cycles of S and sea salt, *J.*
28 *Geophys. Res.- Atmos.*, 97, 20565-20580, 1992.

Deleted: NO. C5,

Deleted: NO. 3,

Deleted: Bortkovskii, R. S. and Novak, V. A.: Statistical dependencies of sea state characteristics on water temperature and wind-wave age, *J. Marine Syst.*, 4, 161-169, 1993.

Deleted:

Deleted: Callaghan, A. H., Stokes, M. D., and Deane, G. B.: The effect of water temperature on air entrainment, bubble plumes, and surface foam in a laboratory breaking-wave analog, *J. Geophys. Res. - Oceans*, 119, 7463-7482, 2014.

Deleted: (NO. D18)

1 Chelton, D. B. and Freilich, M. H.: Scatterometer-based assessment of 10-m wind analyses
2 from the operational ECMWF and NCEP numerical weather prediction models, *Mon.*
3 *Weather Rev.*, 133, 409-429, 2005.

4 Cicerone, R. J.: Halogens in the atmosphere, *Rev. Geophys. Space Ge.*, 19 (NO. 1), 123-139,
5 1981.

6 Clarke, A. D., Owens, S. R., and Zhou, J.: An ultrafine sea-salt flux from breaking waves:
7 Implications for cloud condensation nuclei in the remote marine atmosphere, *J. Geophys.*
8 *Res.*, 111, D06202, 2006.

9 de Leeuw, G., Andreas, E. L., Anguelova, M. D., Fairall, C. W., Lewis, E. R., O'Dowd, C. D.,
10 Schulz, M., and Schwartz, S. E.: Production flux of sea-spray aerosol, *Rev. Geophys.*, 49,
11 RG2001, 2011.

12 Facchini, M. C., Rinaldi, M., Decesari, S., Carbone, C., Finessi, E., Mircea, M., Fuzzi, S.,
13 Ceburnis, D., Flanagan, R., Nilsson, E. D., de Leeuw, G., Martino, M., Woeltjen, J., and
14 O'Dowd, C. D.: Primary submicron marine aerosol dominated by insoluble organic colloids
15 and aggregates, *Geophys. Res. Lett.*, 35, L17814, 2008.

16 Fairall, C. W., Kepert, J. D., and Holland, G. J.: The effect of sea spray on surface energy
17 transports over the ocean, *The Global Atmosphere and Ocean System*, 2, 121-142, 1994.

18 Falkowski, P. G., Barber, R. T., and Smetacek, V.: Biogeochemical controls and feedbacks on
19 ocean primary production, *Science*, 281, 200-206, 1998.

20 Ghan, S. J., Guzman, G., and Hayder, A. -R.: Competition between sea salt and Sulfate
21 particles as cloud condensation nuclei, *J. Atmos. Sci.*, 55, 3340-3347, 1998.

22 Gaiser, P.W., St. Germain, K. M., Twarog, E. M., Poe, G. A., Purdy, W., Richardson, D.,
23 Grossman, W., Linwood Jones, W., Spencer D., Golba, G., Cleveland, J., Choy, L.,
24 Bevilacqua, R. M., and Chang, P. S.: The WindSat spaceborne polarimetric microwave
25 radiometer: sensor description and early orbit performance, *IEEE T. Geosci. Remote*, 42, NO.
26 11, 2347-2361, 2004.

27 Garrett, W. D.: Stabilization of air bubbles at the air-sea interface by surface-active material,
28 *Deep-Sea Res.*, 14, 661-672, 1967.

Deleted: Erickson, D. J., Merrill, J. T., and Duce, R. A.: Seasonal estimates of global atmospheric sea-salt distributions, *J. Geophys. Res. -Atmos.*, 91 (NO.D1), 1067-1072, 1986. ¶

1 Goddijn-Murphy, L., Woolf, D. K., and Callaghan, A. H.: Parameterizations and algorithms
2 for oceanic whitecap coverage, *J. Phys. Oceanogr.*, 41, 742-756, 2011.

3 Gong, S. L.: A parameterization of sea-salt aerosol source function for sub- and super-micron
4 particles, *Global Biogeochem. Cycles*, 17, 1097, 2003.

5 Graedel, T. E. and Keene, W. C.: The budget and cycle of Earth's natural chlorine, *Pure Appl.*
6 *Chem.*, 68, 1689-1697, 1996.

7 Grythe, H., Ström, J., Krejci, R., Quinn, P., and Stohl, A.: A review of sea-spray aerosol
8 source functions using a large global set of sea salt aerosol concentration measurements,
9 *Atmos. Chem. Phys.*, 14, 1277-1297, 2014.

10 Hanson, J. L., and Phillips, O. M.: Wind sea growth and dissipation in the open ocean, *J.*
11 *Phys. Oceanogr.*, 29, 1633-1648, 1999.

12 Jaeglé, L., Quinn, P. K., Bates, T. S., Alexander, B., and Lin, J.-T.: Global distribution of sea
13 salt aerosols: new constraints from in situ and remote sensing observations, *Atmos. Chem.*
14 *Phys.*, 11, 3137-3157, doi:10.5194/acp-11-3137-2011, 2011.

15 Kara, A. B., Wallcraft, A. J., and Bourassa, M. A.: Air-sea stability effects on the 10 m winds
16 over the global ocean: Evaluations of air-sea flux algorithms, *J. Geophys. Res.-Oceans*, 113,
17 C04009, 2008.

18 Keene, W. C., Pszenny, A. A. P., Jacob, D. J., Duce, R. A., Galloway, J. N., Schultz-Tokos, J.
19 J., Sievering, H., and Boatman, J. F.: The geochemical cycling of reactive chlorine through
20 the marine troposphere, *Global Biogeochem. Cy.*, 4 (NO. 4), 407-430, 1990.

21 Keene, W. C., Khalil, M. A. K., Erickson, D. J., McCulloch, A., Graedel, T. E., Lobert, J. M.,
22 Aucott, M. L., Gong, S.-L., Harper, D. B., Kleiman, G., Midgley, P., Moore, R. M., Seuzaret,
23 C., Sturges, W. T., Benkovitz, C. M., Koropalov, V., Barrie, L. A., and Li, Y.-F.: Composite
24 global emissions of reactive chlorine from anthropogenic and natural sources: reactive
25 chlorine emissions inventory, *J. Geophys. Res.*, 104 (NO. D7), 8429-8440, 1999.

26 Kleiss, J. M. and Melville, W. K.: The analysis of sea surface imagery for whitecap
27 kinematics, *J. Atmos. Ocean. Tech.*, 28, 219-243, 2011.

28 Koop, T., Kapilashrami, A., Molina, L.T., and Molina, M. J.: Phase transitions of sea-
29 salt/water mixtures at low temperatures: implications for ozone chemistry in the polar marine
30 boundary layer, *J. Geophys. Res.*, 105 (NO. D21), 26393-26402, 2000.

Deleted: (4)

Deleted: Gong, S. L. and Barrie, L. A.: Modeling sea-salt aerosols in the atmosphere I. Model development, *J. Geophys. Res.*, 102 (NO. D3), 3805-3818, 1997.

Deleted: (NO. 9)

Deleted: Holthuijsen, L. H., Powell, M. D., and Pietrzak, J. D.: Wind and waves in extreme hurricanes, *J. Geophys. Res.*, 117, C09003, 2012.

Deleted:

- 1 | Leckler, F., Arduin, F., Filipot, J.-F., Mironov, A.: Dissipation source terms and whitecap
2 | statistics, *Ocean Modell.*, 70, 62-74, 2013.
- 3 | Lewis, E. R. and Schwartz, S. E.: Sea salt aerosol production: mechanisms, methods,
4 | measurements and models - A critical review, *Geoph. Monog. Series*, 152, American
5 | Geophysical Union, Washington D. C., 413 pp, 2004.
- 6 | Luria, M. and Sievering, H.: Heterogeneous and homogeneous oxidation of SO₂ in the remote
7 | marine atmosphere, *Atmos. Environ.*, 25A, 1489-1496, 1991.
- 8 | Mårtensson, E. M., Nilsson, E. D., de Leeuw, G., Cohen, L. H., and Hansson, H.-C.:
9 | Laboratory simulations and parameterization of the primary marine aerosol production, *J.*
10 | *Geophys. Res.*, 108, 4297, 2003.
- 11 | Medwin, H.: In situ acoustic measurements of microbubbles at sea, *J. Geophys. Res.*, 82, 971-
12 | 976, 1977.
- 13 | Meissner, T. and Wentz, F. J.: The emissivity of the ocean surface between 6 and 90 GHz
14 | over a large range of wind speeds and earth incidence angles, *IEEE T. Geosci. Remote*, 50,
15 | 3004-3026, 2012.
- 16 | Melville, W. K.: The role of surface-wave breaking in air-sea interaction, *Annu. Rev. Fluid*
17 | *Mech.*, 28, 279-321, 1996.
- 18 | Monahan, E. C.: Oceanic Whitecaps, *J. Phys. Oceanogr.*, 1, 139-144, 1971.
- 19 | Monahan, E. C. and O'Muircheartaigh, I.: Optimal power-law description of oceanic
20 | whitecap coverage dependence on wind speed, *J. Phys. Oceanogr.*, 10, 2094-2099, 1980.
- 21 | Monahan, E. C. and O'Muircheartaigh, I.: Whitecaps and the passive remote sensing of the
22 | ocean surface, *Int. J. Remote Sens.*, 7, 627-642, 1986.
- 23 | Monahan, E. C. and Woolf, D. K.: Comments on "Variations of whitecap coverage with wind
24 | stress and water temperature, *J. Phys. Oceanogr.*, 19, 706-709, 1989.
- 25 | Monahan, E. C., Fairall, C. W., Davidson, K. L., and Boyle, P. J.: Observed inter-relations
26 | between 10 m winds, ocean whitecaps and marine aerosols, *Q. J. Roy. Meteor. Soc.*, 109,
27 | 379-392, 1983.
- 28 | Monahan, E. C., Spiel, D. E., and Davidson, K. L.: A model of marine aerosol generation via
29 | whitecaps and wave disruption, in: *Oceanic whitecaps: and their role in air-sea exchange*

Deleted: Liu, X. and Penner, J. E.: Effect of Mount Pinatubo H₂SO₄/H₂O aerosol on ice nucleation in the upper troposphere using a global chemistry and transport model, *J. Geophys. Res.*, 107, D124141, 2002.¶

Deleted: (NO. 8)

Deleted:

Deleted:

Deleted: (NO.D9)

Deleted: (NO. 6)

Deleted: NO. 8,

Deleted: (5)

processes, Monahan, E. C., Mac Niocaill, G., D. Reidel Publishing Company, Dordrecht, The Netherlands, 167-174, 1986.

Norris, S. J., Brooks, I. M., Moat, B. I., Yelland, M. J., de Leeuw, G., Pascal, R. W., Brooks, B. J.: Near-surface measurements of sea spray aerosol production over whitecaps in the open ocean. *Ocean Science*, 9, 133–145, doi: 10.5194/os-9-133-2013, 2013a.

Norris, S. J., Brooks, I. M., and Salisbury, D. J.: A wave roughness Reynolds number parameterization of the sea spray source flux, *Geophys. Res. Lett.*, 40, 4415–4419, 2013b.

O’Dowd, C. D. and de Leeuw, G.: Marine aerosol production: a review of the current knowledge, *Philos. T. R. Soc. A*, 365, 1753-1774, 2007.

O’Dowd, C. D., Lowe, J. A., Smith, M. H., and Kaye, A. D.: The relative importance of non-sea-salt sulphate and sea-salt aerosol to the marine cloud condensation nuclei population: An improved multi-component aerosol-cloud droplet parametrization, *Q. J. Roy. Meteor. Soc.*, 125, 1295-1313, 1999.

O’Dowd, C. D., Facchini, M. C., Cavalli, F., Ceburnis, D., Mircea, M., Decesari, S., Fuzzi, S., Yoon, Y. J., and Putaud, J.-P.: Biogenically driven organic contribution to marine aerosol, *Nature*, 431, 676-680, 2004.

Ovadnevaite, J., Manders, A., de Leeuw, G., Ceburnis, D., Monahan, C., Partanen, A. -I., Korhonen, H., and O’Dowd, C. D.: A sea spray aerosol flux parameterization encapsulating wave state, *Atmos. Chem. Phys.*, 14, 1837-1852, 2014.

Paget, A. C., Bourassa, M. A., and Anguelova, M. D.: Comparing in situ and satellite-based parameterizations of oceanic whitecaps, *J. Geophys. Res. Oceans*, 120, 2826–2843, 2015.

Pandey, P. C. and Kakar, R. K.: An empirical microwave emissivity model for a foam-covered sea, *IEEE J. Oceanic Eng.*, 7, 135-140, 1982.

Partanen, A.-I., Dunne, E. M., Bergman, T., Laakso, A., Kokkola, H., Ovadnevaite, J., Sogacheva, L., Baisnée, D., Sciare, J., Manders, A., O’Dowd, C., de Leeuw, G., and Korhonen, H.: Global modelling of direct and indirect effects of sea spray aerosol using a source function encapsulating wave state, *Atmos. Chem. Phys.*, 14, 11731-11752, 2014.

Quilfen, Y., Prigent, C., Chapron, B., Mouche, A. A., and Houti, N.: The potential of QuikSCAT and WindSat observations for the estimation of sea surface wind vector under severe weather conditions, *J. Geophys. Res.*, 112, C09023, 2007.

Deleted:

Deleted:

Deleted: NO. 3,

Deleted:

- 1 Reising, S., Asher, W., Rose, L., and Aziz, M.: Passive polarimetric remote sensing of the
2 ocean surface: The effects of surface roughness and whitecaps, paper presented at the
3 International Union of Radio Science, URSI Gen. Assem., Maastricht, Netherlands, 2002.
- 4 Saiz-Lopez, A. and von Glasow, R.: Reactive halogen chemistry in the troposphere, *Chem.*
5 *Soc. Rev.*, 41, 6448-6472, 2012.
- 6 Salisbury, D. J., Anguelova, M. D., and Brooks, I. M.: On the variability of whitecap fraction
7 using satellite-based observations, *J. Geophys. Res.-Oceans*, 118, 6201-6222, 2013.
- 8 Salisbury, D. J., Anguelova, M. D., and Brooks, I. M.: Global distribution and seasonal
9 dependence of satellite-based whitecap fraction, *Geophys. Res. Lett.*, 41, 1616–1623, 2014.
- 10 Savelyev, I. B., Anguelova, M. D., Frick, G. M., Dowgiallo, D. J., Hwang, P. A., Caffrey, P.
11 F., and Bobak, J. P.: On direct passive microwave remote sensing of sea spray aerosol
12 production, *Atmos. Chem. Phys.*, 14, 11611-11631, 2014.
- 13 Sievering, H., Boatman, J., Gorman, E., Kim, Y., Anderson, L., Ennis, G., Luria, M., and
14 Pandis, S.: Removal of sulphur from the marine boundary layer by ozone oxidation in sea-salt
15 aerosols, *Nature*, 360, 571-573, 1992.
- 16 Sievering, H., Gorman, E., Ley, T., Pszenny, A., Springer-Young, M., Boatman, J., Kim, Y.,
17 Nagamoto, C., and Wellman, D.: Ozone oxidation of sulfur in sea-salt aerosol particles during
18 the Azores Marine Aerosol and Gas Exchange experiment, *J. Geophys. Res. -Atmos.*, 100,
19 23075-23081, 1995.
- 20 Smith, M. H., Park, P. M., and Consterdine, I. E.: Marine aerosol concentrations and
21 estimated fluxes over the sea, *Q. J. Roy. Meteor. Soc.*, 119, 809–824, 1993.
- 22 Smith, M. H. and Harrison, N. M.: The sea spray generation function, *J. Aerosol Sci.*, 29
23 (Suppl. 1), S189-S190, 1998.
- 24 Sofiev, M., Soares, J., Prank, M., de Leeuw, G., and Kukkonen, J.: A regional-to-global
25 model of emission and transport of sea salt particles in the atmosphere, *J. Geophys. Res.*, 116,
26 D21302, 2011.
- 27 Stramska, M. and Petelski, T.: Observations of oceanic whitecaps in the north polar waters of
28 the Atlantic, *J. Geophys. Res.*, 108, NO. C3, 3086, 2003.

1 Tang, W., Yueh, S. H., Fore, A. G., and Hayashi A.: Validation of Aquarius sea surface
 2 salinity with in situ measurements from Argo floats and moored buoys, J. Geophys. Res.
 3 Oceans, 119, 6171–6189, 2014, doi:10.1002/2014JC010101.

4 Textor, C., Schulz, M., Guibert, S., Kinne, S., Balkanski, Y., Bauer, S., Bernsten, T., Berglen,
 5 T., Boucher, O., Chin, M., Dentener, F., Diehl, T., Easter, R., Feichter, H., Fillmore, D.,
 6 Ghan, S., Ginoux, P., Gong, S., Grini, A., Hendricks, J., Horowitz, L., Huang, P., Isaksen, I.,
 7 Iversen, T., Kloster, S., Koch, D., Kirkevåg, A., Kristjansson, J. E., Krol, M., Lauer, A.,
 8 Lamarque, J. F., Liu, X., Montanaro, V., Myhre, G., Penner, J., Pitari, G., Reddy, S., Seland,
 9 Ø., Stier, P., Takemura, T., and Tie, X.: Analysis and quantification of the diversities of
 10 aerosol life cycles within AeroCom, Atmos. Chem. Phys., 6, 1777-1813, 2006.

11 Toba, Y. and Chaen, M.: Quantitative expression of the breaking of wind waves on the sea
 12 surface, Records of Oceanographic Works in Japan, 12 (NO. 1), 1-11, 1973.

13 Thorpe, S. A.: On the clouds of bubbles formed by breaking wind-waves in deep water, and
 14 their role in air-sea gas transfer, Philos. T. R. Soc. S. -A., 304, 155-210, 1982.

15 Wanninkhof, R., Asher, W. E., Ho, D. T., Sweeney, C., and McGillis, W. R.: Advances in
 16 quantifying air-sea gas exchange and environmental forcing, Annual Review of Marine
 17 Science, 1, 213-244, 2009.

18 Wentz, F. J.: A model function for ocean microwave brightness temperatures, J. Geophys.
 19 Res., 88, NO. C3, 1892-1908, 1983.

20 Wentz, F. J.: A well-calibrated ocean algorithm for special sensor microwave / imager, J.
 21 Geophys. Res., 102, NO. C4, 8703-8718, 1997.

22 Woolf, D. K.: Bubbles and their role in gas exchange, in: The Sea Surface and Global
 23 Change, Liss, P. S. and Duce, R. A., Cambridge Univ. Press, New York, 173-205, 1997.

24 Wu, J.: Variations of whitecap coverage with wind stress and water temperature, J. Phys.
 25 Oceanogr., 18, 1448-1453, 1988.

26 Zhao, D. and Toba, Y.: Dependence of whitecap coverage on wind and wind-wave properties,
 27 J. Oceanogr., 57, 603-616, 2001.

28 |

Deleted: Sugihara, Y., Tsumori, H., Ohga, T., Yoshioka, H., and Serizawa, S.: Variation of whitecap coverage with wave-field conditions, J. Marine Syst., 66, 47-60, 2007.¶
 Takemura, T., Okamoto, H., Maruyama, Y., Numaguti, A., Higurashi, A., and Nakajima, T.: Global three-dimensional simulation of aerosol optical thickness distribution of various origins, J. Geophys. Res., 105 (NO.D14), 17853-17873, 2000.

Deleted: Wentz, F. J.: Measurement of oceanic wind vector using satellite microwave radiators, IEEE T. Geosci. Remote, 30 (NO. 5), 960-972, 1992.¶

Deleted: Zweers, N. C., Makin, V. K., de Vries, J. W., and Burgers, G.: A sea drag relation for hurricane wind speeds, Geophys. Res. Lett., 37, L21811, 2010.¶

Table 1. Coordinates, number of data points, range and mean value for wind speed, and range and mean value of SST of selected regions (a) for January 2006, (b) for July 2006.

a

Region	Lon.	Lat.	Number of samples *	Wind speed* [m s ⁻¹]	SST* [°C]				
					Range	Mean	Median	Range	Mean
1.	86°W – 95°W	23°N–28°N	18896	1.3–15.7	7.5	7.6	19.4–26.0	23.8	24.1
2.	1°W – 15°W	1°S – 30°S	169128	0.2–12.9	6.4	6.4	21.4–27.8	24.2	24.1
3.	75° E – 89° E	1°S –30°S	169056	0.0–13.4	7.0	7.2	23.0–29.4	26.8	27.3
4.	11°W – 20°W	30°N – 44°N	49760	0.2–19.6	8.0	7.6	13.3–20.4	16.4	16.3
5.	86°W –100°W	31°S – 60°S	200360	0.5–23.0	8.7	8.7	4.8–24.1	12.7	11.7
6.	171°W –180°W	15°S–14°N	123328	0.6–15.6	8.2	8.2	26.2–30.4	28.4	28.2
7.	31°W – 50°W	10°N – 29°N	90640	0.3–20.0	8.8	9.0	20.1–27.9	24.9	25.3
8.	140°W – 160°W	20°S – 30°S	50040	0.5–16.3	6.8	6.7	22.2–29.1	26.3	26.6
9.	140°W – 160°W	40°S – 50°S	41840	0.1–20.6	6.9	6.5	9.3–18.2	13.2	13.1
10.	0°W – 30°W	40°S – 50°S	133080	0.5–26.4	9.4	9.3	3.2–16.7	9.6	9.3
11.	50° E – 70° E	40°S – 50°S	50784	0.5–21.6	9.6	9.6	3.2–17.4	9.6	9.5
12.	180° E – 180°W	60°S – 90°S	576576	0.2–20.9	7.0	6.7	-1.9–8.0	1.8	1.4

* For January 2006.

1

2

b

Region	Lon.	Lat.	Number of samples**	Wind speed** [m s ⁻¹]	SST**[°C]				
					Range	Mean	Median	Range	Mean
1.	86°W – 95°W	23°N–28°N	13848	0.4–10.0	4.5	4.4	28.7–30.5	29.5	29.4
2.	1°W – 15°W	1°S – 30°S	189600	0.2–14.0	6.6	6.6	17.7–27.1	23.2	23.7
3.	75° E – 89° E	1°S –30°S	195424	0.6–15.4	8.0	8.1	18.8–30.0	25.4	25.9
4.	11°W – 20°W	30°N – 44°N	43040	0.7–14.0	6.7	6.6	16.9–23.3	20.4	20.5
5.	86°W –100°W	31°S – 60°S	257496	0.7–22.7	9.8	9.6	2.5–19.1	9.3	8.3
6.	171°W –180°W	15°S–14°N	133096	0.1–14.8	6.0	6.0	26.9–29.7	28.8	29.0
7.	31°W – 50°W	10°N – 29°N	88304	0.4–13.6	7.4	7.4	23.6–28.0	26.0	26.1
8.	140°W – 160°W	20°S – 30°S	47504	0.7–24.7	6.9	6.2	18.8–27.0	23.2	23.4
9.	140°W – 160°W	40°S – 50°S	52736	0.5–21.0	10.1	10.3	8.2–14.1	10.9	10.8
10.	0°W – 30°W	40°S – 50°S	160192	0.9–28.9	10.8	10.8	1.8–14.6	8.3	8.3
11.	50° E – 70° E	40°S – 50°S	49344	1.1–28.2	12.9	12.7	2.1–16.1	8.3	7.8
12.	180° E – 180°W	60°S – 90°S	177240	0.8–29.1	11.7	11.9	-1.3–4.3	1.7	1.7

3

** For July 2006

4

5

6

Deleted: ¶
Region .

...

Figure captions

Figure 1. Satellite retrieved 37 GHz W data for 11 March 2006. a) Map ($0.5^\circ \times 0.5^\circ$) of ascending and descending passes for W at 37 GHz; b) W at 10 and 37 GHz (green and magenta symbols, respectively) compared to historical photographic data including total W (diamonds) and active whitecap fraction W_A (squares). Parameterization $W(U_{10})$ of Monahan and O'Muircheartaigh (1980, MOM80) (purple line) is shown for reference.

Figure 2. Selected regions to determine regional variations of $W(U_{10})$.

Figure 3. Seasonal cycle for 2006 in different regions as defined in Fig. 2 and Table 1: a) wind speed U_{10} ; b) Sea surface temperature (SST) T . The regions represent: 4–Temperate zone in Northern hemisphere; 5–Temperate zone in Southern hemisphere; 6–Doldrums along the Equator; 12–Lowest SST.

Figure 4. Scatter plot for March 2006 of (a) global $U_{10\text{ECMWF}}$ versus $U_{10\text{QSCAT}}$ and (b) global T from ECMWF versus T from GDAS. In both figures the colors indicate the amount of data points per hexabin. The black lines are linear fits: the dashed line represents unrestricted fit and the solid line a fit forced through zero. The linear regressions and respective R^2 are listed in each panel.

Figure 5. Global W as function of U_{10} from QuikSCAT for March 2006 where W is obtained with 10 GHz (a) and 37 GHz (b) measurement frequency. The red line indicates the Monahan and O'Muircheartaigh (1980 MOM80) relationship (Eq. (3)). The colors indicate the amount of data points per hexabin.

Figure 6. Global \sqrt{W} as function of U_{10} from QuikSCAT for March 2006, where \sqrt{W} is obtained with 10 GHz (a) and 37 GHz (b) measurement frequency. The black line (in both panels) indicates the best linear fit through the data. The red line in Fig. 6b equals the black line in Fig. 6a. The colors indicate the amount of data points per hexabin.

Figure 7. Scatter plot of \sqrt{W} versus $U_{10\text{ECMWF}}$ for March 2006.

Figure 8. Linear fits of \sqrt{W} versus U_{10} for: region 1 for January 2006 at 10 GHz (a) and 37 GHz (b); region 5 for all months at 10 GHz (c) and 37 GHz (d); regions 1–12 for March 2006 at 10 GHz (e) and 37 GHz (f).

Deleted: 3

Deleted: -

Deleted: 4

Deleted: -

Deleted: the right panel

Deleted: the left panel

Deleted: ¶

Deleted: 5

Deleted: \sqrt{W} versus U_{10} : Scatterplots with linear fits for

Deleted: Linear fits for

Deleted: Linear fits for

Deleted: 7

Figure 9. Seasonal cycle for 2006 of regression coefficients in the $\sqrt{W(U_{10})}$ linear fits for different regions as defined in Fig. 2 and Table 1: a) slope m ; b) y-intercept c . The regions represent: 4–Temperate zone in Northern hemisphere; 5–Temperate zone in Southern hemisphere; 6–Doldrums along the Equator; 12–Lowest SST.

Figure 10. Regional and seasonal variations: a) Regionally averaged b values for each month with error bars (\pm one standard deviation) representing the regional variability; b) Annually averaged b values for each region with error bars representing the seasonal variability.

Figure 11. Sea surface temperature dependences of a) coefficient a (slope) and b) coefficient b (intercept) in the $W(U_{10})$ dependence. Each point is annual mean for different region. The error bars indicate ± 1 standard deviation for SST (horizontal bars) and coefficients (vertical bars). Panel c) shows the monthly means of coefficients b for each region that form one data point in panel b). Regions in Northern hemisphere (NH) are shown with squares; regions in Southern hemisphere (SH) are shown with circles. The diamonds are for region 6 at the Equator.

Figure 12. a) Comparison of the new global $W(U_{10})$ parameterization (based on the global W data set) to parameterizations from different studies; SAL13 (10 GHz) and SAL13 (37 GHz) are parameterizations from Salisbury et al. (2013) (Eq. (1)), CAL08 are parameterizations derived by Callaghan et al. (2008) (Eq. (2)); and MOM80 is the parameterization of Monahan and O’Muircheartaigh (1980) (Eq. (3)).

b) Comparison of the new quadratic parameterization $W(U_{10}, T)$ (Eqs. 13-14) at three fixed SST values ($T = 20^\circ\text{C}$, red line; $T = 12^\circ\text{C}$, green line; $T = 2^\circ\text{C}$, blue line) to the global quadratic parameterization $W(U_{10})$ (Eq. 11, black solid line) and the parameterizations of Salisbury et al. (2013) (Eq. (1)) for 10 GHz (dash-dotted line) and 37 GHz (dashed line).

c) Comparison of the new $W(U_{10}, T)$ parameterizations with quadratic (Eqs. 13-14, purple line) and cubic (red line) wind speed exponents at $T = 20^\circ\text{C}$ to the parameterizations of Salisbury et al. (2013, SAL13) (Eq. (1)) for 37 GHz (dashed line) and Monahan and O’Muircheartaigh (1980, MOM80) (blue solid line).

Figure 13. a) As Fig. 1b with W values added from $W(U_{10})$ for 10 and 37 GHz (black lines, Eqs. (10-11)) and $W(U_{10}, T)$ for 10 (red) and 37 GHz (cyan, Eqs. (13-14)). Wind speed and sea surface temperature from the whitecap database are used for the calculations.

Deleted: 6

Deleted: Regional and s

Deleted: dependency of

Deleted: parameterizations'

Deleted: y-intercept for all months of 2006

Deleted: R

Deleted: as defined in table 1. NH= Northern Hemisphere; EQ = Equator; SH = Southern Hemisphere

Deleted: 7

Deleted: SST – (dots, left vertical axis) and intercept variability of the linear $\sqrt{W(U_{10})}$ parameterization (triangles, right vertical axis) for 2006 for three selected regions as defined in table 1.

Deleted: 8

Deleted: Intrinsic correlation between W and U_{10} from QuikSCAT. (a) Scatterplot of global $U_{10\text{ECMWF}}$ versus $U_{10\text{QSCAT}}$ for March 2006. (b) Scatterplot of \sqrt{W} versus $U_{10\text{ECMWF}}$ for March 2006. In both figures the colors indicate the amount of data points per hexabin. The black lines are linear fits; the dashed line represents the best fit and the solid line the best linear fit forced through zero. Values for R^2 are indicated.

Deleted: ¶

Moved (insertion) [26]

Deleted: ,

Deleted: where

Deleted: and

Deleted: 3

1 b) Difference map of annual average W distribution for 2006 calculated from the
2 Monahan and O’Muircheartaigh (1980, MOM80) $W(U_{10})$ parameterization (Eq. (3)) minus
3 $W(U_{10}, T)$ from Eqs. (13-14). The calculations use wind speed U_{10} is from QuikSCAT in the
4 whitecap database.
5 Figure 14. a) Annual average super-micron mass emission rate for 2006 in $\mu\text{g m}^{-2} \text{s}^{-1}$
6 calculated from from Eq. (4')). b) Difference map between the annual average super-micron
7 SSA mass emission rate calculated from the Monahan et al. (1986) SSSF and the annual
8 average super-micron SSA mass emission rate calculated from the Monahan et al. (1986)
9 SSSF where W is replaced with Eqs. (13-14). The calculations use wind speed U_{10} is e from
10 QuikSCAT in the whitecap database,
11
12
13
14
15

- Deleted: Figure 9. A
- Deleted: 2
- Deleted: (a) and
- Deleted: 9
- Deleted: (b).
- Deleted: extracted
- Deleted: the ECMWF
- Deleted:
- Deleted: 10
- Deleted:
- Deleted: the MOM80 $W(U_{10})$ parameterization (Eq. (2)) (a) and from Eq. (9) (b). U_{10} is extracted from the ECMWF data base.¶
- ¶ Figure 11.
- Deleted: coarse mode
- Deleted: coarse mode
- Deleted: 9
- Deleted: Emission rates are calculated for 2006 in $\mu\text{g m}^{-2} \text{s}^{-1}$.
- Deleted: xtracted
- Deleted: the
- Deleted: ECMWF data base
- Deleted: ¶
- Moved up [26]: Figure 12. $W(U_{10})$ from different studies, where SAL13 (10 GHz) and SAL13 (37 GHz) are parameterizations from Salisbury et al. (2013) (Eq. (1)), and CAL08 are parameterizations derived by Callaghan et al. (2008) (Eq. (3)).

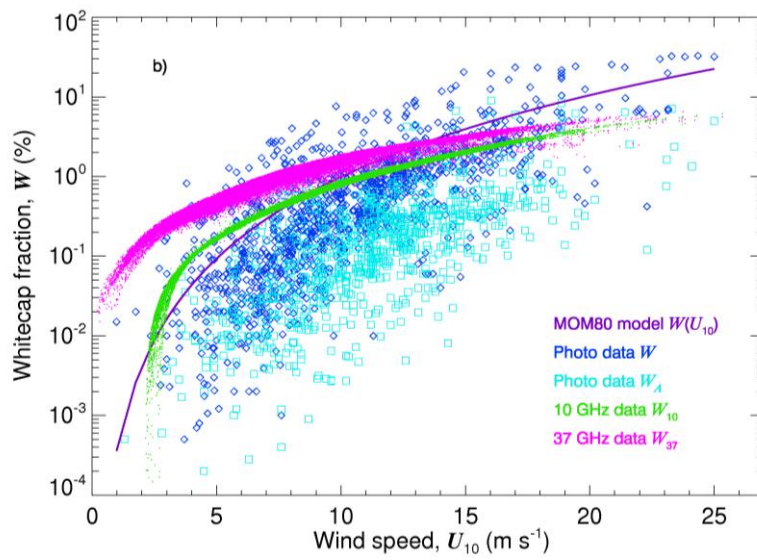
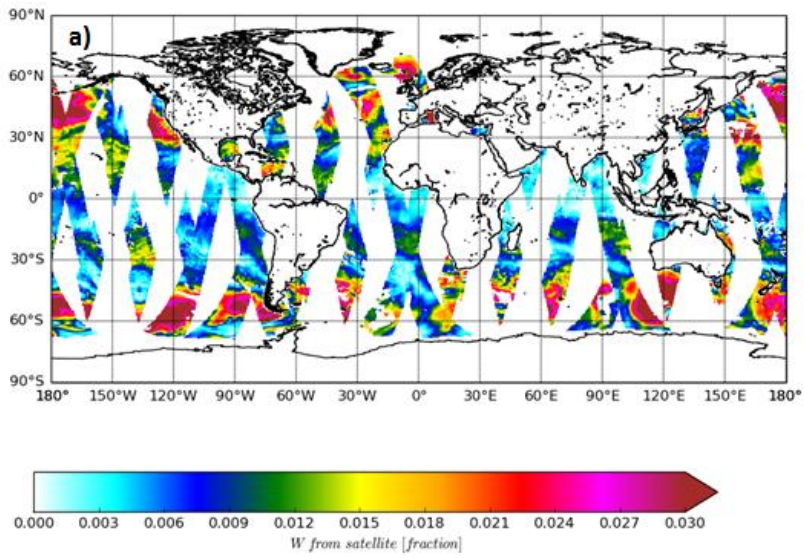


Figure 1

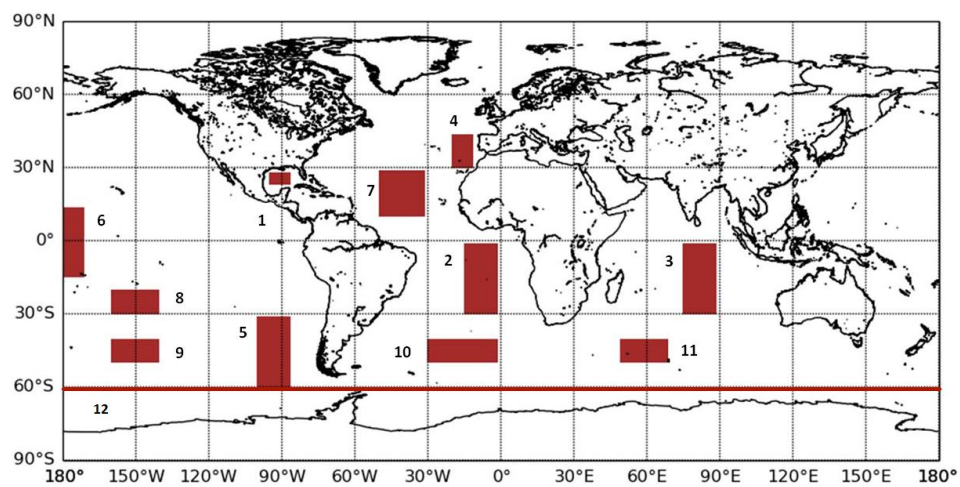


Figure 2

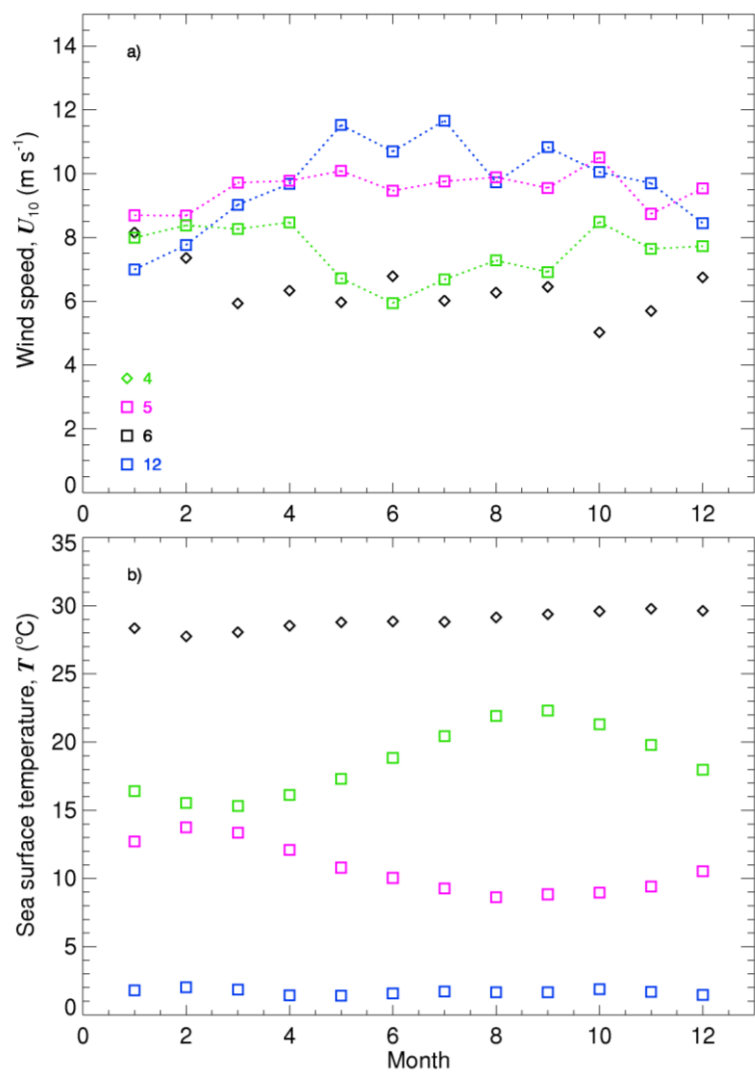


Figure 3

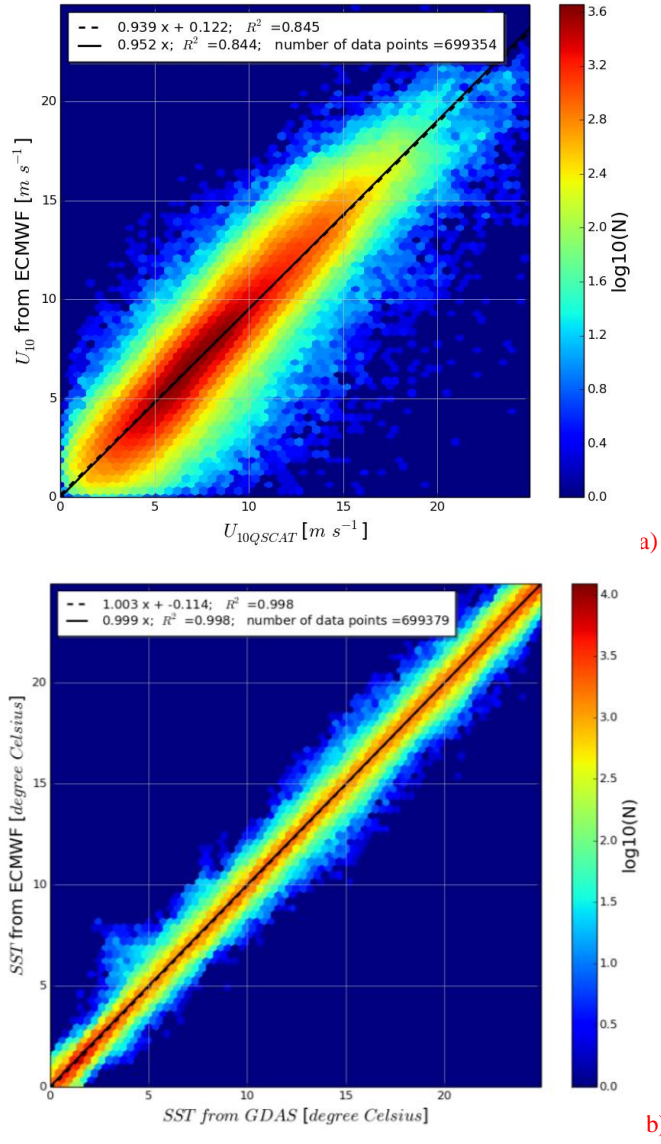
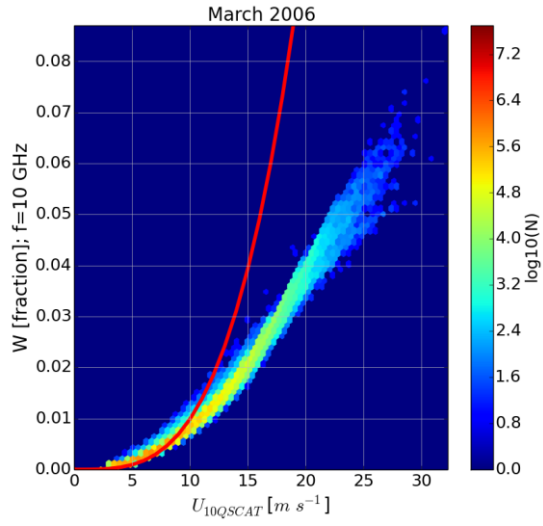
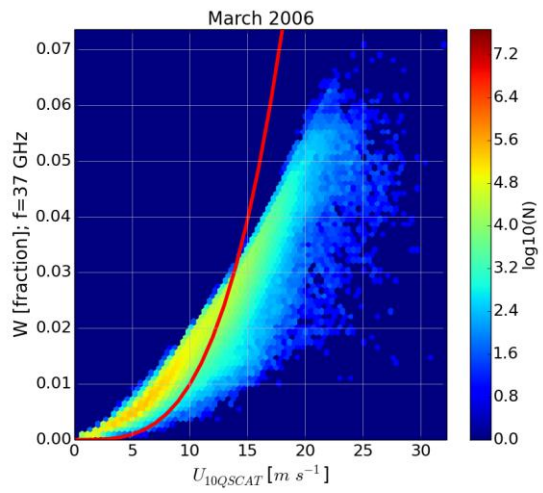


Figure 4

1



2



3

4

5 Figure 5

1

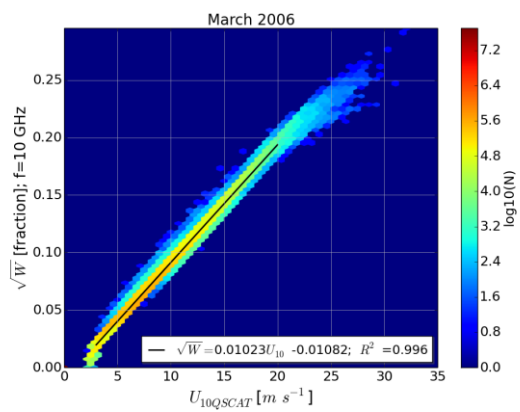
2

3

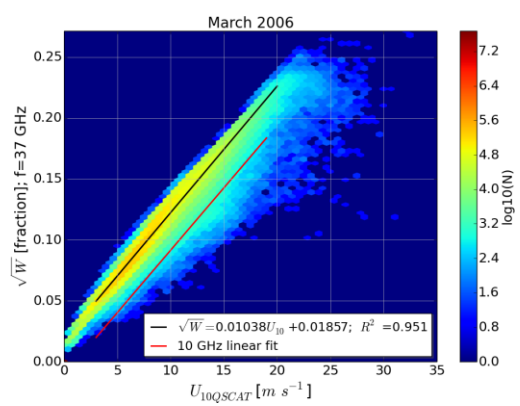
4

5 Figure 6

6

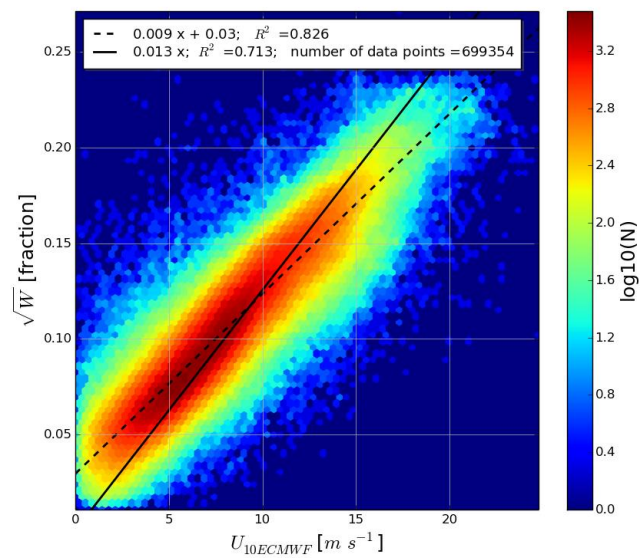


a



b

1



2

3

4 Figure 7

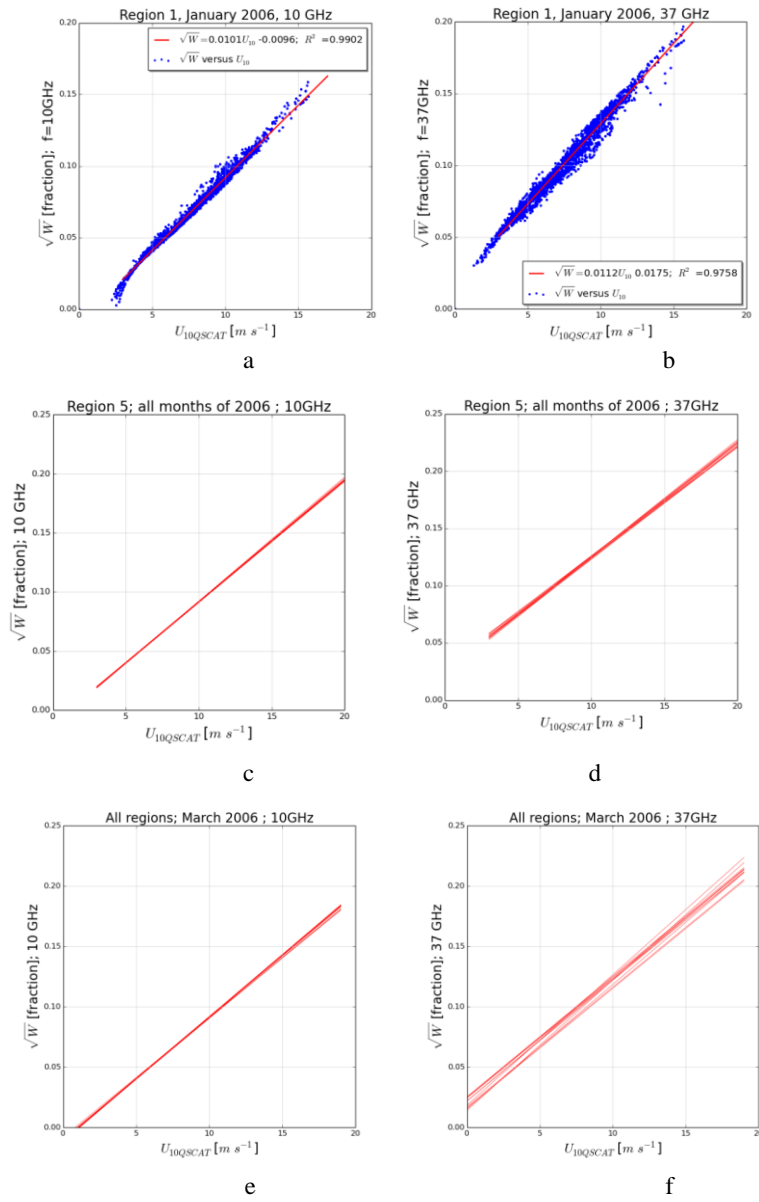
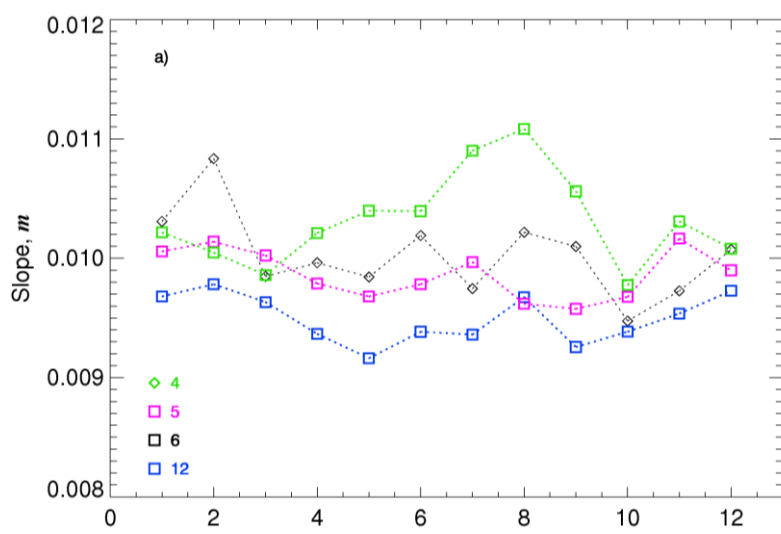
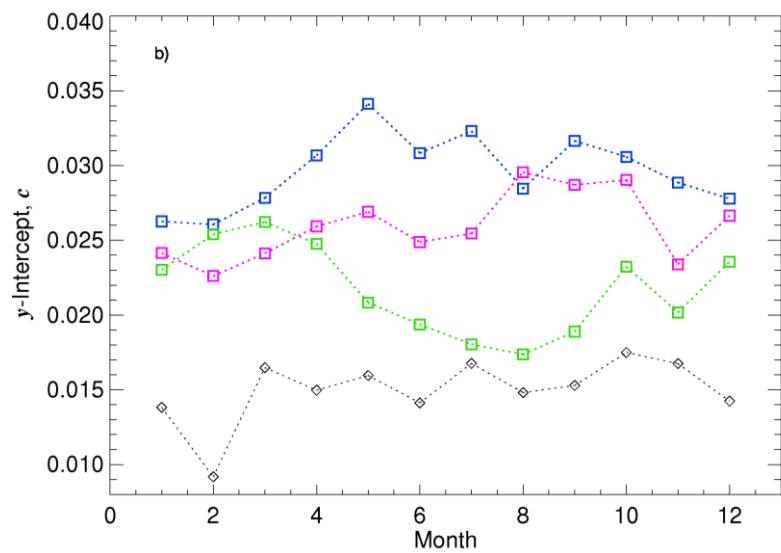


Figure 8

1



2

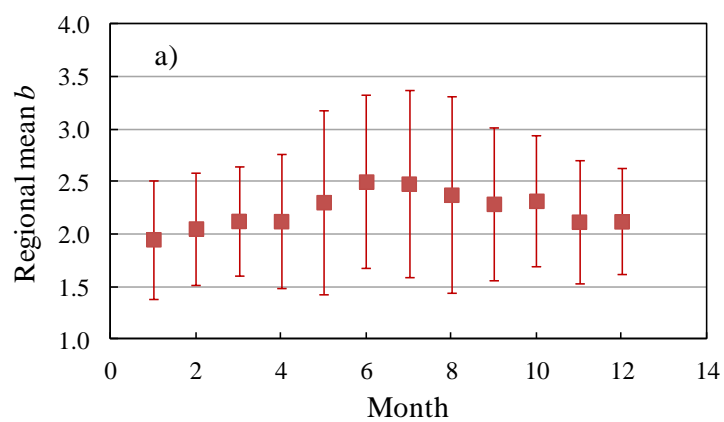


3

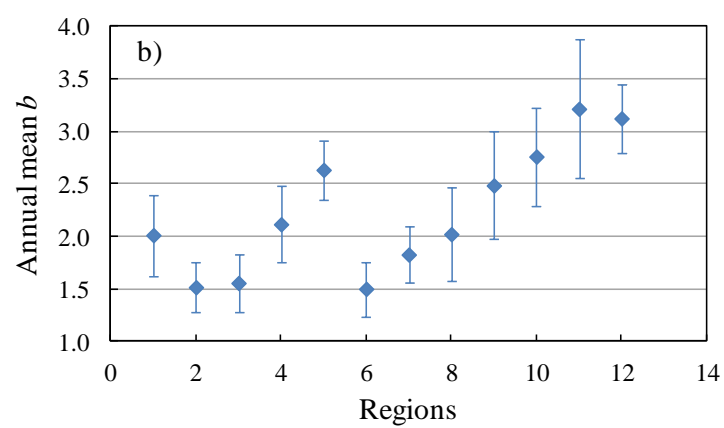
4 Figure 9

5

1



2



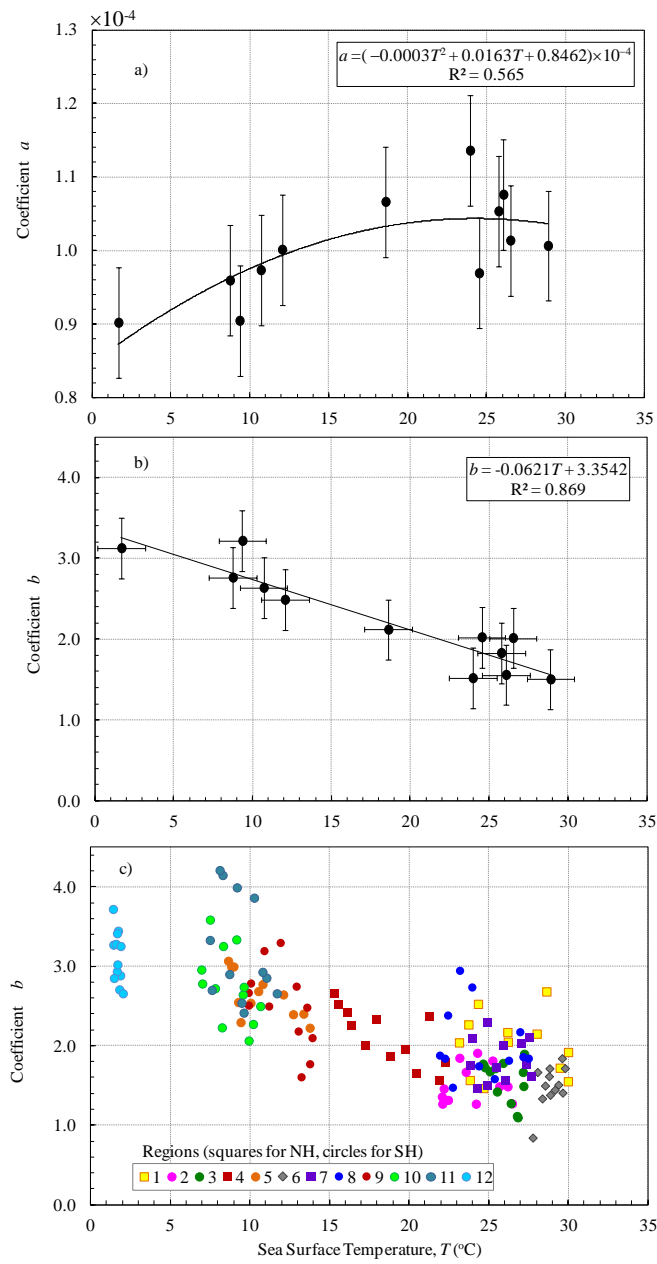
3

4

5 Figure 10

6

7



1
2 Figure 11

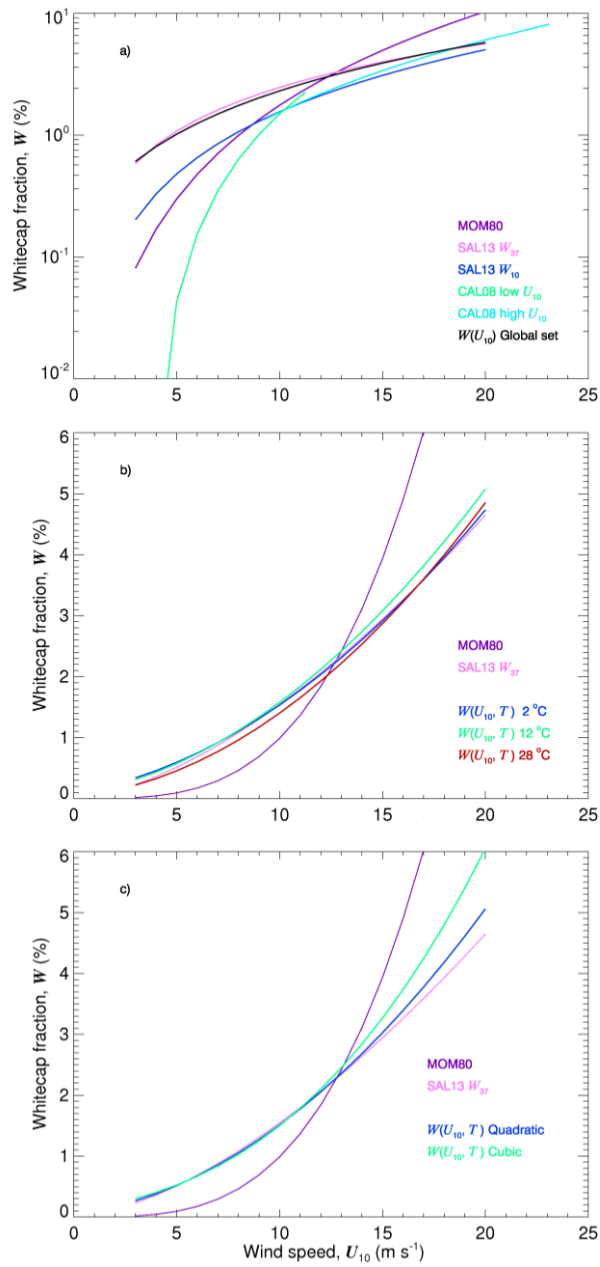


Figure 12

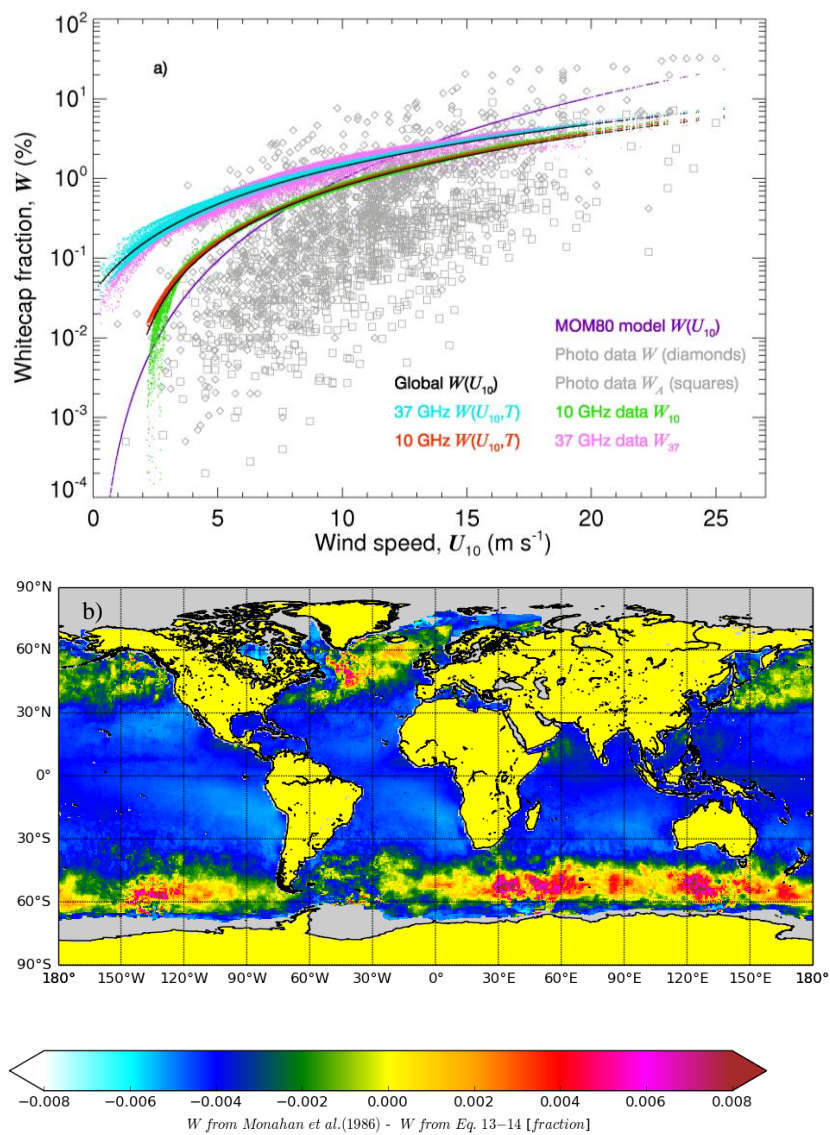
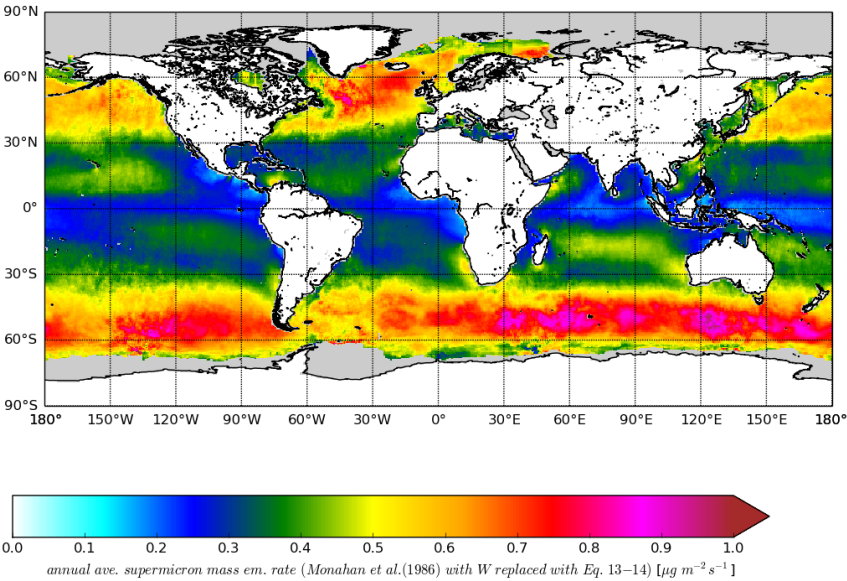
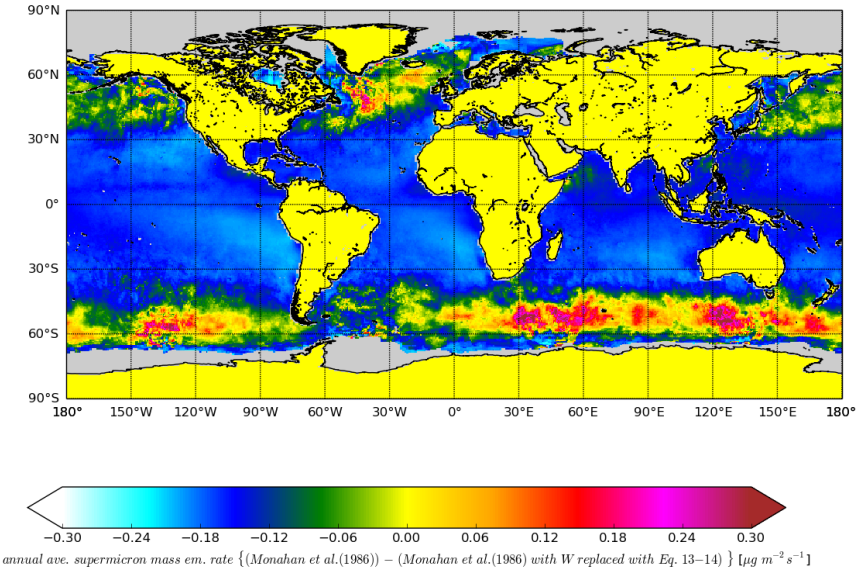


Figure 13

1



2



3

4 Figure 14

5